EXPERIMENTAL AND STATISTICAL MODELING METHODOLOGIES FOR IMPROVING SETTLED SEDIMENT MANAGEMENT IN URBAN STORMWATER SYSTEMS

MARÍA ALEJANDRA PIMIENTO AVELLA

ENGINEERING DOCTORAL PROGRAM
PONTIFICIA UNIVERSIDAD JAVERIANA
BOGOTÁ, COLOMBIA
2022

DOCTORAL DISSERTATION

EXPERIMENTAL AND STATISTICAL MODELING METHODOLOGIES FOR IMPROVING SETTLED SEDIMENT MANAGEMENT IN URBAN STORMWATER SYSTEMS

María Alejandra Pimiento Avella (CE, MSC)

RESEARCH GROUP:
Science and Engineering of Water and the Environment

ADVISOR:
Dr. Andrés Torres. Pontificia Universidad Javeriana, Bogotá, Colombia.

REVIEWERS:
Dr. Nicole Nawrot. Gdansk University of Technology, Gdansk, Poland
Dr. Jose Anta Álvarez. Universidade da Coruña, A Coruña, SpainS
Dr. Juan Pablo Rodríguez. Universidad de los Andes, Bogotá, Colombia
Dr. Andrés Vargas Luna. Pontificia Universidad Javeriana, Bogotá, Colombia

Acknowledgments

Words cannot express my gratitude to my advisor, Ph.D. Andrés Torres who has been the most outstanding support to carry out this investigation, for believing in me and teaching me to research. Who also, has considered me as part of his team for future projects.

This endeavor would not have been possible without the support of Minciencias as a funder to carry out the doctorate through call 785 of 2017. Also, the generous support from the Pontificia Universidad Javeriana, for financing part of the research project and the research seedbed "agua en la ciudad". Nonetheless, I would like to express my gratitude to the University of Coruña for receiving me to do the internship.

Special thanks to the professors and students of the seedbed for their support in collecting samples and analyzing them in the laboratory, and to the students of the tenth semester of medicine in 2022-3.

I'd like to recognize my family, especially my parents and my partner, who offered me their unconditional support throughout this journey. Lastly, I would be remiss not to mention my friends, who have always supported the process, and my colleagues, who inspire me.

Contents

List of figures

List of tables

List of equations

List of abbreviations

A	Basin area
ABF	Dermal absorption factor
Accum	Sediment accumulation
ADD	Lifetime average daily dose
ADP	Antecedent dry weather period
Al	Aluminum
AR	Arzobispo River
AT	Exposure average time
Bn	Geochemical background value
Bw	Body weight
C	Runoff coefficient
Cd	Cadmium
CN	Curve number method
Cn	Measured heavy metal concentration
CR	Carcinogenic risk
Cr	Chromium
Cu	Cooper
CW/ST	Constructed-wetland/storage-tank
D10	particle diameter not to exceed 10% of the sample cumulatively
D50	particle diameter not to exceed 50% of the sample cumulatively
dw	Number of days in dry weather
ED	Exposure duration
EF	Enrichment factor
Ef	Exposure frequency
EPA	US Environmental Protection Agency
FAO	Food and Agriculture Organization of the United Nations
H	Total precipitation height
HCl	Hydrochloric acid
HI	Hazard index
HNO_3	Nitric acid
HM	Heavy metal
HQ	Hazard quotient
I_{ave}	Average rain intensity
ICP	Inductively coupled plasma
I_{geo}	Geo-accumulation index
InhR	Inhalation rate
IngR	Ingestion rate
I_{max}	Maximum rain intensity
K	Conversion factor
MPI	Modified pollution index
MR	Molinos River
MRI	Modified ecological risk index
Ni	Nickel
Pb	Lead
PCA	Principal Component Analysis
PEC	Probable effect concentration
PEF	Particle emission factor
PI	Pollution index

PLI	Pollution load index
PSD	Particle size distribution
PUJ	Pontificia Universidad Javeriana
Q	flow
RDS	Road-deposited sediment
RfD	Reference dose
RI	Potential ecological risk index
RMSE	Root mean square error
rw	Number of days with rainfall weather
S	Maximum infiltration capacity
SA	Exposed skin surface area
SAF	Skin adherence factor
SF	Constant factor for each substance
SVM	Support vector machine
SQG	Sediment quality guidelines
TCR	Total cancer risk
TEC	Threshold effect concentration
Trn	Toxic metal response
Z	Zinc

GENERAL INTRODUCTION

Nowadays, worldwide awareness of the proper management of natural resources has increased, particularly in urban environments where the landscape has been drastically altered. Rapid urbanization and climate change have generated extreme rainfall and increased the washing and transport of sediments by runoff to urban stormwater systems (Faiz et al., 2009; Zhang et al., 2017). Sediment are part of the aquatic ecosystem, and their management is an environmental and economic concern by the quantities dredged in different water bodies, their disposal, relocation, or reuse (SedNet et al., 2007). Particles accumulate on impervious surfaces during dry periods, are washed, and transported through the urban drainage system by stormwater runoff. Thus, sediment are becoming one of the most critical sources of non-point source pollution, causing water quality impairment in receiving water bodies, and are a dominant stressor in urban aquatic ecosystems (Choi et al., 2020; Laxmi Mohanta et al., 2020).

Understanding sediment characterization, such as particle size distribution and pollutants amounts and types, is a fundamental element of sediment management. It is necessary to develop monitoring plans in which measures for quality control are considered during sampling and analysis of sediments' physical and chemical properties (Lintern et al., 2016). However, the composition of the sediments is associated with the characteristics of the basin, which must also be analyzed to improve management practices (if any) or implement adequate management measures (Q. Wang et al., 2019).

In storage environments with long residence times, the accumulation of contaminated sediments can represent an environmental hazard at the site or if they are released by human activity or during important flooding events (Chang et al., 2019). Commonly, the management strategies proposed for the maintenance of urban stormwater systems include sediment dredging to increase the hydraulic capacity of the structures and remove pollutants. Usually, the dredged sediments are disposed of in landfills or confined for aquatic disposal. Thus, some studies have been carried out to reuse sediments in activities such as agriculture, horticulture, forestry, soil restoration, construction material, or gardening (Akcil et al., 2015; Bhairappanavar et al., 2018; L. Wang et al., 2015). The reuse depends mainly on pollutants concentrations which are related to particle size, land use, stormwater surface contact (roads, parking lots, roofs of different materials), rainfall intensity and duration, and antecedent dry weather period (Charters et al., 2015; Pimiento et al., 2018).

Although there are articles in the literature with reports on sediment characterization, these analyzes have been carried out mainly in developed countries. Additionally, in some of these particles' relationship analyzes have been performed primarily to identify sources of contaminants and periods of accumulation. However, information is still lacking on how to use this information in management alternatives. Unfortunately, in Colombia, as in many developing countries, there are no sediment quality standards or technical management guidelines. Specifically, in Bogotá, sediment are collected from different water bodies, mechanically or manually, and are transported to various dumps (Alcaldía Mayor de Bogotá, 2019). However, there is no differentiation between sediment from rainwater systems and sludge from the sewage system during the collection practice, so all the collected material is traditionally considered waste.

Based on the above, the usefulness of generating management elements for sediments carried by runoff and accumulated in Bogotá's drainage systems was evidenced. However, analyzing the basin's hydrology and the sediments' characteristics is necessary as a first step. In addition, dredging and disposal options must be identified to establish management alternatives. On the other hand, it is essential to determine sediments' effects on the environment and people's health. This research proposes experimental and statistical modeling methodologies that allow management alternatives for the sediments retained in urban stormwater systems.

This document is made up of four parts with contributions to close the gap regarding methodologies to be considered for managing urban stormwater sediments. This distribution aims to implement sediment analysis methodologies according to the available information. In turn, each part has an introduction with the state of the art, a chapter with the proposed methodology for data analysis, a chapter with the results and discussion, the conclusions, and finally, the references. Therefore, Part A: Data Characterization shows the methodology used for the collection and experimental analysis of sediment and precipitation data. Part B: sediment pollution, focuses on sediment risk assessment of human health and the environment. Part C: statistical analysis and modeling, a methodology is proposed for determining relationships between variables and prioritizing and modeling variables. Finally, Part D: Sediment Management summarizes how the proposed methodologies provide elements to improve the management of settled urban stormwater sediments.

REFERENCES INTRODUCTION

Akcil, A., Erust, C., Ozdemiroglu, S., Fonti, V., & Beolchini, F. (2015). A review of approaches and techniques used in aquatic contaminated sediments: metal removal and stabilization by chemical and biotechnological processes. Journal of Cleaner Production, 86(Supplement C), 24–36. https://doi.org/10.1016/j.jclepro.2014.08.009

Alcaldía Mayor de Bogotá. (2019). Distrito inaugura moderna planta de lodos para procesar residuos extraídos de alcantarillas. In Bogota.gov.co.

Bhairappanavar, S., Liu, R., & Coffman, R. (2018). Beneficial uses of dredged material in green infrastructure and living architecture to improve resilience of Lake Erie. Infrastructures, 3(4). https://doi.org/10.3390/infrastructures3040042

Chang, H., Allen, D., Morse, J., & Mainali, J. (2019). Sources of contaminated flood sediments in a rural–urban catchment: Johnson Creek, Oregon. Journal of Flood Risk Management, 12(4). https://doi.org/10.1111/jfr3.12496

Charters, F. J., Cochrane, T. A., & O'Sullivan, A. D. (2015). Particle size distribution variance in untreated urban runoff and its implication on treatment selection. Water Research, 85(Supplement C), 337–345. https://doi.org/10.1016/j.watres.2015.08.029

Choi, J. Y., Jeong, H., Choi, K.-Y., Hong, G. H., Yang, D. B., Kim, K., & Ra, K. (2020). Source identification and implications of heavy metals in urban roads for the coastal pollution in a beach town, Busan, Korea. Marine Pollution Bulletin, 161. https://doi.org/10.1016/j.marpolbul.2020.111724

Faiz, Y., Tufail, M., Javed, M. T., Chaudhry, M. M., & Naila-Siddique. (2009). Road dust pollution of Cd, Cu, Ni, Pb and Zn along Islamabad Expressway, Pakistan. Microchemical Journal, 92(2), 186–192. https://doi.org/10.1016/j.microc.2009.03.009

Laxmi Mohanta, V., Naz, A., & Kumar Mishra, B. (2020). Distribution of heavy metals in the water, sediments, and fishes from Damodar river basin at steel city, India: a probabilistic risk assessment. Human and Ecological Risk Assessment, 26(2), 406–429. https://doi.org/10.1080/10807039.2018.1511968

Lintern, A., Leahy, P. J., Heijnis, H., Zawadzki, A., Gadd, P., Jacobsen, G., Deletic, A., & Mccarthy, D. T. (2016). Identifying heavy metal levels in historical flood water deposits using sediment cores. Water Research, 105, 34–46. https://doi.org/10.1016/j.watres.2016.08.041

Pimiento, M. A., Rivera, D. S., Lara Borrero, J. A., & Torres Abello, A. E. (2018). Relationship between hydrological, physical and chemical characteristics present in rainwater runoff sediments. Ingenieria y Competitividad, 20(2), 27. https://doi.org/10.25100/iyc.v20i2.5846

SedNet, Palumbo, L., & Bortone, G. (2007). Sediment and Dredged Material Treatment. In Sustainable Management of Sediment Resources. Elsevier Science.

Wang, L., Kwok, J. S. H., Tsang, D. C. W., & Poon, C.-S. (2015). Mixture design and treatment methods for recycling contaminated sediment. Journal of Hazardous Materials, 283(Supplement C), 623–632. https://doi.org/10.1016/j.jhazmat.2014.09.056

Wang, Q., Zhang, Q., Dzakpasu, M., Chang, N., & Wang, X. (2019). Transferral of HMs pollution from road-deposited sediments to stormwater runoff during transport processes. FRONTIERS OF ENVIRONMENTAL SCIENCE & ENGINEERING, 13(1). https://doi.org/10.1007/s11783-019-1091-x

Zhang, J., Hua, P., & Krebs, P. (2017). Influences of land use and antecedent dry-weather period on pollution level and ecological risk of heavy metals in road-deposited sediment. Environmental Pollution, 228, 158–168. https://doi.org/10.1016/j.envpol.2017.05.029

PART A: DATA CHARACTERIZATION

INTRODUCTION PART A

Owing to rapid urbanization, the percentage of impervious surfaces has increased, restructuring urban hydrology by raising the speed and volume of runoff, increasing the risk of flooding and deterioration of water quality (Ma et al., 2019; Schroer et al., 2018; Wiest et al., 2018). Most cities face pollution at different levels, especially since their ecosystems receive a high load of pollutants due to urbanization and human activities in cities (Ignatavicius et al., 2017; Zhu et al., 2008). Urban stormwater runoff can present a severe water quality problem due to the wide range of pollutants that can be transported from streets, parking lots, rooftops, construction sites, vacant lots, and landscaped by flow through the drainage system of the receiving waters (Charters et al., 2015; Ignatavicius et al., 2017; Wu et al., 2018).

During rainfall events, part of the harmful pollutants contained in the sediments may be dissolved, desorbed, and transported by stormwater, and thus contribute to stormwater pollution because of chemical, biochemical, and mechanical processes, also influenced by rainfall characteristics, antecedent weather conditions and land use (Sałata et al., 2019; Q. Wang et al., 2019; Wijesiri et al., 2016). Adsorption, desorption, and leaching of contaminants into sediments can vary based on water quality parameters such as pH, temperature, specific conductivity, and hardness, additionally to sediment's high atomic weight and density (Laxmi Mohanta et al., 2020; Shojaeezadeh et al., 2020). Sediment act as indicators of environmental quality for stormwater due they can adsorb harmful pollutants such as nutrients, heavy metals, pesticides, and polycyclic aromatic hydrocarbons (PAHs), owing to the extensive and intensive impacts of anthropogenic activities (Q. Wang et al., 2020; J. Zhang et al., 2017). In addition, contaminated sediments can represent a risk for the organisms that inhabit them because they tend to accumulate organic pollutants and transfer them along the food chain, causing adverse effects at different levels (Yun et al., 2015).

There is a lack of studies investigating the prediction of sediment quality in stormwater drainage systems as a source of non-point source pollutants. Sediment quality depends on particle size distribution, hydrological variables, basin characteristics, and land use activities. Findings are generally not supported by statistical analyses focused on sediment quality variability causes (Bąk et al., 2019; Q. Wang et al., 2019; Zhao & Li, 2013a).

Part A of this manuscript describes the data collection and characterization. CHAPTER 1 describes the study site, the data collection, and the data analysis methodologies. CHAPTER 2 presents the results obtained regarding the hydrological description of the basin and the collected sediments.

CHAPTER 1 STUDY SITE

This research was developed in Bogotá, Colombia's capital city. Located in the center of the country, it is within the intertropical confluence zone, producing two rainy seasons: from March to May and from September to November. With an average temperature of 13.1°C and an average annual rainfall of 797mm (IDEAM, n.d.; Ramirez, 2017), Bogotá has four hydrographic drainage basins (Figure 1), which drains directly into the Bogotá River: Salitre, Torca, Fucha, and Tunjuelo rivers, which have numerous sub-basins of minor currents. Table 1 presents the rainwater drainage description for each basin.

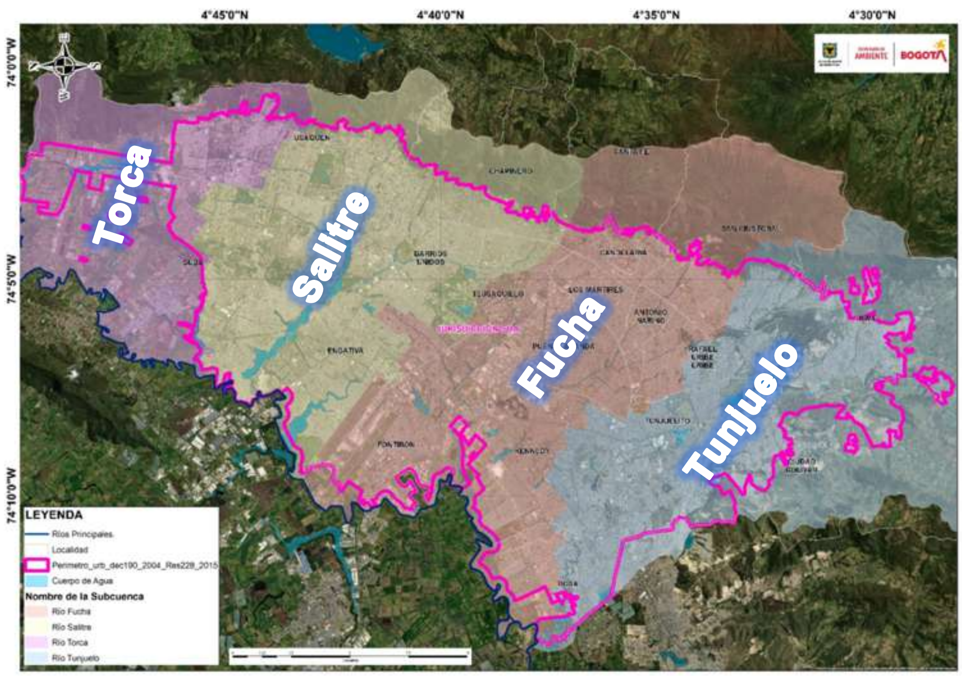

Figure 1 Hydrographic basins of Bogotá.
Source: (Secretaría de Ambiente, 2021)

Table 1: Hydrographic basin description of Bogotá

Basin	Urban area (ha)	Main rainwater network (km)	Local rainwater network (km)
Salitre	13964	229.89	866.90
Fucha	12991	195.77	801.22
Tunjuelo	41427	85.40	595.01
Torca	6009	32.65	65.51

Source: (Secretaría de Ambiente, 2021)

Section 1.1 presents the description of the selected sampling points, section 2.2 the methodology for sediment collection, sections 1.3 and 1.4 include the hydrological data and the variables used from these data to analyze the rainfall and runoff in the basin, and finally, section 1.5 shows the analyzes carried out for the characterization of the sediments.

1.1 Sampling site

The Salitre basin was selected because it has the largest stormwater network in the city, which is in the north-central sector and has a drainage area of 13,964 ha. The main river starts in the eastern hills with the name of Arzobispo River, then changes its name to Salitre River, runs for 19.76 km, and discharges into the Bogotá River. To select the sampling points, a tour of different drainage structures of the city was carried out to identify sediment accumulation points. Once the accumulation points were identified, possible sediment collection methodologies were considered. Three urban drainage structures were selected (Figure 2 and Figure 3): Molinos River (MR), Arzobispo River (AR), and the constructed-wetland/storage-tank (CW/ST) from the Pontificia Universidad Javeriana (PUJ). Additionally, the land uses of the catchments are: MR - residential, AR, and CW/ST - commercial.

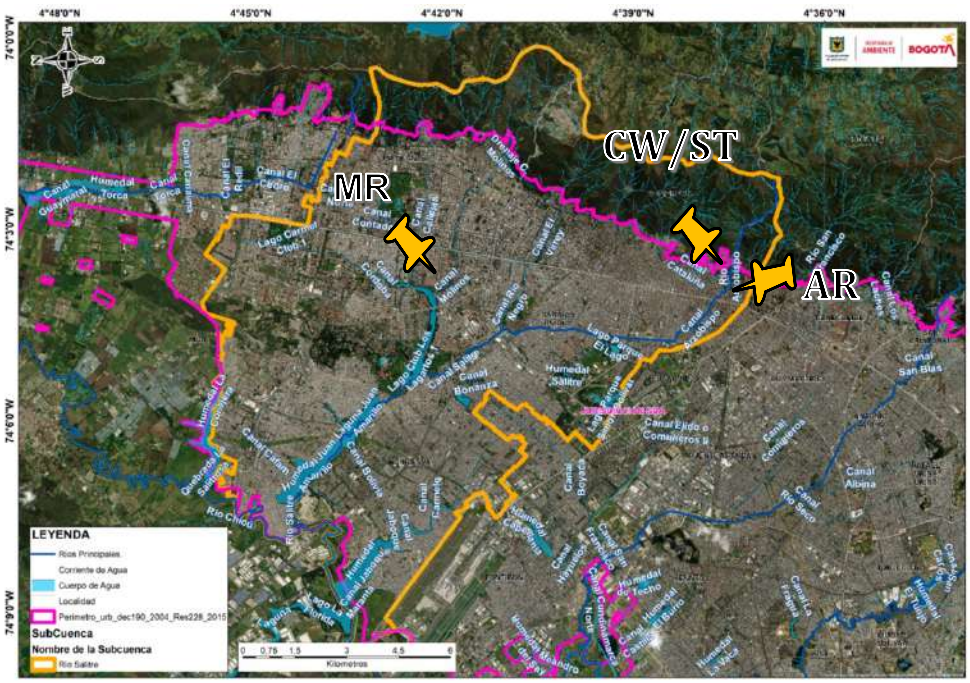

Figure 2 Salitre river basin and sampling points location.MR: Molinos river, CW/ST: constructed-wetland/storage-tank, AR: Arzobispo river.
Source:(Secretaría de Ambiente, 2021)

Figure 3 Sampling sites. Molinos River, Arzobispo River, and Constructed-wetland/storage-tank.

1.2 Sediment sample collection

The most common sediment sampling is discontinuous; an average value of sediment accumulation is obtained over a period, and they do not allow high-frequency analysis over time. Although continuous and automated measurement methodologies enable measurements to be taken for prolonged periods, these devices are expensive. The most used geometry for the design of sediment traps is the cylindrical one, this form of collection allows estimating the accumulation and movement of sediments for a time since the traps remain submerged (Thomas & Ridd, 2004).

Sediment collection was done discontinuously using two methodologies (i) hand-made sediment traps and (ii) a Van Veen grab. The first one facilitates the collection of particles accumulated over some time. However, an analysis of the accumulated sediment matrix is not made. The second methodology collects a point sample from the sediment column. However, it is impossible to determine the particles' characteristics that accumulate in a specific period. Autosamplers were not used despite their effectiveness because it was not feasible to control the equipment installed in the currents and these could easily be lost due to the current or theft. Thus, recycled plastic containers were used to construct the traps, which were tied by nylon to an existing surface above the riverbeds, as shown in Figure 4. Unfortunately, the sediment traps were lost in AR shortly after their installation, so it was decided to collect the sediment with the Van Veen grab. In MR, some traps were also lost due to high currents, which were being replaced (See Appendix A for detailed traps information).

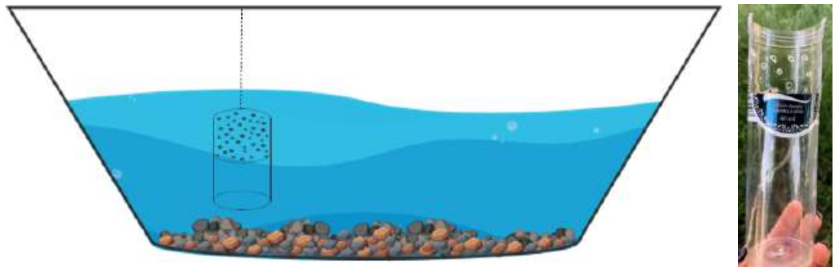

Figure 4 Sample collection with sediments traps

Sediment sampling campaigns were carried out from February 2020 to November 2021 at all sampling points. Due to COVID-19 lockdowns, it was not possible to collect samples consistently as we expected. As shown in Table 2, MR is where the most significant number of samples were collected, a total of 25 every two weeks. A monthly periodicity was implemented in AR and CW/ST; however, only 8 and 7 samples were collected, respectively.

Table 2 Sediment sampling campaigns. MR MR: Molinos river, CW/ST: constructed-wetland/storage-tank, AR: Arzobispo river.

Sample	Location	Date	Instrument	Sample	Location	Date	Instrument
001-5	MR	3/03/20	Trap	**001-28**	CW/ST	4/27/2021	Trap
001-6	MR	3/03/20	Grab	**001-29**	CW/ST	5/26/2021	Trap
001-7	AR	3/04/20	Grab	**001-30**	MR	6/11/21	Grab
001-8	MR	3/17/2020	Trap	**001-31**	MR	6/22/2021	Trap
001-9	MR	3/31/2020	Trap	**001-32**	MR	7/07/21	Trap
001-10	MR	4/14/2020	Trap	**001-33**	CW/ST	7/07/21	Trap
001-11	MR	4/28/2020	Trap	**001-34**	AR	7/07/21	Grab
001-12	MR	5/12/20	Trap	**001-35**	MR	7/22/2021	Trap
001-13	MR	9/24/2020	Trap	**001-36**	MR	8/03/21	Trap
001-14	MR	10/08/20	Trap	**001-37**	AR	8/03/21	Grab
001-15	MR	10/22/2020	Trap	**001-38**	MR	8/17/2021	Trap
001-16	MR	11/19/2020	Trap	**001-39**	MR	8/31/2021	Trap
001-17	MR	12/03/20	Trap	**001-40**	CW/ST	8/31/2021	Grab
001-18	MR	12/17/2020	Trap	**001-41**	AR	8/31/2021	Grab
001-19	MR	2/09/21	Grab	**001-42**	MR	9/14/2021	Trap
001-20	AR	2/09/21	Grab	**001-43**	MR	9/28/2021	Trap
001-21	CW/ST	3/02/21	Trap	**001-44**	CW/ST	9/28/2021	Trap
001-23	MR	3/23/2021	Trap	**001-45**	AR	9/28/2021	Grab
001-24	AR	3/23/2021	Grab	**001-46**	MR	10/12/21	Trap
001-25	CW/ST	3/23/2021	Trap	**001-47**	MR	10/26/2021	Trap
001-26	MR	4/06/21	Trap	**001-48**	AR	11/02/21	Grab
001-27	MR	4/20/2021	Trap				

1.3 Hydrology characterization

Bogotá has an early warning system in which daily precipitation is reported, and this information is freely accessible on the website of the District Risk Management Institute of Bogotá (IDIGER, for its name in Spanish). The closest station to the sampling points with daily accumulated rainfall information was selected: "El Paraíso" climatological station (latitude 4.62802611849305 and longitude -74.05863996311022) for the CW/ST and AR, "Gustavo Morales Morales" pluviometric station (latitude 4.575873, and longitude -74.106178,2578) for the MR (Instituto Distrital de Gestión de Riesgos y Cambio Climático, 2022). Table 3 shows an example of the data downloaded from the Gustavo Morales Morales Station, and in Figure 5 the precipitation data with the sampling periods for MR (see Appendix A for AR and CW/ST figures). Moreover, the period of dry weather in Bogotá is from December to the end of March and from the end of July to the end of September, the other months being rainy seasons (IDEAM, n.d.).

Table 3 Gustavo Morales Morales station accumulated daily rainfall in mm.

Date	Accumulation (mm)	Date	Accumulation (mm)
18/02/20	0.0	**25/02/20**	27.2
19/02/20	0.0	**26/02/20**	20.2
20/02/20	10.1	**27/02/20**	27.5
21/02/20	30.3	**28/02/20**	0.7
22/02/20	7.4	**29/02/20**	19.5
23/02/20	21.2	**1/03/20**	0.0
24/02/20	1.1	**2/03/20**	4.6

Source: (Instituto Distrital de Gestión de Riesgos y Cambio Climático, 2022)

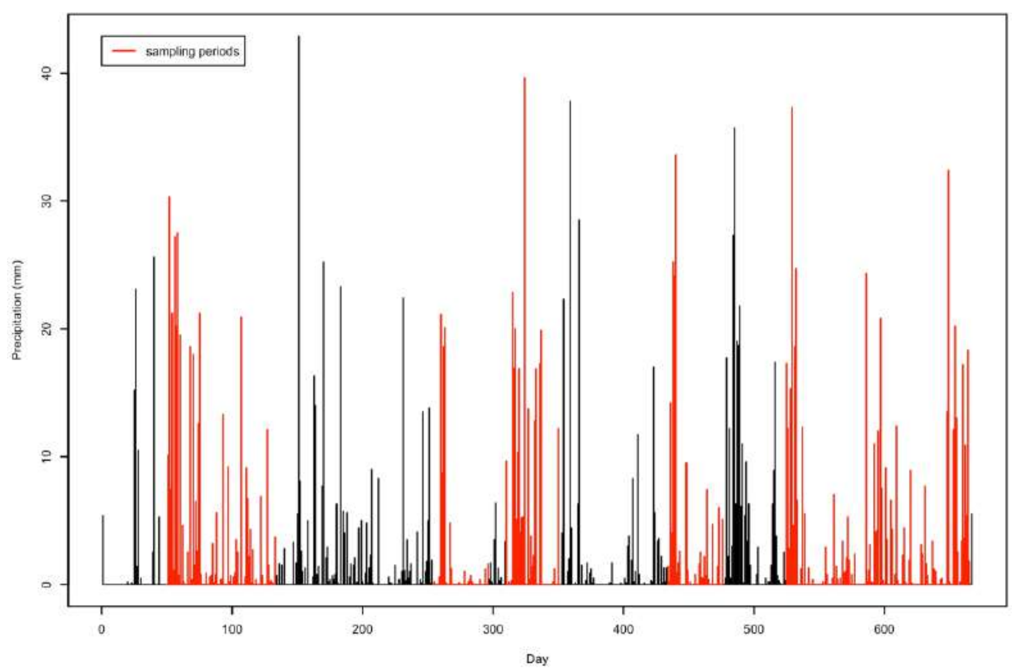

Figure 5 Pluviometric station "Gustavo Morales Morales" precipitation data from 1 January 2020 until 28 October 2021, and Molinos River sampling periods.

With the data downloaded from the stations previously mentioned, the following variables can be estimated for hydrological analysis (Figure 6): total precipitation height in mm (H), average rain intensity in mm/h (I_{ave}) calculated with Equation 1, maximum intensity in mm/h (I_{max}) calculated with Equation 2, number of days with dry weather (dw), number of days with rainfall weather (rw), and antecedent dry weather period in days (ADP).

$$I_{ave} = \frac{H}{n * 24}$$

Equation 1. Average Intensity (mm/h)

$$I_{max} = \frac{H_{i-max}}{24}$$

Equation 2. Maximum Intensity (mm/h)

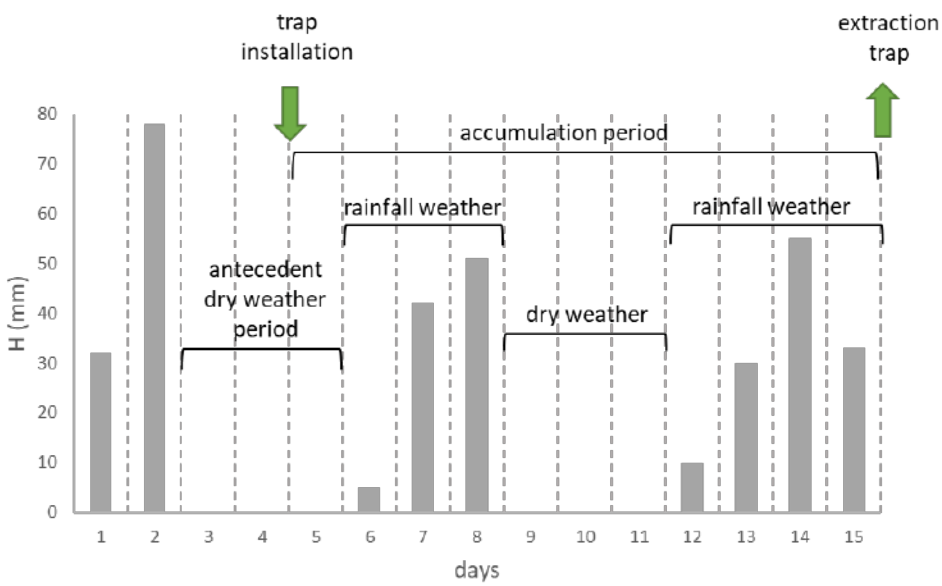

Figure 6 Hydrology characterization

1.4 Rainfall and flow runoff

The rainfall-runoff is calculated using the USDA curve number (CN) method, which estimates the amount of precipitation that becomes runoff depending on the impermeability characteristics of the basin and the antecedent soil saturation conditions: wet - CN I or dry - CN III (USDA, 2004). The study site has a hydrological soil classification of C. Being urban basins with a high impermeability, a CN II = 90 is taken, representing roads with hard surfaces. Equation 3 is used to calculate CN I, and Equation 4 to calculate CN III from CN II.

$$CN(I) = \frac{4.2 * CN(II)}{10 - 0.058 * CN(II)}$$

Equation 3. Curve number I

Source: (USDA, 2004)

$$CN(III) = \frac{23 * CN(II)}{10 + 0.13 * CN(II)}$$

Equation 4. Curve number III
Source: (USDA, 2004)

With the CN estimation is possible to calculate the maximum infiltration capacity (S) in mm using Equation 5, and the runoff coefficient (C) using Equation 6 where H is the total precipitation height in mm.

$$S = 254 * \left(\frac{100}{CN} - 1\right)$$

Equation 5. Maximum infiltration capacity (mm)

$$C = \frac{(H - 0.2S)^2}{H^2 + 0.8HS}$$

Equation 6. Runoff coefficient (dimensionless)

Since there is not flow information for the basins to be studied, the rational method was applied to estimate the average flow of runoff using the average intensity (Equation 7), where Q is the flow in m^3/s, I_{ave} in mm/h, A in the basin area in ha, and K is the conversion factor = 360. The drainage area of MR is 972 m^2, of AR 18592 m^2, and of CW/ST 3776 m^2.

$$Q = \frac{C * I_{ave} * A}{K}$$

Equation 7 Rational method (m^3/s)

1.5 Laboratory analysis

Once the sediments were collected, they are taken to the PUJ water quality laboratory to analyze and obtain information about their physical and chemical composition. The characterization includes particle size distribution (PSD), the common heavy metals (HM) concentrations. In previous analyzes no polycyclic aromatic hydrocarbons (PHAs) were detected, all of them are below the detection limit.

1.5.1 Particle size distribution

PSD is a pollution parameter from diffuse urban sources since it is linked to the adsorption and washing of pollutants and suspended solids (Ma et al., 2018). Smaller particles have higher concentrations of contaminants because these particles have a larger specific surface area, different mineral ratios, and higher organic matter content than larger particles (Gunawardana et al., 2014; Lau & Stenstrom, 2005). On the other hand, according to the Food and Agriculture Organization of the United Nations (FAO), the grain size allows for classifying the type of soil into fines (< 0.075mm), sand (0.075-4.75 mm), gravel (4.75-75 mm), and cobbles (>75 mm) (FAO, n.d.).

PSD is essential in urban runoff sediment mobility, fate, accumulation, and quality. Fine particles are the ones that contribute the most significant contaminant loads and are the ones that move more quickly (Jeong et al., 2020; Q. Wang et al., 2019; X. Zhang et al., 2020). At the same time, larger solids can settle and accumulate in structures, obstructing and affecting aquatic ecosystems (Characklis & Wiesner, 1997).

Urban runoff carries solids, particularly from the road surface. These solids range in size from submicron particles to gravel (Sansalone et al., 1997). The sand fraction was dominant in most cases, followed by mud and gravel (Al-Rubaei et al., 2017). However, there is a significant difference between the content of the dust fractions transported by runoff in the different climatic seasons and land use (Seleznev et al., 2019). Therefore, it is impossible to assume a single PSD profile for a land-use type or drainage area for a watershed because it seems possible to transport a wide range of particle sizes (Charters et al., 2015; Kim & Sansalone, 2008).

A particle size analysis is performed by laser diffraction ranging from 0.1 µm to 1000 µm using the Mastersizer 3000E Particle Size Analyzer (Figure 7). Particle size is calculated from the scattering pattern created when the laser beam passes through a sample (Malvern Panalytical Ltd, 2022). Two analyses are made for each sample; each analysis has five readings.

Figure 7 Malvern Mastersizer 3000E.

1.5.2 Heavy metal concentrations

The simultaneous Atomic Emission Spectrometer Shimadzu ICP-E 9800 (Figure 8) was used to measure HM concentration in sediments, allowing multiple elements to be analyzed simultaneously and rapidly regardless of their concentration levels. In addition, a multiparametric pattern was used to detect 19 metals. For each element, calibration is made through 12 established concentrations from 0.001 mg/L to 10 mg/L. The equipment detects an intensity for each concentration value, and the calibration curves are built. The calibration curves generated for each element make it possible to determine the concentration in each sample. The minimum detection value that is quantified with accuracy and precision for each HM is presented in Table 4.

Table 4 Metal ICP quantification limit in mg/L.

Metal	Quantification limit (mg/L)	Metal	Quantification limit (mg/L)
Al	0.100	**Ni**	0.005
Cd	0.005	**Pb**	0.100
Zn	0.010	**Cu**	0.010
Cr	0.010		

For each sample, two methods are used to analyze the concentration of HM in sediment samples by ICP (Shimadzu, 2020). The first allows estimating the total concentration through microwave-assisted acid digestion of sediments. The second determines the concentration of acid rain leaching through synthetic precipitation. For each analysis, the samples are prepared following the established standard method described below. However, the analysis is carried out under conditions as similar as possible to what the material dredged from the structures would be like, wet and heterogeneous. That is, prior drying or sieving is not carried out. All analyzes were performed in triplicate to avoid bias.

Figure 8 Shimadzu ICP-E 9800.

<u>Total concentration</u>

The Environmental Protection Agency (EPA) method 3051A: microwave-assisted acid digestion is used to prepare solid samples to be analyzed for total HM (EPA., 2007). 0.5 g of material are weighed, and 10.0 ± 0.1 mL of concentrated nitric acid (HNO_3) and 3.0 ± 0.1 mL of concentrated hydrochloric acid (HCl) are added to the container in an extractor hood. The Milestone microwave (Figure 9) is programmed with the following settings: (i) 4 minutes, 90 °C, 800 Watt, (ii) 5 minutes, 130 °C, 800 Watt, (iii) 4 minutes, 190 °C, 800 Watt, (iv) 10 minutes, 190 °C, 800 Watt. Cellulose acetate membrane filters (0.45 µm) are used to eliminate residues. Make up to 100 mL in balloons with deionized water for later analysis in ICP.

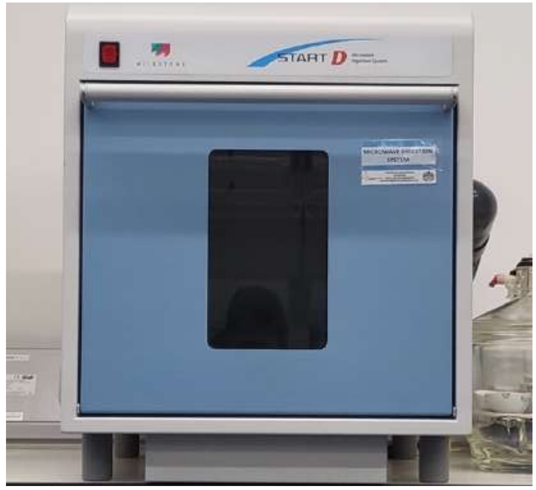

Figure 9 Milestone microwave.

<u>Synthetic precipitation leaching</u>

The EPA method 1312 determines the mobility of inorganic phases present in waste materials in acid conditions caused by acidic rain (EPA., 1994). The extraction fluid must first be prepared by adding a 60/40 weight percent mixture of sulfuric and nitric acids to distilled water until the pH is 4.20 ± 0.05. Next, add 50 g of sediment sample and 500 g of extraction liquid to the container for extraction. The container is secured in the rotary agitator device (Figure 10a) and activated to rotate at 30 ± 2 rpm for 18 ± 2 hours. After extraction, the material is separated into its component solid and liquid phases by filtering through a glass fiber filter. The sample is digested by taking 10 mL of the filtered extract and adding 0.5 mL of ICP grade HNO_3. To preserve the excess filtered extract, bring it to a pH <2 with HNO_3 and preserve it at a temperature of 4 °C. The samples are carried in a thermoreactor CR 3200 (Figure 10b) at 105 °C for 2 hours. Cellulose acetate membrane filters (0.45 μm) are used to eliminate residues for later analysis in ICP.

a. 8 Place Variable-Speed Rotary Agitator *b. Thermoreactor CR 3200*

Figure 10 Equipment for Synthetic Precipitation Leaching

A wide variety of HM has been found in sediments from different urban water bodies. As shown, it is impossible to establish a concentration pattern for any HM. However, it has been found that the concentrations of Cu, Zn, and Pb in urban sediments are closely related to vehicle traffic due to tire and brake wear, which are easily transported by runoff (Choi et al., 2020; Q. Wang et al., 2020; X. Zhang et al., 2020).

Table 5 Heavy metal concentrations measured in sediments from different locations in mg/kg. RDS: Road deposited sediment.

Metal concentration (mg/kg)						Sediment Samples Location
Cd	Pb	Cu	Zn	Cr	Ni	
0.27	34.51	57.47	155.44	207.15	-	RDS[a]
1.74-	199	178	1090	171	19	RDS[b]
1.6	125	191	1029	125	43.1	Storm drain[b]
-	197.30	94.30	329	128.10	72.10	RDS[c]
-	194.60	153.50	472.00	225.70	112.40	RDS[d]
-	412.20	297.20	2652.50	159.80	91.50	Stormwater particles[d]
0.13	5.86	24.20	46.66	-	34.77	Abiete watershed[e]
0.10	5.98	27.80	50.42	-	212.28	Toko watershed[e]
1.50	39.20	-	154.30	-	23.20	Stormwater pond[f]
0.43	39.17	10.66	70.62	29.44	24.05	River coast[g]
6.07	55.95	595.10	-	594.25	-	Top (0-5 cm) Canolly Canal[h]
5.46	36.25	549.45	-	525.35	-	Middle (5-15 cm) Canolly Canal[h]
4.99	40.25	429.30	-	524.70	-	Bottom (15-30 cm) Canolly Canal[h]
1	92	67	212	17	12	Dry sediments road[i]
1	69	134	205	64	33	Runoff sediment road[i]
1.32	88	87	233	21	21	Snow sediment road[i]
-	124.9	69.39	983.43	36.31	23.75	Stormwater sedimentation tank[j]
-	11	64	180	21	-	Surface water bodies in autumn[k]
-	17	20	40	-	-	Surface water bodies in winter[k]
-	589	158	687	129	125	RDS[l]
-	200	120	560	-	160	Urban river[m]
0.70	5.78	55.39	155.20	48.01	26.77	Streams august[r]
0.61	5.71	52.13	97.12	41.18	21.57	Streams december[r]

Source: a(X. Zhang et al., 2020), b(Choi et al., 2020), c(Q. Wang et al., 2020), d(Q. Wang et al., 2019), e(Mandeng et al., 2019), f(Crane, 2019), g(Amor et al., 2019), h(Siddik et al., 2018), i(Pal et al., 2018), j(Sałata & Dąbek, 2017), k(Ignatavicius et al., 2017), l(Zhu et al., 2008), m(Christensen et al., 2006), r (Şimşek et al., 2022).

1.5.3 Sediment accumulation

Sediment accumulation occurs naturally in rivers and lakes due to intensified degradation processes in urbanized river basins (Bhairappanavar et al., 2018). Urban sedimentation constantly occurs through natural processes associated with seasonality, weather conditions, and soil erosion. In addition, anthropic processes such as land excavation and other works are associated with soil and pavement deterioration, tire and brake wear, and oil spills (Sansalone et al., 1997; Seleznev et al., 2019). Sediment accumulate in water bodies until a strong enough water flow moves them to another point downstream or dredged to prevent flooding. This accumulation generates hydraulic and environmental problems, so quantity must be considered an issue of the same importance as quality (Nawrot & Wojciechowska, 2017; Parker et al., 2000; Schroer et al., 2018).

Accumulation increases under poor landscape management and becomes the largest source of water pollution due to the sediment volume in the different urban structures (Seleznev et al., 2019). In addition, sediment in stormwater drainage structures can reduce their capacity, lead to clogging, and require excessive maintenance (Rietveld et al., 2021; Schroer et al., 2018). Usually, the quantity of accumulated sediments is variable and difficult to estimate due to the lack of requirements for their monitoring (Nawrot & Wojciechowska, 2017). The volume of sediments collected in the traps will be measured to analyze the accumulation. The accumulation percentage will be determined with respect to the capacity of the traps used in the accumulation period.

CHAPTER 2 URBAN STORMWATER SEDIMENT CHARACTERIZATION

The data obtained in the previous chapter on daily rain and laboratory analysis were analyzed to obtain different parameters to understand each sampling site's hydrology (section 2.1) and the collected sediments (section 2.2).

2.1 Hydrology and hydraulic characterization

For each sediment sampling period, the hydrological, runoff, and flow variables associated with each basin were estimated. Table 6 shows a fragment of the hydrological variables calculated from the daily rainfall data (See Appendix A for all hydrology characterization).

Table 6 Fragment Molinos River Hydrology Data. H: total precipitation height, I_{ave}: average intensity, I_{max}: maximum intensity, dw: number of days with dry weather, rw: number of days with rainfall weather, ADP: antecedent dry weather period.

Sample	H (mm)	T (days)	dw (days)	rw (days)	ADP (days)	I_{ave} (mm/h)	I_{max} (mm/h)
001-5	169.80	15	4	11	6	0.472	1.263
001-8	84.30	15	6	9	3	0.234	0.883
001-9	11.80	15	9	6	3	0.033	0.233
001-10	30.70	15	8	7	4	0.085	0.554
001-11	46.50	15	8	7	2	0.129	0.871
001-12	24.90	15	10	5	5	0.069	0.504
001-13	75.10	15	8	7	5	0.208	0.879
001-14	2.20	15	13	2	0	0.006	0.050
001-15	3.50	15	12	3	4	0.009	0.066
001-16	155.93	15	4	11	0	0.433	1.651

The CN I and CN III for the conditions mentioned in section 1.4 are 78 and 95, respectively. With this, the runoff coefficient and Q are calculated for each sampling period, as shown in Table 7 for MR (see Appendix A for runoff coefficients and flow rates for AR and CW/ST). The flow estimation depends on hydrology, so there is expected to be a linear relationship between the two variables. Although the contribution of sediments comes from the runoff, for the approach developed in this research the analysis of runoff is not an influential factor. Therefore, hydrology will be used as the primary variable for the analyses.

Table 7 Molinos River Infiltration capacity (S) in mm, Runoff coefficient (C), average flow (Q) in m³/s

Sample	S (mm)	C	Q (m³/s)	Sample	S (mm)	C	Q (m³/s)
001-5	71.64	0.63	0.76	**001-26**	71.64	0.01	0.00
001-8	28.22	0.69	0.41	**001-27**	71.64	0.07	0.01
001-9	13.37	0.31	0.03	**001-31**	71.64	0.61	0.69
001-10	71.64	0.10	0.02	**001-32**	71.64	0.13	0.01
001-11	71.64	0.21	0.07	**001-35**	71.64	0.00	0.00
001-12	71.64	0.05	0.01	**001-36**	71.64	0.00	0.00
001-13	28.22	0.66	0.35	**001-38**	71.64	0.30	0.13
001-14	28.22	0.22	0.00	**001-39**	71.64	0.38	0.21
001-15	71.64	0.55	0.01	**001-42**	71.64	0.09	0.02
001-16	71.64	0.60	0.67	**001-43**	71.64	0.01	0.00
001-17	13.37	0.88	0.81	**001-46**	71.64	0.25	0.09
001-18	13.37	0.36	0.03	**001-47**	13.37	0.87	0.67
001-23	71.64	0.52	0.43				

2.2 Sediment characterization

The characterization of sediments means knowing the physical and chemical properties of the sediments. For this, PSD and HM concentrations are analyzed.

2.2.1 Particle size distribution (PSD)

For a given percentage (10%, 20%, ..., and 100%), the maximum diameter is estimated in which the sample does not exceed said percentage cumulatively. This refers to D10, D20, ..., and D100. Then, the minimum and maximum values and the D median are obtained, excluding outliers. For example, D50 varies as follows: 15 - 307 µm with a median of 117 µm for MR, 2 - 274 µm with a median of 132 µm for AR, and 119 - 143 µm with a median of 1 µm for CW/ST. Figure 11 shows each sampling site's median mass percentage by particle size ranges in µm. Based on grain size, about 40% of the sediments are classified as fine particles and 60% as sand. Therefore, the sediments are expected to have high concentrations of contaminants due to the specific surface area that increases the adsorption capacity (See Appendixix A for all PSD results).

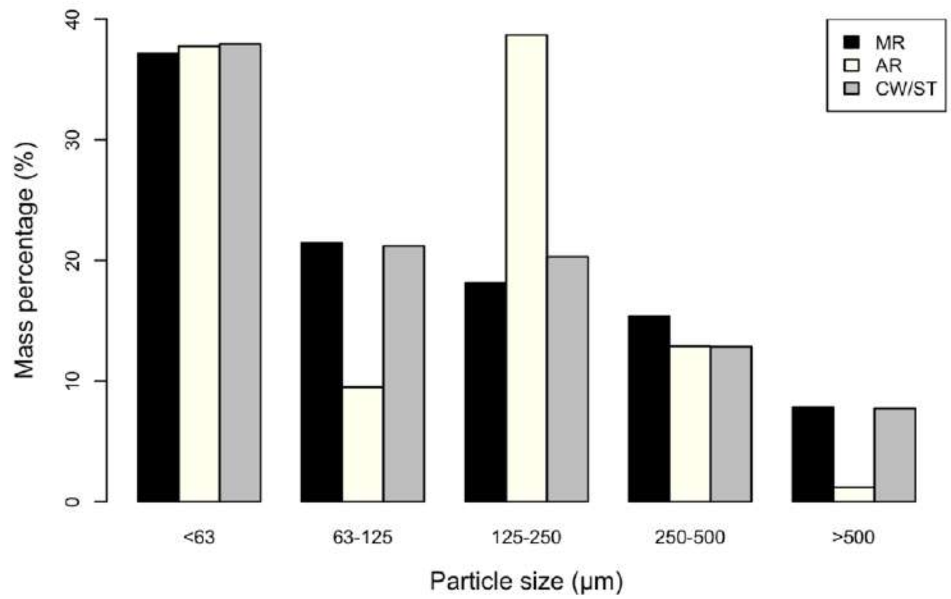

Figure 11 Median mass percentage for each particle size range (µm). Molinos River (MR), Arzobispo River (AR), Constructed-wetland/storage-tank (CW/ST).

When comparing the obtained values with those of other authors, in most cases, the medians are above the reported means in sediments for diverse sources in urban areas. For example, Falco et al., (2020) found a D50 = 27-30 µm for the inflow and 8.68-46 µm for the outflow in a sedimentation tank. Additionally, Rommel et al., (2020) for the particles collected in three locations in Frankfurt, found a D50 variation between 40-63 µm. The most similar results to the obtained in this research are those of Faram et al., (2007), who found a variation of D50 between 7-112 µm on urban roads. However, the medians obtained are below the values presented by Pamuru et al., (2022) on an overview of 77 events in urban watersheds with a D50 = 321 µm and with the one obtained by Wei et al., (2022) for residential areas greater than 500 µm.

For the three sampling sites, about 37% of the particles are in a fraction less than 63 µm. These results partially agree with those found by Zhu et al., (2008) in residential areas and by J. Wang et al., (2021) in commercial and residential zones, who found a variation between 30 and 40% of the total sediment mass for this fraction. The fraction between 250-500 µm represents approximately 14% of the total sample, results that agree with those found for residential and riverside areas by Zhu et al., (2008) and commercial land use by J. Wang et al., (2021).

For MR and CW/ST, the fractions between 63-125 µm and 125-250 µm each represent approximately 20% of the total mass. This result agrees with the results found by Zhu et al., (2008) for heavy traffic, commercial, residential, and riverside park areas. This is also consistent with the results found by Wu et al., (2018) on road and roof surfaces for the 63-125 µm fraction and the 125-250 µm fraction found by Rommel et al., (2020) in RDS. Besides, the fraction higher than 500 µm represents approximately 8% of the mass, which agrees with the 6% mass found in commercial areas by J. Wang et al., (2021) and with Zhu et al., (2008), who found a variation between 5% and 11%.

AR has a different PSD from the other two places, with a mass percentage of around 10%, 39%, and 2% for the fractions 63-125, 125-250, and >500 µm, respectively. Solely, J. Wang et al., (2021) found a similar percentage (9%) for the fraction 63-125 µm.

2.2.2 Heavy metal concentrations by ICP

Metals with the most significant presence in urban environments were selected, which are: cadmium (Cd), chromium (Cr), nickel (Ni), copper (Cu), lead (Pb), and zinc (Zn). With the calibration curves sediment sample's total and soluble HM concentrations were calculated, considering their weight and the volume of reagents used for each sample preparation process (See Appendix A for calibration curves and equations).

Figure 12 shows the variation of the total HM concentration for each site. MR is the one with the lowest concentrations; even for Cd and Cr, no concentrations were found, followed by Pb<Ni<Zn<Cu, with a median concentration of 8.98<17.14<100<570.47 mg/kg, respectively. AR is the one with the highest concentrations except for Cu and Zn, and the total HM was Cd<Cr<Ni<Pb<Zn<Cu with a median concentration of 4.79<5.33<22.34<43.08<114.19<613.66 mg/kg respectively. CW/ST concentrations were Cd<Cr<Ni<Pb<Zn<Cu with a median of 1.66<5.02<20.83<33.6<476.09<818.24 mg/kg, respectively. The high concentrations of Cu and Zn can be attributed to the runoff from the parking area (See Appendix A for all HM concentrations).

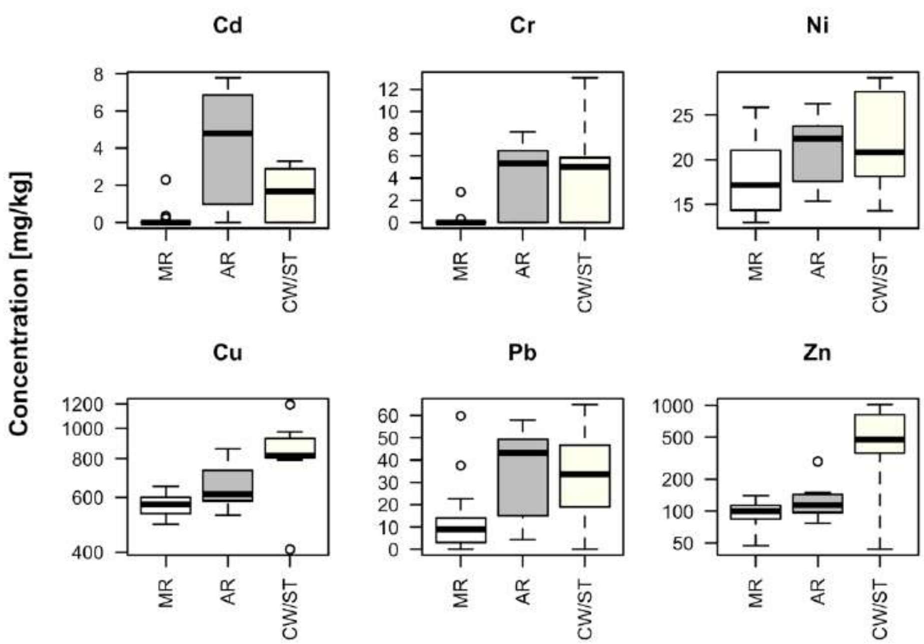

Figure 12 Total heavy metals concentrations in sediments. MR: Molinos River, AR: Arzobispo River, CWST: Constructed wetland storage tank.

Cr measured concentrations are much lower than those found by other researchers (Table 5), contrary to Cu concentrations, which are much higher than those reported by others for the three study cases. The highest concentrations of Cd, Cr, and Cu were found in a canal that receives untreated municipal and industrial discharges. The magnitude range of the Cd concentrations coincides with those measured in the AR and those of Cu in the MR (Siddik et al., 2018).

Table 8 shows the variation between total and soluble concentrations for some samples. For example, the concentrations obtained for the soluble fraction are 0% for Cd and Cr, around 1% for Pb and Zn, and about 5% of the total concentration for Ni and Cu, as shown in Figure 13 (See Appendix A for all HM concentrations). It means that the HM remains in the sediments, making them the top pollutants carriers. Thus, it is inconvenient to consider the soluble fraction to evaluate the pollutant load of HM in an urban stormwater drainage system.

Table 8 Fragment of total and soluble (SPLP) heavy metals concentrations in mg/kg. MR: Molinos River, AR: Arzobispo River, CW/ST: Constructed-wetland/storage-tank (See Appendix A for all concentrations results).

Sample	Site	Cd (mg/kg)		Cr (mg/kg)		Ni (mg/kg)		Cu (mg/kg)		Pb (mg/kg)		Zn (mg/kg)	
		TOT	SPLP	TOT	SPLP	TOT	SPLP	TOT	SPLP	TOT	SPLP	TOT	SPLP
001-5	MR	0.0	0.0	0.0	0.0	20.0	1.0	586.9	34.0	15.8	0.7	47.1	3.1
001-13	MR	0.0	0.0	0.0	0.0	21.1	1.2	650.8	35.2	14.0	0.5	128.9	13.8
001-17	MR	0.0	0.0	0.0	0.0	21.5	1.2	524.6	34.3	11.5	0.8	64.6	7.0
001-28	CW/ST	2.8	0.0	6.6	0.0	27.3	1.0	1192.9	32.4	39.5	0.1	476.1	1.0
001-29	CW/ST	3.3	0.0	13.0	0.0	29.2	1.1	818.2	29.4	64.8	0.2	929.8	1.5
001-34	AR	7.8	0.2	6.8	0.0	26.3	1.2	859.1	31.1	50.1	0.3	149.4	0.7
001-37	AR	6.8	0.0	6.2	0.3	23.9	0.8	669.8	28.5	40.3	0.0	139.2	0.6

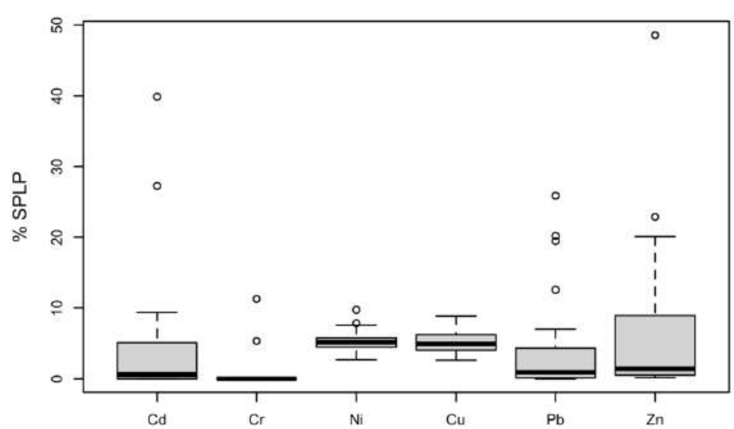

Figure 13 Percentage of soluble (SPLP) concentration to total concentration for each metal.

2.2.3 Sediment accumulation

Sediment accumulation volumes will only be considered for MR because it was the only place with continuous sampling. Therefore, the sediment accumulated volume in traps is divided by the volume of the traps to obtain the sample accumulation percentage. As shown in Table 9, the minimum accumulation is 18%, and the maximum is 93%.

Table 9 Molinos river sediments accumulation volume

Sample	Accum volume (ml)	Trap volume (ml)	Accum (%)	Sample	Accum volume (ml)	Trap volume (ml)	Accum (%)
001-5	70	196.35	35.65%	**001-23**	150	192.00	78.13%
001-8	50	62.83	79.58%	**001-26**	110	287.43	38.27%
001-9	75	345.58	21.70%	**001-27**	100	287.43	34.79%
001-10	55	190.07	28.94%	**001-31**	62	95.43	64.97%
001-11	150	328.61	45.65%	**001-32**	125	287.43	43.49%
001-12	60	328.61	18.26%	**001-35**	120	287.43	41.75%
001-13	170	537.67	31.62%	**001-36**	48	95.43	50.30%
001-14	500	537.61	93.00%	**001-38**	75	287.43	26.09%
001-15	200	410.43	48.73%	**001-39**	180	287.43	62.62%
001-16	80	127.23	62.88%	**001-42**	148	287.43	51.49%
001-17	50	127.23	39.30%	**001-43**	110	287.43	38.27%
001-18	75	127.23	58.95%	**001-46**	200	287.43	69.58%
001-22	40	95.43	41.92%	**001-47**	80	287.43	27.83%

Sediment accumulation assessment is a helpful decision-making tool for urban stormwater management practices, not only from a hydraulic capacity point of view but also considering water quality. Accumulation could be related to the basin's hydrology and the PSD, which allows the establishment of a management tool based on hydrology to decide when it is most appropriate to dredge the stormwater structures.

CONCLUSIONS PART A

Sediment particle size distribution (PSD) shows that the sediments collected in the three sampling points can be classified as fine particles due to the D50 being around 110 µm and the D90 being less than 500 µm. Additionally, approximately 37% of the samples are lower than 63 µm. However, other authors have reported D50 greater than those found in this investigation, and few studies have found coincidences with the relative mass percentage of particles smaller than 63 µm. Being fine particles, the capacity to adsorb contaminants such as heavy metals (HM) increases, implying more significant effects on the environment and the need to establish management tools that promote the capture of these particles at the source to avoid contamination of water bodies.

The heavy metal (HM) concentrations measured in the sediments for the three points show variations between them. Molinos River (MR) is the one with the lowest concentrations, and Arzobispo River (AR) is the one with the highest, except for Cu and Zn, which are higher in constructed-wetland/storage-tank (CW/ST). Additionally, the soluble fraction is a tiny percentage of the total concentrations, which means that the HM remains attached to the particles of the sediments. Thus, the sediments have a high load of HM that affects the stormwater quality since these do not dissolve, and their concentrations tend to magnify. Further investigation is needed to know the relation between land use and HM concentrations to establish their source. Additionally, these concentrations may risk the environment and human health, which is essential to analyze to give more tools for stormwater best management practices.

Understanding the physical and chemical characterization of sediments is essential to determining sources of stormwater pollution. Besides, it provides local authorities with adequate information to implement management practices and reduce environmental and aquatic pollution in urban environments. With the HM concentrations, it is possible to establish the degree of affectation these may generate. For this reason, in PART B of this manuscript, the risk associated with the sediments were analyzed. Information that will be helpful for decision-making regarding managing urban stormwater sediments.

REFERENCES PART A

Al-Rubaei, A. M., Merriman, L. S., III, Hunt, W. F., Viklander, M., Marsalek, J., & Blecken, G. T. (2017). Survey of the operational status of 25 Swedish municipal stormwater management ponds. Journal of Environmental Engineering, 143(6), 05017001. https://doi.org/10.1061/(ASCE) EE.1943-7870.0001203

Amor, R. B., Yahyaoui, A., Abidi, M., Chouba, L., & Gueddari, M. (2019). Bioavailability and Assessment of Metal Contamination in Surface Sediments of Rades-Hamam Lif Coast, around Meliane River (Gulf of Tunis, Tunisia, Mediterranean Sea). Journal of Chemistry, 2019. https://doi.org/10.1155/2019/4284987

Bąk, Ł., Szeląg, B., Sałata, A., & Studziński, J. (2019). Modeling of Heavy Metal (Ni, Mn, Co, Zn, Cu, Pb, and Fe) and PAH Content in Stormwater Sediments Based on Weather and Physico-Geographical Characteristics of the Catchment-Data-Mining Approach. Water, 11(3), 626. https://doi.org/10.3390/w11030626

Bhairappanavar, S., Liu, R., & Coffman, R. (2018). Beneficial uses of dredged material in green infrastructure and living architecture to improve resilience of Lake Erie. Infrastructures, 3(4). https://doi.org/10.3390/infrastructures3040042

Characklis, G. W., & Wiesner, M. R. (1997). Particles, metals, and water quality in runoff from large urban watershed. Journal of Environmental Engineering, 123(8), 753-759.

Charters, F. J., Cochrane, T. A., & O'Sullivan, A. D. (2015). Particle size distribution variance in untreated urban runoff and its implication on treatment selection. Water Research, 85(Supplement C), 337–345. https://doi.org/10.1016/j.watres.2015.08.029

Choi, J. Y., Jeong, H., Choi, K.-Y., Hong, G. H., Yang, D. B., Kim, K., & Ra, K. (2020). Source identification and implications of heavy metals in urban roads for the coastal pollution in a beach town, Busan, Korea. Marine Pollution Bulletin, 161. https://doi.org/10.1016/j.marpolbul.2020.111724

Christensen, A. M., Nakajima, F., & Baun, A. (2006). Toxicity of water and sediment in a small urban river (Store Vejleå, Denmark). Environmental Pollution, 144(2), 621–625. https://doi.org/10.1016/j.envpol.2006.01.032

Crane, J. L. (2019). Distribution, Toxic Potential, and Influence of Land Use on Conventional and Emerging Contaminants in Urban Stormwater Pond Sediments. Archives of Environmental Contamination and Toxicology, 76(2), 265–294. https://doi.org/10.1007/s00244-019-00598-w

EPA., U. S. (1994). SW-846 Test Method 1312: Synthetic Precipitation Leaching Procedure (p. 30).

EPA., U. S. (2007). Method 3051A (SW-846): Microwave Assisted Acid Digestion of Sediments, Sludges, and Oils, (p. 30).

Falco, S., Brunetti, G., Grossi, G., Maiolo, M., Turco, M., & Piro, P. (2020). Solids Removal Efficiency of a Sedimentation Tank in a Peri-Urban Catchment. Sustainability 2020, Vol. 12, Page 7196, 12(17), 7196. https://doi.org/10.3390/SU12177196

FAO. (n.d.). 11. Soil Suitability Classification For Aquaculture. Retrieved October 23, 2022, from https://www.fao.org/fishery/docs/CDrom/FAO_Training/FAO_Training/General/x6706e/x6706e11.htm

Faram, M. G., Iwugo, K. O., & Andoh, R. Y. G. (2007). Characteristics of urban run-off derived sediments captured by proprietary flow-through stormwater interceptors. Water Science and Technology, 56(12), 21–27. https://doi.org/10.2166/wst.2007.747

Gunawardana, C., Egodawatta, P., & Goonetilleke, A. (2014). Role of particle size and composition in metal adsorption by solids deposited on urban road surfaces. Environmental Pollution, 184, 44–53. https://doi.org/10.1016/j.envpol.2013.08.010

IDEAM. (n.d.). Características Climatológicas de Ciudades Principales y Municipios Turísticos. Http://Www.Ideam.Gov.Co/Documents/21021/418894/Caracter%C3%ADsticas+de+Ciudades+Principales+y+Municipios+Tur%C3%ADsticos.Pdf/C3ca90c8-1072-434a-A235-91baee8c73fc.
https://doi.org/10.3176/earth.2017.04

Ignatavicius, G., Valskys, V., Bulskaya, I., Paliulis, D., Zigmontienė, A., & Satkunas, J. (2017). Heavy metal contamination in surface runoff sediments of the urban area of Vilnius, Lithuania. Raskmetallid Vilniuse Linnakeskkonna Pindmise Äravoolu Setendites., 66(1), 13–20. https://doi.org/10.3176/earth.2017.04

Instituto Distrital de Gestión de Riesgos y Cambio Climático. (2022, May 20). Sistema de Alerta Bogotá (SAB). Https://Www.Sire.Gov.Co/Web/Sab/Informacion-Hidrometeorologica.

Jeong, H., Choi, J. Y., Lee, J., Lim, J., & Ra, K. (2020). Heavy metal pollution by road-deposited sediments and its contribution to total suspended solids in rainfall runoff from intensive industrial areas. Environmental Pollution, 265. https://doi.org/10.1016/j.envpol.2020.115028

Kim, J.-Y., & Sansalone, J. J. (2008). Event-based size distributions of particulate matter transported during urban rainfall-runoff events. Water Research, 42(10–11), 2756–2768. https://doi.org/10.1016/j.watres.2008.02.005

Lau, S.-L., & Stenstrom, M. K. (2005). Metals and PAHs adsorbed to street particles. Water Research, 39(17), 4083–4092. https://doi.org/10.1016/j.watres.2005.08.002

Laxmi Mohanta, V., Naz, A., & Kumar Mishra, B. (2020). Distribution of heavy metals in the water, sediments, and fishes from Damodar river basin at steel city, India: a probabilistic risk assessment. Human and Ecological Risk Assessment, 26(2), 406–429. https://doi.org/10.1080/10807039.2018.1511968

Ma, Y., Hao, S., Zhao, H., Fang, J., Zhao, J., & Li, X. (2018). Pollutant transport analysis and source apportionment of the entire non-point source pollution process in separate sewer systems. Chemosphere, 211, 557–565. https://doi.org/10.1016/j.chemosphere.2018.07.184

Ma, Y., He, W., Zhao, H., Zhao, J., Wu, X., Wu, W., Li, X., & Yin, C. (2019). Influence of Low Impact Development practices on urban diffuse pollutant transport process at catchment scale. Journal of Cleaner Production, 213, 357–364. https://doi.org/10.1016/j.jclepro.2018.12.198

Malvern Panalytical Ltd. (2022, September 26). Mastersizer 3000E. https://www.malvernpanalytical.com/en/products/product-range/mastersizer-range/mastersizer-3000e

Mandeng, E. P. B., Bidjeck, L. M. B., Bessa, A. Z. E., Ntomb, Y. D., Wadjou, J. W., Doumo, E. P. E., & Dieudonné, L. B. (2019). Contamination and risk assessment of heavy metals, and uranium of sediments in two watersheds in Abiete-Toko gold district, Southern Cameroon. Heliyon, 5(10). https://doi.org/10.1016/j.heliyon.2019.e02591

Nawrot, N., & Wojciechowska, E. (2017). Review on the quality of sediments from the stormwater drainage system in the urban area. E3S Web of Conferences, 17, 00064. https://doi.org/10.1051/e3sconf/20171700064

Pal, S. K., Wallis, S. G., & Arthur, S. (2018). An assessment of heavy metals pollution potential of road sediment derived from a suburban road network under different weather conditions. Environmental Engineering and Management Journal, 17(8), 1955–1966. https://doi.org/10.30638/EEMJ.2018.195

Pamuru, S. T., Forgione, E., Croft, K., Kjellerup, B. v., & Davis, A. P. (2022). Chemical characterization of urban stormwater: Traditional and emerging contaminants. Science of The Total Environment, 813, 151887. https://doi.org/10.1016/J.SCITOTENV.2021.151887

Parker, J. T. C., Fossum, K. D., & Ingersoll, T. L. (2000). Chemical characteristics of urban stormwater sediments and implications for environmental management, Maricopa County, Arizona. Environmental Management, 26(1), 99–115. https://doi.org/10.1007/s002670010074

Ramirez, L. V. (2017, November 21). Ubicación de la Ciudad. Https://Bogota.Gov.Co/Ubicacion-de-Bogota-Sitios-Turisticos-Vias-y-Alrededores-de-Bogota.

Rietveld, M., Clemens, F., & Langeveld, J. (2021). Monitoring and characterising the solids loading dynamics to drainage systems via gully pots. Urban Water Journal, 18(9), 699–710. https://doi.org/10.1080/1573062X.2021.1925706

Rommel, S. H., Gelhardt, L., Welker, A., & Helmreich, B. (2020). Settling of Road-Deposited Sediment: Influence of Particle Density, Shape, Low Temperatures, and Deicing Salt. Water 2020, Vol. 12, Page 3126, 12(11), 3126. https://doi.org/10.3390/W12113126

Sałata, A., Bak, L., & Górski, J. (2019). Ecological risk assessment of chemical contaminants in stormwater sediments. E3S Web of Conferences, 86. https://doi.org/10.1051/e3sconf/20198600017

Sałata, A., & Dąbek, L. (2017). Methods of assessment of stormwater sediments quality. E3S Web of Conferences, 17. https://doi.org/10.1051/e3sconf/20171700080

Sansalone, J. J., Buchberger, S. G., Koran, J. M., & Smithson, J. A. (1997). Relationship between particle size distribution and specific surface area of urban roadway stormwater solids. Transportation Research Record, 1601(1), 95–108.

Schroer, W. F., Benitez-Nelson, C. R., Smith, E. M., & Ziolkowski, L. A. (2018). Drivers of Sediment Accumulation and Nutrient Burial in Coastal Stormwater Detention Ponds, South Carolina, USA. Ecosystems, 21(6), 1118–1138. https://doi.org/10.1007/s10021-017-0207-z

Secretaría de Ambiente. (2021). DESCRIPCIÓN Y CONTEXTO DE LAS CUENCAS HÍDRICAS DEL DISTRITO CAPITAL (TORCA, SALITRE, FUCHA Y TUNJUELO).

Seleznev, A., Yarmoshenko, I., Malinovsky, G., Kiseleva, D., Ilgasheva, E., Ryanskaya, A., & Teterin, A. (2019). Surface stormwater runoff in the formation of contemporary urban surface deposited sediments. E3S Web of Conferences, 98, 07028. https://doi.org/10.1051/e3sconf/20199807028

Shimadzu. (2020). ICPE-9800 Series (p. 20). https://www.shimadzu.com/an/products/elemental-analysis/inductively-coupled-plasma-emission-spectroscopy/icpe-9800-series/index.html

Shojaeezadeh, S. A., Nikoo, M. R., Mirchi, A., Mallakpour, I., AghaKouchak, A., & Sadegh, M. (2020). Probabilistic hazard assessment of contaminated sediment in rivers. Science of the Total Environment, 703. https://doi.org/10.1016/j.scitotenv.2019.134875

Siddik, A. M., Chand, A., Varghese, G. K., & Alappat, B. J. (2018). Assessment of trace metal contamination and its anthropogenic influence in the sediments of an urban water body in Kozhikode, Kerala, India. Environmental Forensics, 19(4), 288–297. https://doi.org/10.1080/15275922.2018.1519737

Şimşek, A., Özkoç, H. B., & Bakan, G. (2022). Environmental, ecological and human health risk assessment of heavy metals in sediments at Samsun-Tekkeköy, North of Turkey. Environmental Science and Pollution Research, 29(2), 2009–2023. https://doi.org/10.1007/S11356-021-15746-W/TABLES/12

Thomas, S., & Ridd, P. v. (2004). Review of methods to measure short time scale sediment accumulation. Marine Geology, 207(1–4), 95–114. https://doi.org/10.1016/j.margeo.2004.03.011

USDA. (2004). Appendixix I: USDA/SCS curve number method for estimating daily runoff. https://hrsl.ba.ars.usda.gov/SPAW/Appendixices/AppendixixI.htm

Wang, J., Qin, M., Huang, T., Tu, N., & Li, B. (2021). Particle size distribution and pollutant dissolution characteristics of road-deposited sediment in different land-use districts: a case study of Beijing. Environmental Science and Pollution Research, 28(29), 38497–38505. https://doi.org/10.1007/S11356-021-13426-3/FIGURES/4

Wang, Q., Zhang, Q., Dzakpasu, M., Chang, N., & Wang, X. (2019). Transferral of HMs pollution from road-deposited sediments to stormwater runoff during transport processes. FRONTIERS OF ENVIRONMENTAL SCIENCE & ENGINEERING, 13(1). https://doi.org/10.1007/s11783-019-1091-x

Wang, Q., Zhang, Q., Wang, X. C., Huang, J., & Ge, Y. (2020). Impacts of key factors on heavy metal accumulation in urban road-deposited sediments (RDS): Implications for RDS management. Chemosphere, 261. https://doi.org/10.1016/j.chemosphere.2020.127786

Wei, H., Muthanna, T. M., Lundy, L., & Viklander, M. (2022). An evaluation of temporal changes in physicochemical properties of gully pot sediments. Environmental Science and Pollution Research, 1, 1–14. https://doi.org/10.1007/S11356-022-20341-8/TABLES/3

Wiest, L., Baudot, R., Lafay, F., Bonjour, E., Becouze-Lareure, C., Aubin, J.-B., Jame, P., Barraud, S., Kouyi, G. L., Sébastian, C., Sébastian, C., & Vulliet, E. (2018). Priority substances in accumulated sediments in a stormwater detention basin from an industrial area. Environmental Pollution, 243, 1669–1678. https://doi.org/10.1016/j.envpol.2018.09.138

Wijesiri, B., Egodawatta, P., McGree, J., & Goonetilleke, A. (2016). Understanding the uncertainty associated with particle-bound pollutant build-up and wash-off: A critical review. Water Research, 101, 582–596. https://doi.org/10.1016/j.watres.2016.06.013

Wu, X., Yu, J., Qiu, H., & Fang, H. (2018). Pollution and ecological risk assessment of nutrients associated with deposited sediments collected from roof and road surfaces. Environmental Science and Pollution Research, 25(9), 8943–8950. https://doi.org/10.1007/s11356-017-1132-6

Yun, X., Yang, Y., Liu, M., & Wang, J. (2015). Concentrations and risk assessment of polychlorinated biphenyls and polybrominated diphenyl ethers in surface sediments from the East Lake, China. Ecotoxicology, 24(1), 172–180. https://doi.org/10.1007/s10646-014-1370-z

Zhang, J., Hua, P., & Krebs, P. (2017a). Influences of land use and antecedent dry-weather period on pollution level and ecological risk of heavy metals in road-deposited sediment. Environmental Pollution, 228, 158–168. https://doi.org/10.1016/j.envpol.2017.05.029

Zhang, X., Wang, Y., Guo, S., Li, H., Liu, J., Zhang, Z., Yan, L., Tan, C., Yang, Z., & Guo, X. (2020). Concentration and speciation of trace metals and metalloids from road-deposited sediments in urban and rural areas of Beijing, China. Journal of Soils and Sediments, 20(9), 3487–3501. https://doi.org/10.1007/s11368-020-02702-3

Zhao, H., & Li, X. (2013). Understanding the relationship between heavy metals in road-deposited sediments and washoff particles in urban stormwater using simulated rainfall. Journal of Hazardous Materials, 246–247, 267–276. https://doi.org/10.1016/j.jhazmat.2012.12.035

Zhu, W., Bian, B., & Li, L. (2008). Heavy metal contamination of road-deposited sediments in a medium size city of China. Environmental Monitoring and Assessment, 147(1–3), 171–181. https://doi.org/10.1007/s10661-007-0108-2

PART B: SEDIMENT POLLUTION

INTRODUCTION PART B

Pollutants in urban areas occur through their attachment to fine-grained sediments. In urban environments, particles are transported by runoff and accumulate in low-energy places in drainage structures, evidencing an increase associated with sediment quantity and rainfall (Chang et al., 2019). Road-deposited sediments (RDS) are the predominant source of particles with high concentrations of pollutants carried by runoff into the urban drainage system during a storm, associated with cars, pavement, fences, and roads (Choi et al., 2020; Q. Wang et al., 2019; X. Zhang et al., 2020). Another essential pollutant source is related to particles washed from rooftops, releasing enormous amounts of all the most critical elements like Pb and Zn (Casey et al., 2007; Van Metre & Mahler, 2003).

During rainfall events, part of the harmful elements in the sediment may be dissolved, desorbed, and transported by stormwater, and thus contribute to stormwater pollution because of chemical, biochemical, and mechanical processes, also influenced by rainfall characteristics, antecedent weather conditions and land use (Sałata et al., 2019; Q. Wang et al., 2019; Wijesiri et al., 2016). In addition, adsorption, desorption, and leaching of contaminants into sediments vary according to water quality parameters such as pH, temperature, specific conductivity, and hardness, additionally to sediment's high atomic weight and density (Laxmi Mohanta et al., 2020; Shojaeezadeh et al., 2020).

Contaminated sediments can represent a risk for the organisms that inhabit them because they tend to accumulate pollutants and transfer them along the food chain, causing adverse effects at various levels (Yun et al., 2015). Heavy metals (HM) are one of the most dangerous pollutants in aquatic environments. They are among the primary pollutants in urban watersheds because they are divided into several environmental components: water, suspended solids, biota, and sediments (Ignatavicius et al., 2017; Siddik et al., 2018). For that reason, much consideration has been paid to sediment pollution by HM worldwide in the last few decades (Saleem et al., 2018). Some HMs are essential to life and play vital roles as a source of vitamins and minerals in the functioning of the organism, though most of them become toxic at higher concentrations, while others are often neither toxic nor essential (Karna et al., 2017; Laino-Guanes et al., 2015; Nawrot et al., 2020). HM are enriched in urban environments, leading to their concentration values exceeding the background values (Parker et al., 2000; Sébastian et al., 2014; X. Zhang et al., 2020). HM pollution can become a much more genuine problem as these pollutants are non-biodegradable and prevail in soil and sediment from where they are gradually released into water bodies and accumulate in plants, animals, and humans (Karna et al., 2017; Laxmi Mohanta et al., 2020; Saleem et al., 2018; Sivalingam et al., 2021).

PART B presents the evaluation of the environmental and human health risk associated with the sediments collected from the three urban drainage structures described in section 1.1. The risk assessment is determined by the total HM concentrations measured in the sediments (see section 2.2.2).

CHAPTER 3 POLLUTION ASSESSMENT METHODS

Urban stormwater sediments are associated with environmental pollution. In some countries, quality criteria and standards have been implemented to reduce the risk of contaminated sediments for biota and human health, including natural compounds and hazardous chemicals that do not meet applicable standards (Arakel, 1995). Determination of the sediment's quality from the stormwater drainage system and its effects on the natural environment is frequently performed based on evaluating the contamination degree (Sałata et al., 2019) as tools for proper sediment management (L. Y. Li et al., 2009). Section 3.1 presents the standards used to assess the criticality of heavy metal concentrations associated with the sediments studied in this thesis.

Pollutant accumulation on impervious urban surfaces such as roads, driveways, and roofs during dry weather periods is called pollutant build-up (Wijesiri et al., 2016). Knowledge of the concentrations of contaminants attached to the sediments is essential to assess their toxicity and their potential to affect water quality since they can represent a severe ecological risk (Ignatavicius et al., 2017; Karlavičienė et al., 2009). In addition, long-term monitoring of sediments provides critical information on temporal trends of pollution in waterways, thereby improving the risk assessment process (Sharley et al., 2016). Sections 3.2 and 3.3 present the methodologies used to assess the environmental and human health risks.

3.1 Sediment quality guidelines (SQG)

Sediment quality guidelines (SQGs) were developed to protect the aquatic fauna and surface water quality from sediment-bound contaminants and prioritize chemicals of interest (Sharley et al., 2016; Y. Zhang et al., 2021). Moreover, they are a helpful tool for researchers and administrators, which, when combined with risk indices, appropriately evaluate the quality standards of sediments and design sediment quality goals which are used to assess the risk caused by the presence of PHAs and HM (Nawrot & Wojciechowska, 2017). However, properly implementing an SQG can be daunting for sediment management assessors because there is currently limited guidance on recommended uses. For example, limit concentrations established in different SGGs can differ by several orders of magnitude for the same substance (MacDonald et al., 2000). Therefore, these guidelines are used to (i) assess sediment pollution by associating the measured concentration levels with the matching guidelines; (ii) evaluate the influence of pollutants on the aquatic biota (Saleem et al., 2018).

In general, SQG establishes two limits: threshold effect concentration (TEC), below which no adverse effects are expected to occur, and probable effect concentration (PEC), above which adverse effects will occur more frequently (Sharley et al., 2016, 2017; Yun et al., 2015). Table 10 shows the limit concentrations of HM mentioned in section 2.2.2 for the two thresholds mentioned above, compiled by MacDonald et al., (2000), from different SQGs.

Table 10 Heavy metals sediment quality guidelines. Threshold effect concentration (TEC) and probable effect concentration (PEC).

Substance	TEC	PEC
HM (mg/kg)		
Cd	0.99	4.98
Cr	43.40	111.00
Cu	31.60	149.00
Pb	35.80	128.00
Ni	22.70	48.60
Zn	121.00	459.00

Source: Adapted from (MacDonald et al., 2000)

Some researchers have found in different water bodies that HMs exceed PEC, suggesting the possibility of widespread toxicity from these contaminants, which may have adverse biological effects (Al-Rubaei et al., 2017; Nawrot & Wojciechowska, 2017; Sharley et al., 2017). These concentrations also vary according to the local area and weather conditions (Scoggins et al., 2007; Yun et al., 2015).

3.2 Environmental assessment methods

Given the impact on aquatic ecosystems associated with urban runoff drains, evaluating the potential risks caused by pollutants such as HM and human activities' influence on these pollutants' concentrations is necessary. Different sediment quality indices have been proposed to assess HM contamination and their toxicity evolution in river sediments, RDS, and wetland sediments (Ali et al., 2022; Amor et al., 2019; Shojaeezadeh et al., 2020; Q. Wang et al., 2019). Two or more methods should be applied to improve the precision of the risk assessment (Zhan et al., 2020).

3.2.1 Geo-accumulation index

The geo-accumulation index (I_{geo}) analyzes natural fluctuations in the content of a given substance in the environment (Barbieri, 2016) and highlights the influences of anthropogenic activities. I_{geo} is calculated using Equation 8 initially proposed by (Müller, 1979), to determine the pollution in aquatic bottom sediments. Where Cn is the measured HM concentration (mg/kg), Bn is the geochemical background value (mg/kg), and factor 1.5 represents natural fluctuations influenced by anthropogenic activities (Laxmi Mohanta et al., 2020; Sałata & Dąbek, 2017). In the search for information, no reports of Bn values were found for the study area or the region. Although there are some data on the Bn values in the coastal region of a country, these will not represent the behavior of the study area and will not report the Bn concentrations for all the HM studied in this research. Due to the lack of information, the global average concentrations in soils reported by Rauch & Pacyna, 2009 will be used: Cd = 0.5 mg/kg, Cr = 130 mg/kg, Ni = 25 mg/kg, Cu = 39 mg/kg, Pb = 27 mg/kg, and Zn = 48 mg/kg. The risk classification according to the I_{geo} is shown in Table 11.

$$I_{geo} = log_2\left(\frac{C_n}{1.5 * B_n}\right)$$

Equation 8. Geo-accumulation index (I_{geo})

Table 11. Geo-accumulation index (I_{geo}) classification

G0	unpolluted environment	$I_{geo} \leq 0$
G1	weakly polluted	$0 < I_{geo} \leq 1$
G2	moderately polluted	$1 < I_{geo} \leq 2$
G3	moderately to heavily polluted	$2 < I_{geo} \leq 3$
G4	heavily polluted	$3 < I_{geo} \leq 4$
G5	heavily to extremely polluted	$4 < I_{geo} \leq 5$
G6	extremely polluted	$I_{geo} > 5$

Source: (Laxmi Mohanta et al., 2020)

Table 12 presents the results of the evaluation of the I_{geo} determined by other authors in sediments collected from different sources, such as roads, and watersheds, among others. The table shows that the sediments with the highest risk come from places with human intervention.

Table 12. Geo-accumulation index (I_{geo}). Road deposited sediments (RDS). G0: unpolluted environment, G1: unpolluted to moderately polluted, G2: moderately polluted, G3: moderately to heavily polluted, G4: heavily polluted, G5: heavily to extremely polluted, G6: extremely polluted

I_{geo}						Sediment Samples Location
Cu	Cd	Cr	Pb	Zn	Ni	
G0	G0	G1	G1	G2	-	Tropical Freshwater Lakes[a]
G0	G1	G0	G0	G0	-	RDS[b]
G2	-	G1	G3	G3	G2	RDS[c]
G3	-	G1	G3	G5	G1	Stormwater particles[c]
G0	G0	-	G0	G0	G0	Abiete watershed[d]
G0	G0	-	G0	G0	G0	Toko watershed[d]
G2	G3	G3	G3	G4	G3	lif coast[e]
G3	G0	G3	G3	G4	G2	Stormwater sedimentation tank[f]
G0	G0	G0	G0	G0	-	Haizhou Bay[g]
G0	G0-G3	-	G0	G0	G0	River[h]
-	G0	G0	G0	-	-	Urban river in summer[i]
-	G1	G0	G0	-	-	Urban river in winter[i]

Source: a (Sivalingam et al., 2021), b (X. Zhang et al., 2020), c (Wang et al., 2019), d (Mandeng et al., 2019), e (Amor et al., 2019), f (Sałata & Dąbek, 2017), g (Liu et al., 2021), h (Arisekar et al., 2022), I (Ali et al., 2022).

3.2.2 Enrichment factor

The enrichment factor (EF) helps establish the HM's natural or anthropogenic sources using Equation 9. EF is the normalization of an HM concentration concerning a reference element (Choi et al., 2020; X. Zhang et al., 2020). Al is commonly used as indicator element (Joshi et al., 2009). Where Cn and Bn are the same as in Equation 8, C_{AL} and B_{AL} are the aluminum measured, and the mean background earth's concentration in soils = 62000 μm/g (Rauch & Pacyna, 2009). The EF is generally classified into five categories, described in Table 13.

$$EF = \frac{C_n/C_{Al}}{B_n/B_{Al}}$$

Equation 9. Enrichment factor (EF)

Table 13. Enrichment factor (EF) classification.

No	deficiency to minimal enrichment	EF<1
M	moderate enrichment	1<EF<5
S	significant enrichment	5<EF<20
VH	very high enrichment	20<EF<40
E	extreme enrichment	EF>40

Source: (Choi et al., 2020)

Table 14 shows the EF evaluation carried out by other authors, and there is no evidence of heavy metal enrichment in the sediments from natural water bodies. In environments with significant anthropogenic influence, the enrichment level reaches a very high enrichment by Cu, Ni, Pb, and Zn and an extreme enrichment by Cd and Cr.

Table 14. Enrichment factor (EF) results. Road deposited sediments (RDS). No: deficiency to minimal enrichment, M: moderate enrichment, S: significant enrichment, VH: very high enrichment, E: extreme enrichment

EF						Sediment Samples Location
Cu	**Cd**	**Cr**	**Pb**	**Zn**	**Ni**	
No	No	No	No	No	-	Tropical Freshwater Lakes[a]
M	S	M	M	M	-	RDS[b]
VH	S	S	S	VH	M	Storm Drain[c]
M	S	M	M	M	-	RDS[d]
S	M	-	M	M	M	Abiete watershed[e]
S	M	-	M	M	VH	Toko watershed[e]
S	No	S	S	S	S	Stormwater sedimentation tank[f]
No	No	No	No	No	No	River[g]
-	E	E	VH	-	-	Urban river in summer[h]
-	E	E	VH	-	-	Urban river in winter[h]
M	M	S	M	M	S	Coastal[i]

Source: a (Sivalingam et al., 2021),*b* (X. Zhang et al., 2020), *c* (Choi et al., 2020), *d* (Q. Wang et al., 2019), *e* (Mandeng et al., 2019), *f (Sałata & Dąbek, 2017), g* (Arisekar et al., 2022), *h*(Ali et al., 2022), *i* (Jahromi et al., 2021)

3.2.3 Pollution index

The pollution index (PI), also known as the degree of contamination or contamination factor, is the ratio of the HM concentration to their background concentration. It is calculated using Equation 10, where Cn and Bn are the same as for Equation 8 (Laxmi Mohanta et al., 2020; Pal et al., 2018). The risk classification by PI is shown in Table 15.

$$PI = \frac{C_n}{B_n}$$

Equation 10. Pollution load index (PI)

Table 15. Pollution load index (PI) classification.

Low	low level of pollution	PI≤1
Med	medium level of pollution	1<PI≤3
High	high level of pollution	PI > 3

Source: (Laxmi Mohanta et al., 2020)

Table 16 presents the PI results in sediments collected from different sources.

Table 16. Pollution index results. Road deposited sediments (RDS). L: low level of pollution, M: medium level of pollution, H: high level of pollution.

PI						Sediment Samples Location
Cu	Cd	Cr	Pb	Zn	Ni	
L-M	L-H	L	L	L	L	River[a]
-	M	L	L	-	-	Urban river in summer[b]
-	M	L	L	-	-	Urban river in winter[b]
L	L	L	L	L	L	Coastal[c]

Source: a (Arisekar et al., 2022)*, b* (Ali et al., 2022)*, c* (Jahromi et al., 2021)

3.2.4 Modified pollution index

To interpret the contamination by different HM instead of one by one Brady et al., (2015) proposed the modified pollution index (MPI) based on the EF. With this, the background concentrations and the complex and non-conservative behavior of the sediments are considered (Jahromi et al., 2021). It is calculated using Equation 11 and is classified into six categories, as shown in Table 17. It is possible to use the same classification of EF as a basis for sediment quality (Brady et al., 2015; Jahromi et al., 2021).

$$MPI = \sqrt{\frac{EFaverage^2 + EFmax^2}{2}}$$

Equation 11. Modified Pollution index (MPI)

Table 17. Modified Pollution index (MPI).

No	unpolluted	MPI < 1
S	Slightly polluted	1< MPI ≤2
M	moderately unpolluted	2< MPI ≤3
MH	moderately to heavy polluted	3< MPI ≤5
H	heavily polluted	5< MPI ≤10
E	severely polluted	MPI>10

3.2.5 Potential ecological risk

The potential ecological risk index (RI) represents the sensitivity of the biological community to toxic substances (Pal et al., 2018; Q. Wang et al., 2019; Zhao & Li, 2013b). RI is calculated using Equation 12 proposed by Hakanson, (1980), where Cn and Bn are the same as for Equation 8, and Trn is the toxic metal response (Mandeng et al., 2019; Nawrot et al., 2020). Trn suggested for Cr, Ni, Cu, Cd, Pb, and Zn are 2, 6, 5, 30, 5, and 1, respectively (Zhao & Li, 2013b). The RI is generally classified into four categories, described in Table 18.

$$RI = \sum_{i=1}^{m} Tr_n^i \times \frac{C_n^i}{B_n^i}$$

Equation 12. Potential ecological risk index (RI)

Table 18. Potential ecological risk index (RI) classification.

G0	low ecological risk	RI≤150
G1	moderate ecological risk	150<RI≤300
G2	considerable ecological risk	300<RI≤600
G3	very high ecological risk	RI≥600

Source: (Nawrot et al., 2020)

As stated by different authors summarized in Table 19 the more significant ecological risk is associated with stormwater sediments. However, other classifications are found in each investigation, which makes it difficult to establish a contamination pattern.

Table 19. Ecological risk index (RI). RDS: road deposited sediments. G0: low ecological risk, G1: moderate ecological risk, G2: considerable ecological risk, G3: very high ecological risk.

RI	Sample location
G0	Haizhou Bay[a]
G0-G1	RDS[b]
G1-G2	RDS[c]
G1-G3	Stormwater particles[c]
G2	Abiete watershed[d]
G3	Toko watershed[d]
G2	Lif coast[e]
G0-G1	River[f]
G0	Urban river in summer[g]
G0	Urban river in winter[g]

Source: a (Liu et al., 2021), b (X. Zhang et al., 2020), c (Wang et al., 2019), d (Mandeng et al., 2019), e (Amor et al., 2019), f (Arisekar et al., 2022), g (Ali et al., 2022)

3.2.6 Modified potential ecological risk

Modified ecological risk index (MRI) is a variation of RI to assess the contamination degree at a specific site using EF (Jahromi et al., 2021), calculated using Equation 12. MRI risk classification is shown in Table 20

$$MRI = \sum_{i=1}^{m} Tr_n^i \times \text{EF}$$

Equation 13. Modified ecological risk index (MRI)

Table 20. Modified ecological risk index (MRI) classification.

L	low ecological risk	MRI≤150
M	moderate ecological risk	150<MRI≤300
C	considerable ecological risk	300<MRI≤600
VH	very high ecological risk	MRI>600

3.2.7 Pollution load index

The pollution load index (PLI) is used to assess the cumulative pollution level of HM in sediments. It is calculated using Equation 14, where Cn and Bn are the same as for Equation 8, and is classified into seven categories, as shown in Table 21 (Choi et al., 2020; Mandeng et al., 2019; Saleem et al., 2018)

$$PLI = \sqrt[n]{{C_1}/{B_1} \times {C_2}/{B_2} \times \dots {C_n}/{B_n}}$$

Equation 14. Pollution load index (PLI)

Table 21. Pollution load index (PLI).

Back	Background concentration	PLI = 0
Unp	unpolluted	0<PLI≤1
M-Unp	moderately to unpolluted	1<PLI≤2
M-Poll	moderately to polluted	2<PLI≤3
M-High	moderately to highly polluted	3<PLI≤4
High	highly polluted	4<PLI≤5
VH	very highly polluted	PLI > 5

Source: (Choi et al., 2020)

Only a few researchers have analyzed the PLI sediments, especially in natural water bodies, finding variations between unpolluted and moderately polluted (Table 22).

Table 22. Pollution load index (PLI). Bn: background concentration, No: unpolluted, MN: moderately to unpolluted, MP: moderately to polluted, MH: moderately to highly polluted, H: highly polluted, VH: very high polluted

PLI	Sample location
MN-MP	Lif coast[a]
No	River[b]
No	Urban river in summer[c]
No-MN	Urban river in winter[c]

Source: a (Amor et al., 2019)*, b* (Arisekar et al., 2022)*, c* (Ali et al., 2022)

3.3 Human health risk assessment methods

The human health risk assessment is based on the mean lifetime average daily dose (ADD) of inadvertent human exposure for children and adults populations to sediment through three different pathways: ingestion of contaminated food or water (Equation 15), dermal contact (Equation 16), and inhalation (Equation 17) using the EPA RAGS methodology of carcinogenic HM (Cd, Cr, Ni) and non-carcinogenic HM (Cu, Pb, Zn) (Kumar et al., 2020; Nawrot et al., 2020; US EPA, 1989). Therefore, it is crucial to establish the degree of affectation by different pathways in humans by the contaminated sediments since local social conditions.

$$ADD_{ing} = C_n \times \frac{IngR * Ef * ED}{BW * AT} \times 10^{-6}$$

Equation 15. Human health risk by ingestion ($mg*kg^{-1}*d^{-1}$)

Where Cn is the mean concentration in the analyzed sample (mg/kg); $IngR$ is the ingestion rate for adults = 100mg/d, for children = 200mg/d; Ef is the exposure frequency = 350days/year; ED is the exposure duration for adults =30 years, for children = 6years; BW is the body weight of exposed individual for adults = 60kg, for children 15kg; and AT is the average time for non-carcinogenic pollutants = 10950 days, for carcinogenic pollutants = 28105, for children = 2190 (Nawrot et al., 2020).

$$ADD_{dermal} = C_n \times \frac{SA * SAF * ABF * Ef * ED}{BW * AT} \times 10^{-6}$$

*Equation 16. Human health risk by dermal contact (mg*kg^{-1}*d^{-1})*

Where Cn, Ef, ED, BW, and AT are the same as in the Equation 15; SA is the exposed skin surface area for adults = 5700 cm^2, for children = 2800 cm^2; and SAF is the skin adherence factor for adults = 0.07 mg/(cm^2*h), for children = 0.02; and ABF is the dermal absorption factor = 0.001 (Nawrot et al., 2020).

$$ADD_{inh} = C_m \times \frac{InhR * Ef * ED}{PEF * BW * AT} \times 10^{-6}$$

*Equation 17. Human health risk by inhalation (mg*kg^{-1}*d^{-1})*

Where Cm, Ef, ED, BW, and AT are the same as in Equation 15; $InhR$ is the inhalation rate for adults = 12.8 m^3/day, for children = 7.63 m^3/day; and PEF is the particle emission factor = 1.36*10^9 m^3/kg (Nawrot et al., 2020).

The hazard quotient (HQ) is the health risk associated with non-carcinogenic HM for each pathway, calculated using Equation 18. The hazard index (HI) is the sum of HQ for all paths, which represents the total potential threat from non-cancer pollutants and is calculated using Equation 19. HQ and HI values greater than 1 represent a threat to health due to the adverse effects of HM (Kumar et al., 2020; Şimşek et al., 2022).

$$HQ = \frac{ADD}{RfD}$$

Equation 18. Hazard quotients (HQ) for non-carcinogenic HM

where ADD (mg*kg^{-1}*d^{-1}) is calculated using equations 8 to 10, and RfD (mg*kg^{-1}*d^{-1}) is the reference dose for each pathway. RfD Ingestion: Cu = 0.04, Pb = 0.0035, Zn = 0.3. RfD dermal: Cu = 0.012, Pb = 0.000525, Zn = 0.06. RfD inhalation: Cu = 0.04, Pb = 0.0035, Zn = 0.3 (Nawrot et al., 2020).

$$HI = HQ_1 + HQ_2 + \cdots + HQ_n$$

Equation 19. Hazard index (HI) for non-carcinogenic HM

The carcinogenic risk (CR) estimates the probability of developing cancer in humans. It is calculated with the ADD and a constant factor (SF) for each substance (Equation 20). The total cancer risk (TCR) is the sum of the CR for all HMs on each pathway and all paths (Equation *21*).

A tolerable risk of cancer is expected when the CR varies between 10^{-6} and 10^{-4}, and a high risk of developing cancer when the CR is greater than 10^{-4} (Nawrot et al., 2020; US EPA, 1989).

$$CR = ADD * SF$$

Equation 20. Carcinogenic Risk (CR)

where ADD is the daily intake of carcinogens ($mg*kg^{-1}*d^{-1}$) and SF is the slope factor of hazardous substances ($mg*kg^{-1}*d^{-1}$): Cd = 6.3, Cr = 42, Ni = 0.84 (Nawrot et al., 2020).

$$TCR = \sum CR_{Path}$$

$$CR_{path} = \sum CR_{HM}$$

Equation 21. Total Carcinogenic Risk (TCR)

CHAPTER 4 SEDIMENT RISK ASSESSMENT

As a tool for decision-making on sediments, the methodologies described in CHAPTER 3 were used to assess the risk of the sediments collected in the Molinos River (MR), the Arzobispo River (AR), and the constructed-wetland/storage tank (CW/ST) described in section 1.1. Section 4.1 compares the HM concentrations measured in the sediments with the thresholds determined for the SQG. Section 4.2 show the results of the risk evaluation to the environment by HM, and section 4.3 the possible effects that HM concentrations in sediments can generate on human health.

4.1 Risk assessment by sediment quality guidelines thresholds

As a tool to assess the risk to aquatic fauna derived from sediments contaminated by HM, the total concentrations measured in sediments from the three sampling points were compared with the established limit values (Table 10) (See Appendix A for all HM concentrations). As shown in Figure 14, no adverse effects are expected from Cr, while Cu will adversely affect the fauna interacting with sediments from the three sampling sites. Due to the Ni concentrations, 96%, 62.5%, and 57.1% of the samples collected from MR, AR, and CW/ST are below TEC. Besides, 25% for Zn and 50% for Cd are below the TEC for RA samples. Regarding Pb, 8% of the RM, 42.9% of the CW/ST, and 62.5% of the RA are between TEC and PEC. PEC was found in 50% of the RA samples by Cd and in 57.1% of the CW/ST samples by Zn.

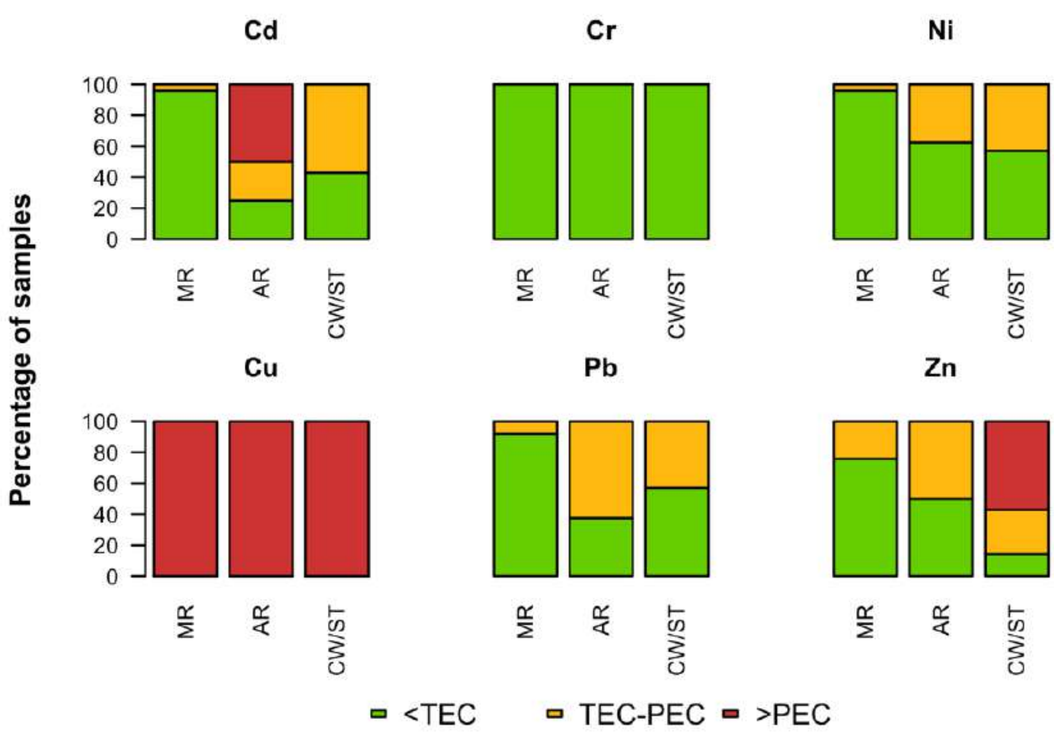

Figure 14 Sediment quality guidelines evaluation by heavy metal. MR: Molinos River, AR: Arzobispo River, CW/ST: Constructed-wetland/storage-tank. TEC: threshold effect concentration, PEC: probable effect concentration.

The SQG evaluation carried out by other authors for Cr agrees with the assessment for the analyzed sediments. For Cu, in all cases, it is below the level found in the sediments evaluated in Bogotá. Sharley et al., (2016) evaluated the PEC from six streams sediments in Melbourne, Australia, that have different land uses and found that for all points, Cr is below the threshold, 77% of points for Cu, and 50% of points for Pb and Zn. Residential land use is the most affected due to poor waste disposal and an increasing traffic load. On the contrary, in this study, residential use is the place with the lowest risk. The evaluation of Pb and Zn are lower in the three sampling points, except in CW/ST, which has the same risk for Zn. Saleem et al., (2018) evaluated freshwater reservoir sediments and found that 100% by Cr, 87.5% by Cu, and 50% by Zn are below TEC. 100% by Pb, 37.5 by Cd and Ni, and 12.5% by Cu are between TEC and PEC thresholds. Finally, 62.5% of sediment samples are above PEC by Cd and Ni. The sediments from a River in China were evaluated below the TEC by Cd, Pb, and Cu. Above TEC by Ni and Zn, sediments have potential toxicity by the last two HM (Y. Zhang et al., 2021).

4.2 Sediment environmental risk assessment

Following the I_{geo} classification for the analyzed sediments shown in Figure 15, the HMs contamination degrees were established in the sediments of the three sampling points: an unpolluted environment (G0) by Cr, Ni, and Pb, secondly an environment uncontaminated to highly contaminated (G0-G4) by Cd and Zn, and finally, the highest degree of environmental contamination is due to Cu, which is highly contaminated (G4) and reaches heavily to extremely polluted (G5) in some samples. Notably, in MR, 84% of the sediment samples are classified as unpolluted to moderately polluted (G0) by Zn, 96% are not contaminated (G1) by Cd and Pb, and all the samples are highly contaminated (G4) by Cu. 50% of AR sediment samples can be classified as uncontaminated to moderately polluted (G0 -G1) by Pb, 75% unpolluted to moderately polluted (G1) by Zn, highly contaminated (G2-G4) by Cd, and the most significant risk is due to Cu, 100% of samples are highly contaminated (G4). 85.7% of the CW/ST sediments samples are classified as heavily to extremely polluted environment (G5) by Cu and between heavily polluted and heavily to extremely polluted (G4-G5) by Zn, while 67.1% are classified as moderately to heavily polluted (G2-G3) by Cd. Thus, MR has the lowest degree of contamination, followed by AR and CW/ST.

The highest I_{geo} degrees of contamination by Zn for CW/ST agree with those obtained by other authors, as shown in Table 12. The highest degrees of contamination by Zn for CW/ST agree with those obtained by other authors (G3 to G5). However, they found a higher classification degree than those obtained for MR and AR. In addition, they found moderate to heavy Pb and Cu contamination degree (G3), which is lower for Cu and higher for Pb for those found in the sediments of this research. Cd classification for most places agrees with that found for the MR and the variation found by (Arisekar et al., 2022) in a river with the category of the CW/ST. A range between uncontaminated and moderately contaminated (G0-G3) was reported regarding Cr and Ni. These results represent a greater risk than those found for sediments from the three sampling points. Due to the significant variability of the I_{geo} results, it is impossible to associate the sediments analyzed in this research with those reported by others.

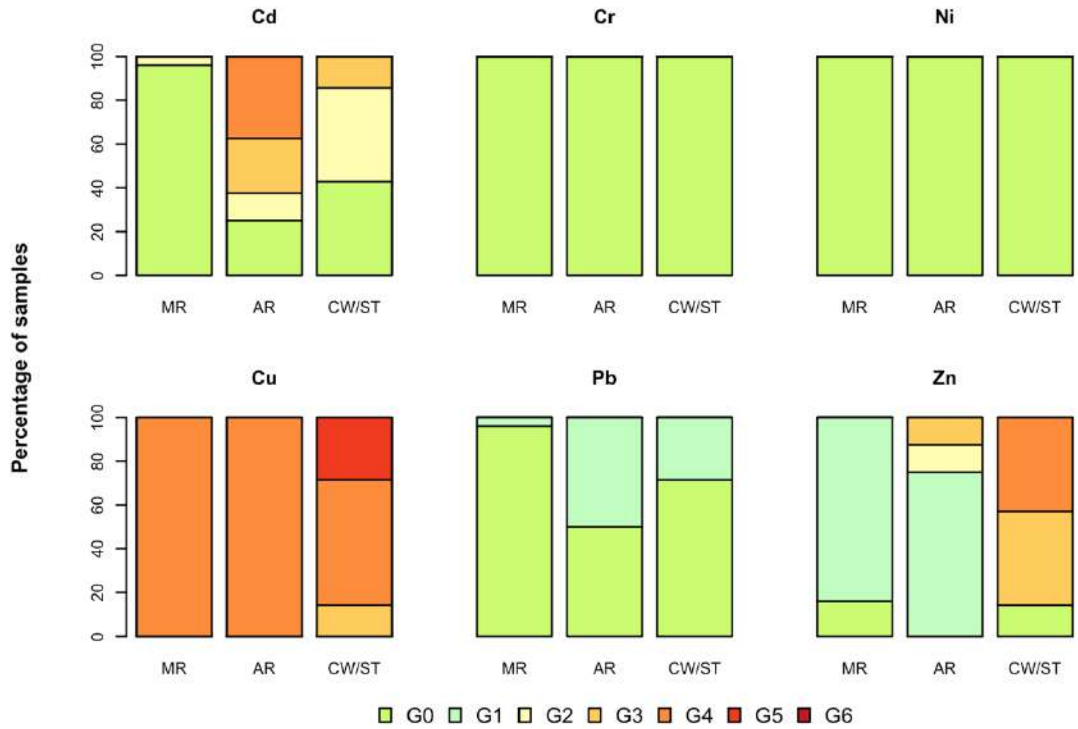

Figure 15 Geo-accumulation index (I_{geo}) concerning the percentage of samples in each place. Molinos River (MR): 25 samples, Arzobispo River (AR): 8 samples, Constructed-wetland/storage-tank (CW/ST): 7 samples. G0: unpolluted environment, G1: unpolluted to moderately polluted, G2: moderately polluted, G3: moderately to heavily polluted, G4: heavily polluted, G5: heavily to extremely polluted, G6: extremely polluted

For each of the studied HM, the EF classifications are shown in Figure 16. For the three sampling points' highest enrichment level is for Cu and Zn, while the lowest is for Cr. CW/ST has extreme enrichment by Cu and Zn in 100% of the sediment samples and by Cd in 57.1%, from significant to extreme enrichment in 100% and 85.7% of sediment samples by Ni and Pb, respectively, and moderate enrichment by Cr in 14.3% of sediment samples. On the other hand, AR has an enrichment from significant to extreme by Cu, Zn, Ni, and Cd in 50%, 37.5%, 37.5%, and 25% of the samples, respectively, from moderate to significant enrichment by Pb in 50% of sediment samples, and no enrichment by Cr in 100% of samples. Finally, MR is classified in 84% and 96% of the samples with extreme enrichment by Zn and Cu, a very high enrichment by Ni in 60% of samples, significant enrichment by Pb in 56 % of samples, and no enrichment by Cr in 100% of samples. Therefore, the sediments have high contamination of Cu, Zn, and Ni of anthropogenic origin.

Regarding the results presented in Table 14 these results agree with the Cr enrichment for the three sampling points with those found in natural water bodies and with the Cd enrichment in MR and AR for most of the samples. Considering enrichment levels found for the other HM, all sediment samples analyzed exceed the reported levels when compared with the results of other researchers.

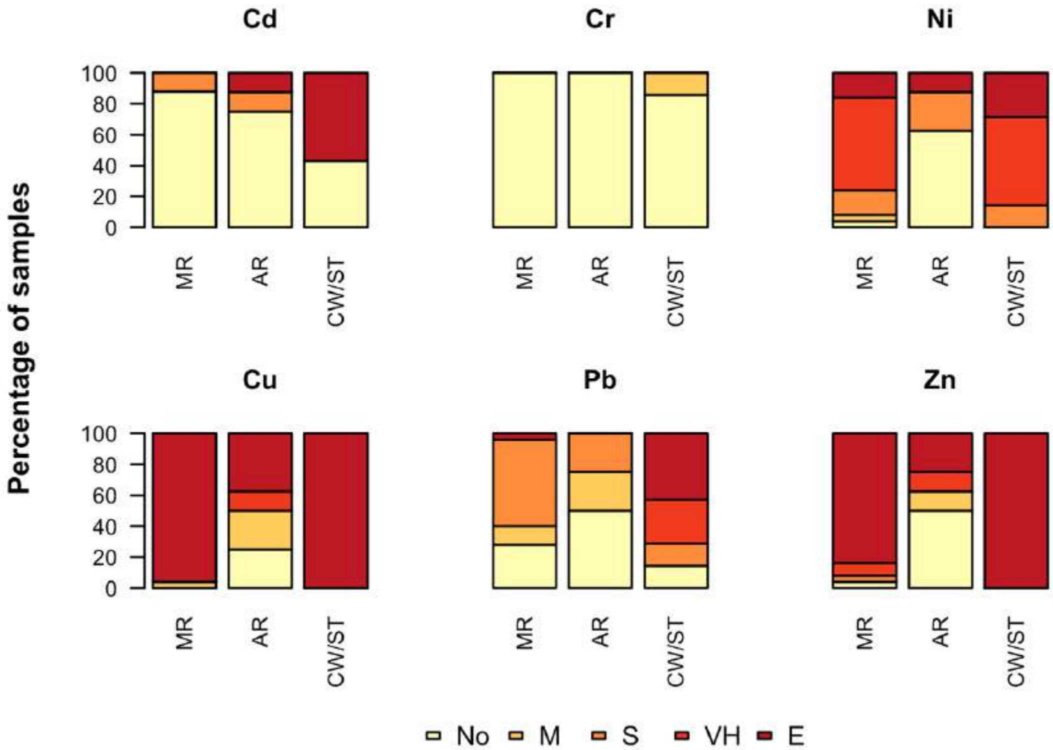

Figure 16 Enrichment factor (EF) concerning the percentage of samples in each place. Molinos River (MR): 25 samples, Arzobispo River (AR): 8 samples, Constructed-wetland/storage-tank (CW/ST): 7 samples. No: deficiency to minimal enrichment, M: moderate enrichment, S: significant enrichment, VH: very high enrichment, E: extreme enrichment.

The pollution index of the sediments collected in all sampling points shows the following pollution levels: a low level by Cr, a low to medium level by Ni and Pb, a low to a high level by Cd, a medium to high by Zn, and a high pollution level by Cu (Figure 17). Specifically, MR has a low level of contamination in more than 90% of the samples for all HMs except Zn and Cu, which has a medium level in 96% and a high level of contamination in 100% of the sediment samples, respectively. AR has a low level of contamination by Cd and Ni at 100% and 87.5%, a medium level by Pb and Zn at 62.5% and 75%, and a high level by Cd and Cu at 75% and 100% of the collected sediments samples, respectively. AR and CW/ST have almost the same contamination levels, being low for Cr and Ni, high for more than 50% of the samples for Cd, Cu, and Zn, and medium for about 30% of the sediment samples by Pb. While CW/ST has a high pollution level of Cu, Zn, and Cd at 100% and 85.7%, respectively. 57.1% of samples have a medium pollution level of Pb and a low pollution level of Ni. Cr has a low pollution level at 100% of sediments analyzed. In general terms, it is evident that the measured concentrations of Cd, Cu, Pb, and Zn greatly exceed the respective base concentrations, which implies medium to high levels of contamination for the urban drainage systems.

The contamination levels have been analyzed in sediments from a few places, which mainly determined a low pollution level of Cr, Pb, Zn, and Ni. Low to medium level of Cu and a low to high level of Cd (Table 16). According to these classifications, the measured PI is higher in the sediments for Zn and Cu; Pb and Ni are higher in some samples, while the Cd and Cr categories agree with those from other researchers. Despite the concordance in some classifications, it is impossible to thoroughly compare the sediments of a specific site with those analyzed here.

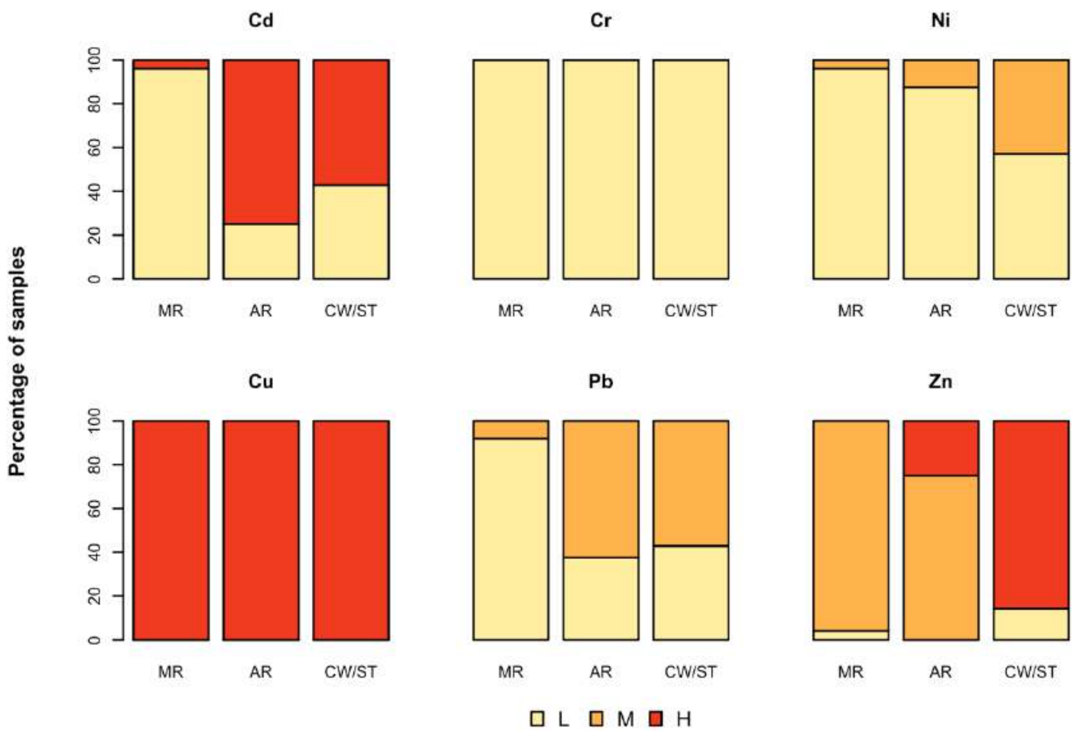

Figure 17 Pollution index (PI) concerning the percentage of samples in each place. Molinos River (MR): 25 samples, Arzobispo River (AR): 8 samples, Constructed-wetland/storage-tank (CW/ST): 7 samples. L: low level of pollution, M: medium level of pollution, H: high level of pollution.

From the ecological risk results shown in Figure 18 - left, it is possible to identify that MR has a low ecological risk impact, followed by CW/ST and AR, which both have a low to considerable ecological risk impact. This means there is no sensitivity of the biological community to HMs for 96% of the MR, 25% of the AR, and 28.6% of the CW/ST sediments. For this reason, it is necessary to pay special attention to the sediments of the AR and CW/ST. They must be removed from the basins to avoid the magnification of the concentrations. On the other hand, MR agrees with the classification reported in RDS and an urban river, and the risk variation in AR and CW/ST for some samples agrees with almost all the results reported by other authors (Arisekar et al., 2022; X. Zhang et al., 2020).

The PLI of the HM analyzed by each site (Figure 18-right) shows an unpolluted environment in MR for 96% of the samples. 37.5 % of AR samples are classified from unpolluted to moderately unpolluted. Finally, 86% of the CW/ST vary equally between uncontaminated and moderately polluted. The classification of the unpolluted environment is found in urban river sediments, especially in summer, which agrees with the contamination found in MR (Ali et al., 2022;

Arisekar et al., 2022). AR and CW/ST classification agrees with the classification of river sediments in winter, and sediments from the lift coast, respectively (Ali et al., 2022; Amor et al., 2019).

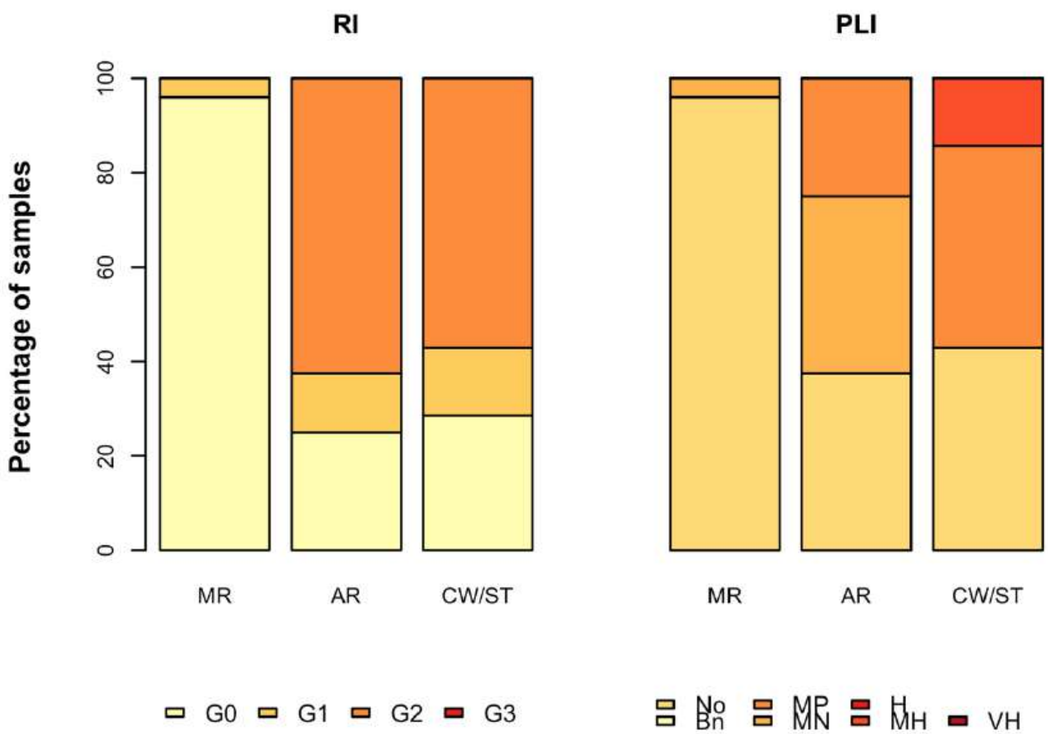

Figure 18 Ecological risk index (RI) and pollution load index (PLI) concerning the percentage of samples in each place. Molinos River (MR): 25 samples, Arzobispo River (AR): 8 samples, Constructed-wetland/storage-tank (CW/ST): 7 samples. G0: low ecological risk, G1: moderate ecological risk, G2: considerable ecological risk, G3: very high ecological risk. Bn: background concentration, No: unpolluted, MN: moderately to unpolluted, MP: moderately to polluted, MH: moderately to highly polluted, H: highly polluted, VH: very high polluted.

Considering that the MPI and MRI use the EF to classify the level of contamination, which mainly presents an enrichment above a very high level, severe pollution MPI in 96%, 50%, and 100% are obtained in sediment samples from MR, AR, and CW/ST, respectively. Regarding MRI, 80%, 37.5%, and 57.1% of MR, AR, and CW/ST sediment samples, respectively, have considerable ecological risk. Thus, the risk assessment using the modified methods considers the anthropogenic source of HM, and the three sampling points imply a higher level of contamination with respect to the original indices.

4.3 Human health risk assessment

The evaluation of ADD in adults and children by each pathway and non-carcinogenic HM is shown in Figure 19. In terms of exposure route, the highest is through ingestion, followed by dermal contact, and finally, inhalation. Exposure by HMs decreases as follows: Cu>Zn>Pb, with CW/ST being the one with the highest exposure by Cu and Zn and AR by Pb. The most significant exposure by contact occurs in adults, while inhalation and ingestion occur in children (See Appendix B for detailed ADD).

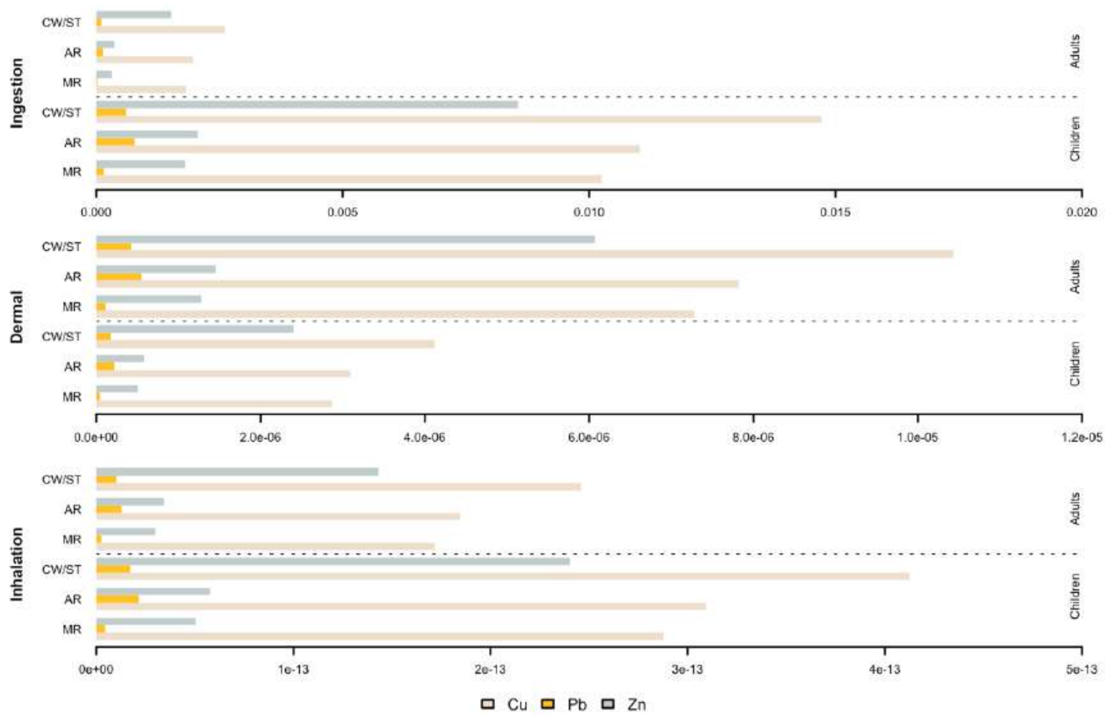

*Figure 19 Average daily dose (ADD) for no carcinogenic HM for each pathway in children and adults [mg/(kg*day)]. MR: Molinos River, AR: Arzobispo River, CW/ST: Constructed wetland storage tank.*

For all pathways, the non-carcinogenic ADD is less than the RfD. Therefore, the HQ is less than 1. The HQ results for all sediment samples decrease the same way as the ADD, as shown in Table (Table 23); no harmful effect is expected from exposure to stormwater sediment in urban areas contaminated with non-carcinogenic HM. As shown in Figure 20 the HI at three sampling points is also less than 1, so there is no threat to human health from any non-carcinogenic HM.

Table 23. Hazard quotients (HQ) for each pathway and heavy metal in children and adults. MR: Molinos River, AR: Arzobispo River, CW/ST: Constructed wetland storage tank

HM	Population	Ingestion			Dermal			Inhalation		
		MR	AR	CW/ST	MR	AR	CW/ST	MR	AR	CW/ST
Cu	Adults	4.6E-2	4.9E-2	6.5E-2	6.1E-4	6.5E-4	8.7E-4	4.3E-12	4.3E-12	6.1E-12
	Children	2.6E-1	2.6E-1	3.7E-1	2.4E-4	2.6E-4	3.4E-4	7.2E-12	7.7E-12	1.0E-11
Pb	Adults	8.2E-3	3.9E-2	3.1E-2	2.2E-4	1.0E-3	8.2E-4	7.7E-13	3.7E-12	2.9E-12
	Children	4.6E-2	2.2E-1	1.7E-2	8.6E-5	4.1E-4	3.2E-4	1.3E-12	6.2E-12	4.8E-12
Zn	Adults	1.1E-3	1.2E-3	5.1E-3	2.1E-5	2.4E-5	1.0E-4	1.0E-13	1.1E-13	4.8E-13
	Children	6.9E-3	6.8E-3	2.9E-2	8.4E-6	9.6E-6	4.0E-5	1.7E-13	1.9E-13	8.0E-13

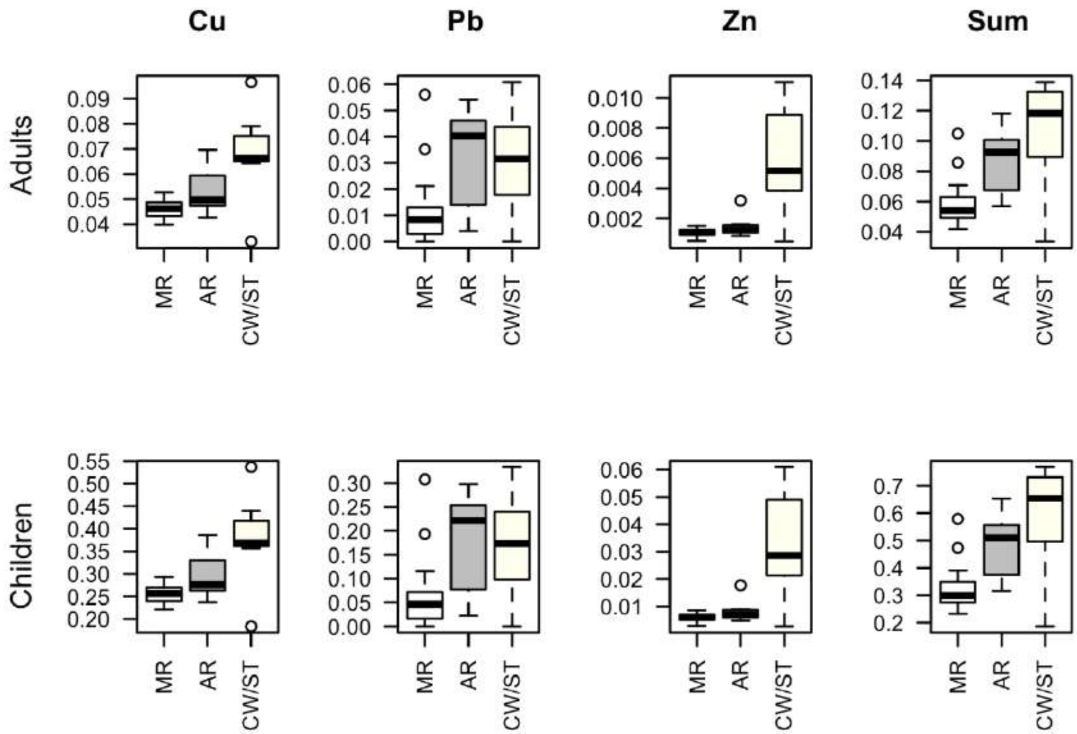

Figure 20 The hazard index (HI) for the same metal, the sum of the HQ for the three pathways, and the sum of the HI for HM in children (bottom) and adults (top). MR: Molinos River, AR: Arzobispo River, CW/ST: Constructed wetland storage tank.

Figure 21 shows each pathway's carcinogenic HM ADD in adults and children. The exposure occurs from highest to lowest: ingestion, dermal contact, and inhalation. Children have the most significant exposure through ingestion and inhalation. For both population groups, Ni is the one that represents the most significant exposure, followed by Cr and, finally, Cd. Regarding the sampling sites, the MR has the lowest degree of exposure, contrary to the AR, which has the highest exposure (See Appendix B for detailed ADD).

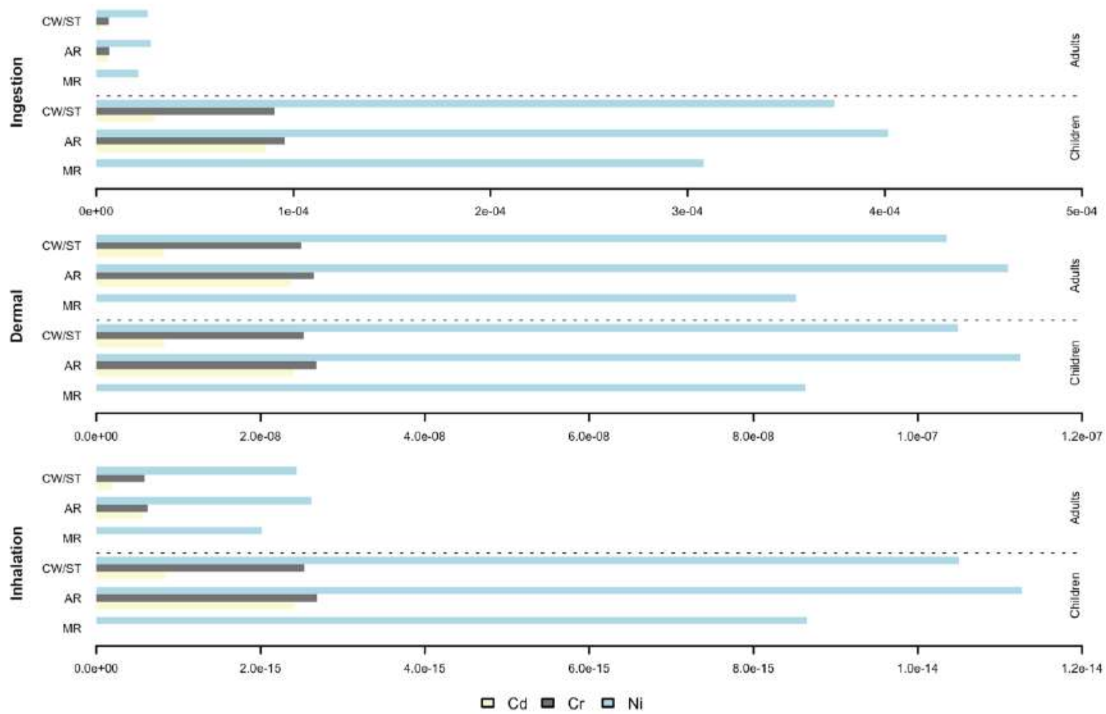

*Figure 21 Average daily dose (ADD) for carcinogenic HM for each pathway in children and adults [mg/(kg*day)]. MR: Molinos River, AR: Arzobispo River, CW/ST: Constructed wetland storage tank.*

Regarding the total cancer risk associated with HM shown in Figure 22 and Figure 23, children have a high risk of developing cancer from contact with sediments. However, it is mainly due to accidental ingestion since 100% of the samples of the three places analyzed have a high risk due to Ni concentrations. Additionally, more than 60% of AR and more than 57% of CW/ST represents a high risk by Cd and Cr. Despite this, there is a low risk for inhalation of sediments and a tolerable risk for associated dermal contact, mainly by Cr.

MR sediments have a tolerable and high risk for the adult population in approximately 60% of the AR and CW/ST samples. The most significant risk is related to ingestion associated with Cr. The tolerable risk is related to ingesting material contaminated with Ni and Cd for the three sampling points and the dermal contact in about 50% of the samples from AR and CW/ST by Cr. No risk is expected from the inhalation of particles. Additionally, AR and CW/ST have a tolerable contact risk due to Cr concentrations.

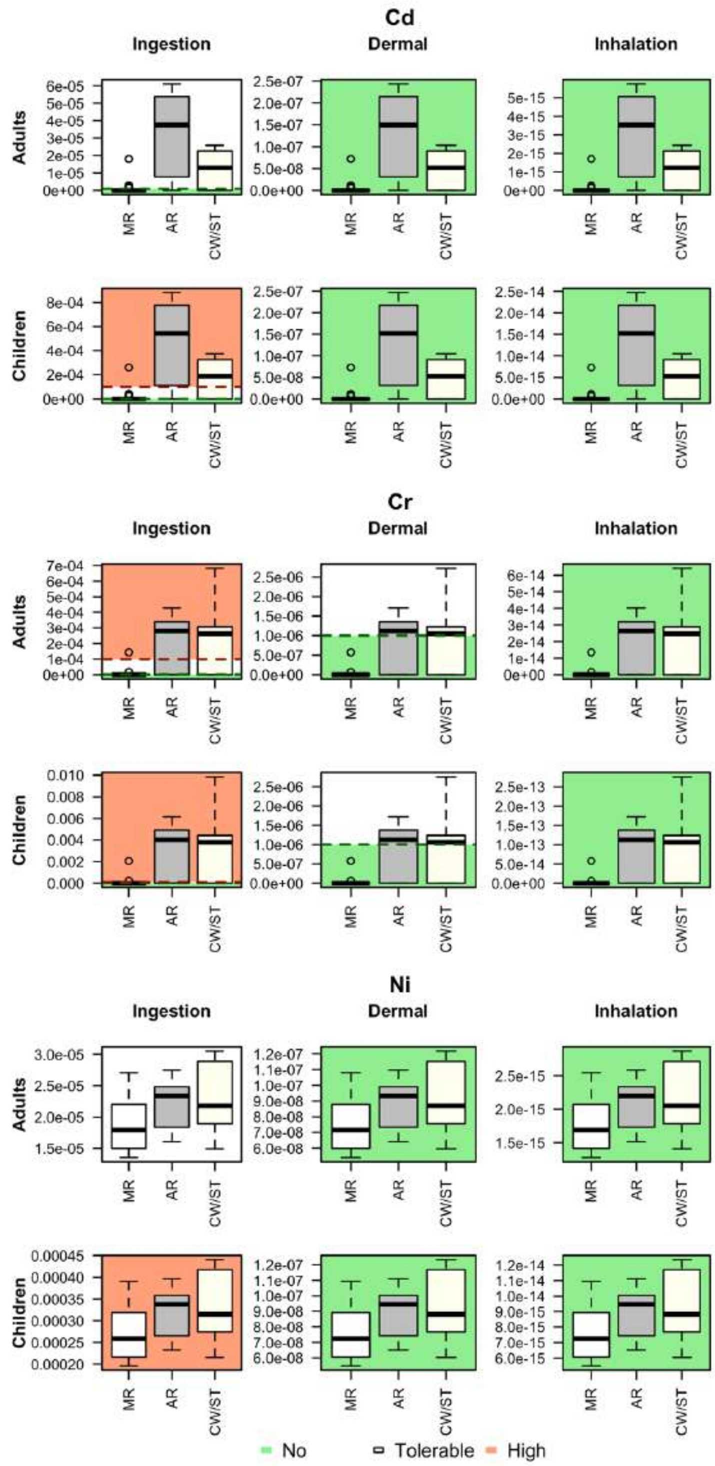

*Figure 22. Cancer Risk (CR) by HM and pathway for children (bottom) and adults (top). No: No cancer risk, Tolerable: tolerable risk of developing cancer. High: high risk of developing cancer. MR: Molinos River, AR: Arzobispo River, CW/ST: Constructed-wetland/storage-tank. *No tolerable CR was found*

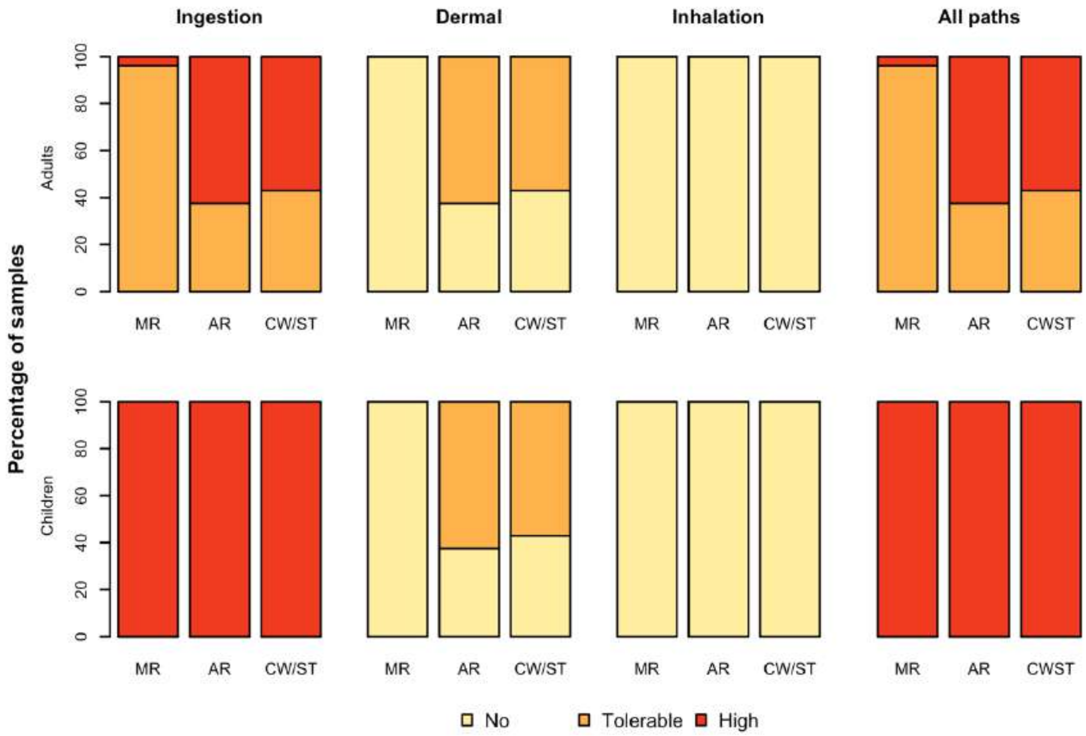

Figure 23. Total Cancer Risk by pathways in children (bottom) and adults (top). No: No cancer risk, Tolerable: tolerable risk of developing cancer. High: high risk of developing cancer. MR: Molinos River, AR: Arzobispo River, CW/ST: Constructed wetland storage tank.

Health risk results agree with those presented by other authors for urban sediments. They show that the most significant route of exposure is through ingestion, which is a risk to human health, especially in children, the most vulnerable population. Other authors' carcinogenic risk analyses carried out for urban sediments have shown that there is always a high risk, mainly due to the Cr content (Kumar et al., 2020; Nawrot et al., 2020; Şimşek et al., 2022).

Due to the above, it is necessary to review the protocols for the extraction and disposal of sediments from the urban drainage system in Bogotá. In cases where manual extraction is carried out, the risk increases for the workers in charge of these tasks, and inadequate disposal may increase exposure to different population groups.

CONCLUSIONS PART B

Sediment quality guidelines evaluation shows that Cu will expect adverse effects on fauna at the three sampling points, Zn in constructed-wetland/storage-tank (CW/ST) and Cd in Arzobispo River (AR). Probable adverse effects by Ni and Pb in AR and CW/ST, Cd in CW/ST, and Zn in Molinos River (MR) and AR. On the other hand, potential ecological risk shows low risk from MR sediments and considerable risk for AR and CW/ST sediments, which can be attributed to the concentrations of Cd, Cu, and Zn, which present high levels of contamination for the sediments. The results of the enrichment factor show that there is a variation in the source of the metals, and therefore when using this index for the calculation of the modified pollution index and the modified ecological risk index, higher risk values are obtained. Thus, there is a threat to aquatic fauna due to interaction with sediments, especially in areas with high vehicular traffic. Therefore, to assess sediment risk, the use of modified indices will provide more accurate information in urban settings.

Concerning the results of the environmental indices, the MR sediments are those that represent the lowest risk. However, the concentrations of Cu and Zn represent a threat to this basin, in addition to the fact that they come from anthropic activities, which is why they widely exceed background concentrations. On the other hand, CW/ST has the highest levels of Cu and Zn contamination. In terms of environmental conservation, it is necessary to remove sediments from urban areas in the source before they are discharged into natural water bodies since most pollutants come from human activities and remain attached to the particles, causing environmental contamination and pollutant magnification.

Regarding human health, sediments represent a high risk for children and above tolerable risk for adults associated with carcinogenic metals (Cr, Cd, and Ni), primarily due to accidental ingestion followed by dermal contact due to Ni and Cr content. On the other hand, non-carcinogenic metals do not represent a risk to human health in any population group. This implies that sanitary protocols are needed for sediment management due to carcinogenic HM. Due to the above, it is necessary to review the protocols for the extraction and sediment disposal dredged from the urban drainage system in Bogotá. In cases where manual extraction is carried out, the risk increases for the workers in charge of these tasks, and inadequate disposal may increase exposure to different population groups.

The analysis of the sediments presented in this document up to this part has required several collection campaigns and expensive laboratory analyses. Hence, as an alternative to improve understanding and facilitate decision-making, in PART C, we focus on doing different statistical analyses to find options to reduce sample collection and the number of laboratory tests and data analyses to determine sediments' effect on the environment and human health.

REFERENCES PART B

Ali, M. M., Rahman, S., Islam, M. S., Rakib, M. R. J., Hossen, S., Rahman, M. Z., Kormoker, T., Idris, A. M., & Phoungthong, K. (2022). Distribution of heavy metals in water and sediment of an urban river in a developing country: A probabilistic risk assessment. International Journal of Sediment Research, 37(2), 173–187. https://doi.org/10.1016/j.ijsrc.2021.09.002

Al-Rubaei, A. M., Merriman, L. S., III, Hunt, W. F., Viklander, M., Marsalek, J., & Blecken, G. T. (2017). Survey of the operational status of 25 Swedish municipal stormwater management ponds. Journal of Environmental Engineering, 143(6), 05017001. https://doi.org/10.1061/(ASCE) EE.1943-7870.0001203

Amor, R. B., Yahyaoui, A., Abidi, M., Chouba, L., & Gueddari, M. (2019). Bioavailability and Assessment of Metal Contamination in Surface Sediments of Rades-Hamam Lif Coast, around Meliane River (Gulf of Tunis, Tunisia, Mediterranean Sea). Journal of Chemistry, 2019. https://doi.org/10.1155/2019/4284987

Arakel, A. V. (1995). Towards developing sediment quality assessment guidelines for aquatic systems: An Australian perspective. Australian Journal of Earth Sciences, 42(4), 335–369. https://doi.org/10.1080/08120099508728207

Arisekar, U., Shakila, R. J., Shalini, R., Jeyasekaran, G., Keerthana, M., Arumugam, N., Almansour, A. I., & Perumal, K. (2022). Distribution and ecological risk assessment of heavy metals using geochemical normalization factors in the aquatic sediments. Chemosphere, 294, 133708. https://doi.org/10.1016/j.chemosphere.2022.133708

Barbieri, M. (2016). The Importance of Enrichment Factor (EF) and Geoaccumulation Index (Igeo) to Evaluate the Soil Contamination. Journal of Geology & Geophysics, 5(1). https://doi.org/10.4172/2381-8719.1000237

Brady, J. P., Ayoko, G. A., Martens, W. N., & Goonetilleke, A. (2015). Development of a hybrid pollution index for heavy metals in marine and estuarine sediments. Environmental Monitoring and Assessment, 187(5), 306. https://doi.org/10.1007/s10661-015-4563-x

Casey, R. E., Simon, J. A., Atueyi, S., Snodgrass, J. W., Karouna-Renier, N., & Sparling, D. W. (2007). Temporal trends of trace metals in sediment and invertebrates from stormwater management ponds. Water, Air, and Soil Pollution, 178(1–4), 69–77. https://doi.org/10.1007/s11270-006-9132-z

Chang, H., Allen, D., Morse, J., & Mainali, J. (2019). Sources of contaminated flood sediments in a rural–urban catchment: Johnson Creek, Oregon. Journal of Flood Risk Management, 12(4). https://doi.org/10.1111/jfr3.12496

Choi, J. Y., Jeong, H., Choi, K.-Y., Hong, G. H., Yang, D. B., Kim, K., & Ra, K. (2020). Source identification and implications of heavy metals in urban roads for the coastal pollution in a beach town, Busan, Korea. Marine Pollution Bulletin, 161. https://doi.org/10.1016/j.marpolbul.2020.111724

Hakanson, L. (1980). An ecological risk index for aquatic pollution control.a sedimentological approach. Water Research, 14(8), 975–1001. https://doi.org/10.1016/0043-1354(80)90143-8

Ignatavicius, G., Valskys, V., Bulskaya, I., Paliulis, D., Zigmontienė, A., & Satkunas, J. (2017). Heavy metal contamination in surface runoff sediments of the urban area of Vilnius, Lithuania. Raskmetallid Vilniuse Linnakeskkonna Pindmise Äravoolu Setendites., 66(1), 13–20. https://doi.org/10.3176/earth.2017.04

Joshi, U. M., Vijayaraghavan, K., & Balasubramanian, R. (2009). Elemental composition of urban street dusts and their dissolution characteristics in various aqueous media. Chemosphere, 77(4), 526–533. https://doi.org/10.1016/j.chemosphere.2009.07.043

Jahromi, F. A., Keshavarzi, B., Moore, F., Abbasi, S., Busquets, R., Hooda, P. S., & Jaafarzadeh, N. (2021). Source and risk assessment of heavy metals and microplastics in bivalves and coastal sediments of the Northern Persian Gulf, Hormogzan Province. Environmental Research, 196, 110963. https://doi.org/10.1016/j.envres.2021.110963

Karlavičienė, V., Švedienė, S., Marčiulionienė, D. E., Randerson, P., Rimeika, M., & Hogland, W. (2009). The impact of storm water runoff on a small urban stream. Journal of Soils and Sediments, 9(1), 6–12. https://doi.org/10.1007/s11368-008-0038-9

Karna, R. R., Luxton, T., Bronstein, K. E., Hoponick Redmon, J., & Scheckel, K. G. (2017). State of the science review: Potential for beneficial use of waste by-products for in situ remediation of metal-contaminated soil and sediment. Critical Reviews in Environmental Science and Technology, 47(2), 65–129. https://doi.org/10.1080/10643389.2016.1275417

Kumar, V., Sharma, A., Pandita, S., Bhardwaj, R., Thukral, A. K., & Cerda, A. (2020). A review of ecological risk assessment and associated health risks with heavy metals in sediment from India. International Journal of Sediment Research, 35(5), 516–526. https://doi.org/10.1016/J.IJSRC.2020.03.012

Laino-Guanes, R. M., Bello-Mendoza, R., González-Espinosa, M., Ramírez-Marcial, N., Jiménez-Otárola, F., & Musálem-Castillejos, K. (2015). Metal concentrations in water and sediments in the upper Grijalva river basin, Mexico-Guatemala border | Concentración de metales en agua y sedimentos de la cuenca alta del río Grijalva, frontera México-Guatemala. Tecnologia y Ciencias Del Agua, 6(4), 61–74.

Laxmi Mohanta, V., Naz, A., & Kumar Mishra, B. (2020). Distribution of heavy metals in the water, sediments, and fishes from Damodar river basin at steel city, India: a probabilistic risk assessment. Human and Ecological Risk Assessment, 26(2), 406–429. https://doi.org/10.1080/10807039.2018.1511968

Li, L. Y., Hall, K., Yuan, Y., Mattu, G., McCallum, D., & Chen, M. (2009). Mobility and Bioavailability of Trace Metals in the Water-Sediment System of the Highly Urbanized Brunette Watershed. Water, Air, and Soil Pollution, 197(1–4), 249–266. https://doi.org/10.1007/s11270-008-9808-7

Liu, B., Xu, M., Wang, J., Wang, Z., & Zhao, L. (2021). Ecological risk assessment and heavy metal contamination in the surface sediments of Haizhou Bay, China. Marine Pollution Bulletin, 163, 111954. https://doi.org/10.1016/j.marpolbul.2020.111954

MacDonald, D. D., Ingersoll, C. G., & Berger, T. A. (2000). Development and evaluation of consensus-based sediment quality guidelines for freshwater ecosystems. Archives Of Environmental Contamination And Toxicology, 39(1), 20–31.

Mandeng, E. P. B., Bidjeck, L. M. B., Bessa, A. Z. E., Ntomb, Y. D., Wadjou, J. W., Doumo, E. P. E., & Dieudonné, L. B. (2019). Contamination and risk assessment of heavy metals, and uranium of sediments in two watersheds in Abiete-Toko gold district, Southern Cameroon. Heliyon, 5(10). https://doi.org/10.1016/j.heliyon.2019.e02591

Müller, G. (1979). Schwermetalle in den Sedimenten des Rheins—Veränderungen seit 1971. UMSCH. WISSENSCH. TECHN., 79(24), 778–783.

Nawrot, N., & Wojciechowska, E. (2017). Review on the quality of sediments from the stormwater drainage system in the urban area. E3S Web of Conferences, 17, 00064. https://doi.org/10.1051/e3sconf/20171700064

Nawrot, N., Wojciechowska, E., Rezania, S., Walkusz-Miotk, J., & Pazdro, K. (2020). The effects of urban vehicle traffic on heavy metal contamination in road sweeping waste and bottom sediments of retention tanks. Science of The Total Environment, 749, 141511. https://doi.org/10.1016/j.scitotenv.2020.141511

Pal, S. K., Wallis, S. G., & Arthur, S. (2018). An assessment of heavy metals pollution potential of road sediment derived from a suburban road network under different weather conditions.

Environmental Engineering and Management Journal, 17(8), 1955–1966. https://doi.org/10.30638/EEMJ.2018.195

Parker, J. T. C., Fossum, K. D., & Ingersoll, T. L. (2000). Chemical characteristics of urban stormwater sediments and implications for environmental management, Maricopa County, Arizona. Environmental Management, 26(1), 99–115. https://doi.org/10.1007/s002670010074

Rauch, J. N., & Pacyna, J. M. (2009). Earth's global Ag, Al, Cr, Cu, Fe, Ni, Pb, and Zn cycles. Global Biogeochemical Cycles, 23(2), 1–16. https://doi.org/10.1029/2008GB003376

Sałata, A., Bak, L., & Górski, J. (2019). Ecological risk assessment of chemical contaminants in stormwater sediments. E3S Web of Conferences, 86. https://doi.org/10.1051/e3sconf/20198600017

Sałata, A., & Dąbek, L. (2017). Methods of assessment of stormwater sediments quality. E3S Web of Conferences, 17. https://doi.org/10.1051/e3sconf/20171700080

Saleem, M., Iqbal, J., Akhter, G., & Shah, M. H. (2018). Fractionation, bioavailability, contamination and environmental risk of heavy metals in the sediments from a freshwater reservoir, Pakistan. Journal of Geochemical Exploration, 184, 199–208. https://doi.org/10.1016/j.gexplo.2017.11.002

Scoggins, M., McClintock, N. L., Gosselink, L., & Bryer, P. (2007). Occurrence of polycyclic aromatic hydrocarbons below coal-tar-sealed parking lots and effects on stream benthic macroinvertebrate communities. Journal of the North American Benthological Society, 26(4), 694–707. https://doi.org/10.1899/06-109.1

Sébastian, C., Barraud, S., Ribun, S., Zoropogui, A., Blaha, D., Becouze-Lareure, C., Kouyi, G. L., & Cournoyer, B. (2014). Accumulated sediments in a detention basin: Chemical and microbial hazard assessment linked to hydrological processes. Environmental Science and Pollution Research, 21(8), 5367–5378. https://doi.org/10.1007/s11356-013-2397-z

Sharley, D. J., Sharp, S. M., Bourgues, S., & Pettigrove, V. J. (2016). Detecting long-term temporal trends in sediment-bound trace metals from urbanised catchments. Environmental Pollution, 219, 705–713. https://doi.org/10.1016/j.envpol.2016.06.072

Sharley, D. J., Sharp, S. M., Marshall, S., Jeppe, K., & Pettigrove, V. J. (2017). Linking urban land use to pollutants in constructed wetlands: Implications for stormwater and urban planning. Landscape and Urban Planning, 162, 80–91. https://doi.org/10.1016/j.landurbplan.2016.12.016

Shojaeezadeh, S. A., Nikoo, M. R., Mirchi, A., Mallakpour, I., AghaKouchak, A., & Sadegh, M. (2020). Probabilistic hazard assessment of contaminated sediment in rivers. Science of the Total Environment, 703. https://doi.org/10.1016/j.scitotenv.2019.134875

Siddik, A. M., Chand, A., Varghese, G. K., & Alappat, B. J. (2018). Assessment of trace metal contamination and its anthropogenic influence in the sediments of an urban water body in Kozhikode, Kerala, India. Environmental Forensics, 19(4), 288–297. https://doi.org/10.1080/15275922.2018.1519737

Şimşek, A., Özkoç, H. B., & Bakan, G. (2022). Environmental, ecological and human health risk assessment of heavy metals in sediments at Samsun-Tekkeköy, North of Turkey. Environmental Science and Pollution Research, 29(2), 2009–2023. https://doi.org/10.1007/S11356-021-15746-W/TABLES/12

Sivalingam, P., al Salah, D. M. M., & Poté, J. (2021). Sediment Heavy Metal Contents, Ostracod Toxicity and Risk Assessment in Tropical Freshwater Lakes, Tamil Nadu, India. Soil and Sediment Contamination: An International Journal, 30(2), 231–252. https://doi.org/10.1080/15320383.2020.1835822

US EPA. (1989). Risk Assessment: Guidance for Superfund Volume 1 Human Health Evaluation Manual (Part A). http://www.epa.gov/swerrims/riskassessment/risk_superfund.html

Van Metre, P. C., & Mahler, B. J. (2003). The contribution of particles washed from rooftops to contaminant loading to urban streams. Chemosphere, 52(10), 1727–1741.

Wang, Q., Zhang, Q., Dzakpasu, M., Chang, N., & Wang, X. (2019). Transferral of HMs pollution from road-deposited sediments to stormwater runoff during transport processes. FRONTIERS OF ENVIRONMENTAL SCIENCE & ENGINEERING, 13(1). https://doi.org/10.1007/s11783-019-1091-x

Wijesiri, B., Egodawatta, P., McGree, J., & Goonetilleke, A. (2016). Understanding the uncertainty associated with particle-bound pollutant build-up and wash-off: A critical review. Water Research, 101, 582–596. https://doi.org/10.1016/j.watres.2016.06.013

Yun, X., Yang, Y., Liu, M., & Wang, J. (2015). Concentrations and risk assessment of polychlorinated biphenyls and polybrominated diphenyl ethers in surface sediments from the East Lake, China. Ecotoxicology, 24(1), 172–180. https://doi.org/10.1007/s10646-014-1370-z

Zhan, Y., Yang, B., Hong, N., Guan, Y., Liu, A., Du, Y., Wu, Q., & Guan, Y. (2020). Developing an equivalent toxicity area approach to comparing toxicity of urban road deposited sediments. Environmental Pollution, 257, 113588. https://doi.org/10.1016/j.envpol.2019.113588

Zhang, X., Wang, Y., Guo, S., Li, H., Liu, J., Zhang, Z., Yan, L., Tan, C., Yang, Z., & Guo, X. (2020). Concentration and speciation of trace metals and metalloids from road-deposited sediments in urban and rural areas of Beijing, China. Journal of Soils and Sediments, 20(9), 3487–3501. https://doi.org/10.1007/s11368-020-02702-3

Zhang, Y., Li, H., Yin, J., & Zhu, L. (2021). Risk assessment for sediment associated heavy metals using sediment quality guidelines modified by sediment properties. Environmental Pollution, 275. https://doi.org/10.1016/J.ENVPOL.2020.115844

Zhao, H., & Li, X. (2013). Risk assessment of metals in road-deposited sediment along an urban–rural gradient. Environmental Pollution, 174, 297–304. https://doi.org/10.1016/j.envpol.2012.12.00

PART C: STATISTICAL ANALYSIS AND MODELING

INTRODUCTION PART C

Sediment pollution depends on particle size distribution (PSD), hydrological variables, basin characteristics, and land use activities. Understanding the load contaminants require detailed knowledge of pollutant concentrations as a function of each storm event (Karlavičienė et al., 2009). Findings are generally not supported by statistical analyses focused on sediment quality variability causes (Bąk et al., 2019).

Many investigations have found that the concentration of pollutants attached to sediments varies with the PSD. The finest are those with the highest amounts of contaminants, approximately 75% of the heavy metals (HM), and are easily transported by stormwater runoff (Y. Ma et al., 2019; Sivalingam et al., 2021; Wang et al., 2019). In contrast, coarser particles are not significant carriers of pollutants (Blecken et al., 2012). At the same time, PSD is influenced by basin geometry, land use, geology, hydrology, and sediment collection methodologies (Charters et al., 2015; Kim & Sansalone, 2008).

The transport of particulate matter of different sizes by runoff varies according to weather characteristics as rain frequency, intensity, duration, and dry periods. (Liu et al., 2017; Sansalone et al., 1997; Zhao & Li, 2013). The mass of finer particles decreases after rain events due to runoff because finer particles can easily be washed off (Y. Ma et al., 2019; Wang et al., 2020). Pollutants transported depend on the rain intensity, the impervious surface, and the pollutants' characteristics (Y. Ma et al., 2018; Wijesiri et al., 2016). Dry weather lends itself to a pollutant build-up that will influence the load and composition of hydrophobic pollutants in the wash of impervious surfaces, contrary to the wet season, where a degree of dilution of contaminants can be evidenced (Gorgoglione et al., 2018; Li et al., 2019). Therefore, there are several relationships of variables found by different authors, especially with the sediment's characterization as HM concentrations and PSD. No reports of relationships with risk assessment, implementing these variables for management strategies, or developing statistical models were found. These analyses would greatly help facilitate decision-making in urban drainage structures with high accumulation amounts.

In PART C of this thesis, statistical, probabilistic, and modeling tools are prosed to identify and synthesize the relationships between variables of the collected sediments to provide elements for sediment management decisions. CHAPTER 5 presents a methodology for data prediction based on statistical and modeling tools used to find relationships between variables. CHAPTER 6 shows the results obtained by applying the proposed methodology to analyze the relationships between the three sampling points' variables and focuses on the prediction analysis for Molinos River (MR), the one with the most significant number of collected samples, as shown in section 1.2.

CHAPTER 5 STATISTICAL AND MODELING TOOLS

Determining relations between the variables analyzed in CHAPTER 2 and CHAPTER 4 helps reduce data field collection and laboratory analysis, which is a useful tool for analyzing sediment management strategies. Additionally, finding patterns between the sampling sites allows the sediment characterization and risk assessment extrapolation to other basins and rainfall events in the same location. Section 5.1 focuses on the statistical tools used to find relationships between the analyzed variables, and section 5.2 presents a methodology for statistical modeling variables, which do not represent the physical behavior of the sediments, but facilitate the analysis of variables, from the statistical point of view to improve sediment management. The analyzes were done through the free software R (R Core Team, 2021).

For the analysis of the variables, these are classified into two groups (i) Y or dependent variables: sediments accumulation (section 2.2.3), contaminant concentrations (section 2.2.2), and risk indices (sections 4.2 and 4.3); (ii) X or independent variables: PSD (section 2.2.1), hydraulic or hydrology characterization (Section 2.1).

5.1 Statistical tools

Statistical tools are the basis for finding relationships between variables through tests such as Cohen's Kappa coefficient, correlations, principal component analysis, and probability.

5.1.1 Cohen's Kappa Coefficient

Cohen's kappa coefficient determines the proportion of agreements (or disagreements) between two categorical variables concerning what could occur after the chance agreement is removed from consideration. 0 means equal chance agreement (no agreement), and 1 means a perfect agreement between the judges (Cohen, 1960). Therefore, the Kappa coefficient was used to categorically compare all variables by estimating the degree of agreement and the p-value using the command kappa.test from the fmsb library (Nakazawa, 2021). The coefficient categorization is divided into six groups: <0: no agreement, 0-0.2: slight agreement, 0.2-0.4: fair agreement, 0.4-0.6: moderate agreement, 0.6-0.8: substantial agreement, and 0.8-1.0: almost perfect agreement (Landis & Koch, 1977). Pairs of variables with a p-value less than 0.05, which is the significant probability because of the null hypothesis test, that is, from slight to almost perfect agreement. This analysis defines pairs of related variables, of which the Y variables and the respective related X variables are defined.

5.1.2 Correlations

The correlation coefficient determines the degree of association between two variables. A positive correlation means Y increases when X increases, and a negative correlation implies Y increases as X decreases. However, this does not necessarily indicate a causal or linear relationship (Asuero et al., 2006). A Pearson correlation analysis was performed to corroborate numerically the correlation between the parametric variables and the Spearman correlation for no parametric variables using the chart.correlation command from the PerformanceAnalytics library (Peterson & Carl, 2020). It allows a graphic display of the correlation matrix with histograms, density functions, regression lines, and significance levels. The correlation seeks to identify if it is possible to carry out linear regression models between the selected variables, using the p-value between the variables to ensure that the correlation found is not given by chance. Red symbols in the diagram represent P-value: • p-value ≤0.1, * p-value ≤0.05, ** p-value ≤0.01, *** p-value ≤0.001.

5.1.3 Limits

Probability was used to establish the value of variable X from which variable Y presents significant changes, that is, to determine the value of X from which Y generates a turning point. Initially, it is necessary to establish the correlation between the variables and the sign of the correlation to evaluate the behavior of Y regarding X, if both increase linearly or if one increases while the other decreases (section 5.1.2). Secondly, the observations are organized with respect to the variable X in ascending order if the correlation is positive or descending if the correlation is negative. Then, the alert value of the Y variable is defined, and the observations with the same or greater value are identified. Subsequently, the probability of occurrence of the alert value Y or greater for each observation is calculated. Finally, preserving the order of the observations with respect to X, if the correlation is positive, the last sample in which the probability of obtaining the alert value is less than one is selected. Otherwise, for negative correlations, the first sample is selected. Thus, the value of the variable X for the chosen sample is set as the turning point.

For example, to determine the turning point of developing cancer risk in children by Cd (Cd_ch), using D50. The samples are ordered from lowest to highest (assuming a positive correlation) according to D50 (variable X). As stated in section 3.3, the alert value for Cd_ch is $1x10^{-4}$. Then, the probability of obtaining a value greater or equal to the alert value is calculated. Finally, the last sample (ordered by D50) is selected, in which the probability is less than 1, thus establishing the maximum value of D50 for which there is no risk of developing cancer in children by Cd.

5.1.4 Multivariate data analysis

Principal components analysis (PCA) is a multivariate analysis that estimates the correlation structure of the variables and provides the necessary weights to obtain the new variable that best explains the variation in the entire data set. It can be used as a data reduction with a well-selected set of objects and variables to build a model (Bro & Smilde, 2014; Wold et al., 1987). In this case, the PCA is proposed to rank the X variables related to the Y variable (section 5.1.1), which will be used for model generation. PCA is performed using the dudi.pca command from the ade4 library (Dray et al., 2017).

5.2 Modeling tools

There are different statistical models for predicting variables, using easily measured variables such as hydrology and PSD. Among the models that can be explored are linear regression models or support vector machine (SVM), the latter due to its great potential to solve nonlinear systems (H. Ma et al., 2022). The proper model selection will depend on the relations between the variables. The predicted variables will require specific knowledge for their interpretation or those that facilitate decision-making for sediment management (*Y* variables). Thus, the variables to be expected will be the accumulation, the concentration of pollutants, and their associated risks.

On the other hand, models can be implemented to detect outliers if errors are found in the prediction of data, which can be attributed to one or several specific observations and not to the implemented methodology. Each sample's root mean square error (RMSE) will be calculated to detect observations outliers. The outlier observations would be those in which the RMSE between the predicted range and the measured data is greater than 1.5. This means that the observations in which these differences occur can be eliminated to improve the modeling results.

The Monte Carlo method was used to select calibration and validation data, generating a thousand combinations to evaluate the variability in the data prediction, avoid a bias in the data selection, and have robustness in the data analysis. 2/3 of the observations will be randomly selected to be used as calibration data and 1/3 as validation data. Thus, the model will be evaluated for each validation and calibration data combination, generating a thousand prediction models.

5.2.1 Linear regression model

The linear regression model is used to predict a variable *Y* from one (simple linear regression) or more variables (multivariate linear regression) (Tranmer et al., 2020). The correlation results will identify the variables *Y* and *X* that have a linear relationship. The best-fit equation will be generated using the lm command from the stats package (R Core Team, 2021). As a result of each model, the constants of the equation are obtained. When generating a thousand models, the constant will not be a single value but will be a range of values. Each model's RMSE is calculated between the predicted and measured data for calibration and validation. In addition to the correlated variables, it is possible to include all the variables related to the *Y* variable (based on the Kappa coefficient) in the multiple linear models.

5.2.2 Support vector machine

If no correlation or weak correlation was found to use a linear regression model, a SVM model could be used due to its ability to solve nonlinear problems using pattern recognition and function estimation (Hernández et al., 2021). SVM is used as a prediction tool, separating the sample into two planes, since solves the adjustment of a function that describes a relationship between *X* (object) and the answer *Y* using S (the data set) (Galarza-Molina, 2017). The ksvm command from the kernlab library was used (Karatzoglou et al., 2004), which has the most popular kernel functions for data training and prediction: Radial Basis kernel "Gaussian" – rbfdot, polynomial kernel - polydot, linear kernel – vanilladot, hyperbolic tangent kernel – tanhdot, laplacian kernel – laplacedot, Bessel kernel -besseldot, ANOVA RBF kernel – anovadot, spline kernel – splinedot.

According to PCA results, SVM models are generated with selected variables, eliminating *X* variables one by one, from least to most relevant. The kernel and the group of variables *X* with the best *Y* prediction were selected. Each model's RMSE is calculated between the predicted and measured data for validation and calibration. The best model will be the one with the lowest median RMSE for the validation data. If two or more models have the same RMSE, the selection will be made according to the lowest validation RMSE variation. For example, if A model RMSE variation is between 5 and 20 with a median of 10; and B model RMSE variation is between 1 and 30 with a median of 10, then the best model is A because it has the slightest variation.

Figure 24 shows the proposed methodology for modeling variables according to the first statistical tests evaluating the relationship between variables.

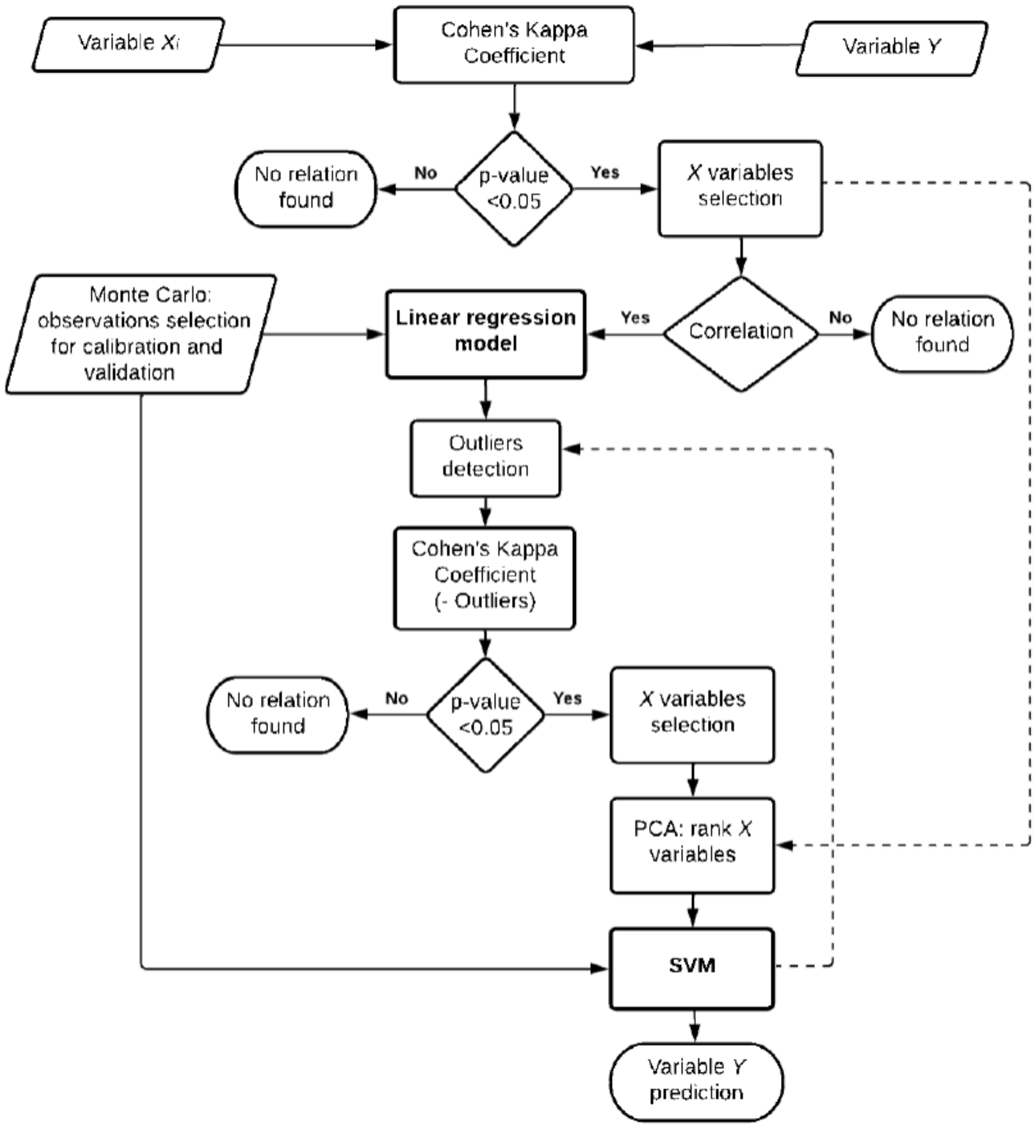

Figure 24 Modeling methodology. Variable X_i: D1 to D100, precipitation height, rain intensity, antecedent dry weather period, number of dray/rainy days, or flow runoff. Variable Y: contaminant concentrations, risk indices, or accumulation

CHAPTER 6 SEDIMENT DATA PREDICTION

As mentioned in the previous chapter, statistical analysis is done by defining the dependent and independent variables. Y or dependent variables are sediment accumulation, contaminant concentrations, and risk indices; X or independent variables are PSE, hydraulic or hydrology characterization. The analysis was carried out between variables X and Y by statistical tools for the three sampling points. No consistent relationships were found between the sites, as shown in section 6.1. For this reason, we can affirm that extrapolations cannot be made from one sampling site to another. Therefore, section 7.2 focuses on the Molinos River (MR) (section 1.1) because it is the sampling point with the most extensive data.

6.1 General relationships

Following the methodology to analyze relationships between variables, Cohen's Kappa coefficient was evaluated for the three sampling points jointly (Table 24) and individually. However, no common relationships were found for the three points. Even so, it is evaluated the PCA and correlation analysis was used as a support tool to find relationships between variables.

Table 24 Cohen's Kappa Coefficient for the three sampling points. Zn_I_{geo}: Zn geo-accumulation index, PLI: pollution load index, Cd_CRc: children cancer risk by Cd, Cd_CRa: adults cancer risk by Cd, Zn_PI: pollution index by Zn, RI: ecological risk index, Pb_EF: enrichmdent factor by Pb, Ni_EF: enrichmdent factor by Ni, ADP: antecedent dry weather period (days), rw: days with rain, dw: days without rain , I_{max}: maximum intensity (mm/h).

var1	var2	p-value	Agreement	Estimate	var1	var2	p-value	Agreement	Estimate
D20	**Zn_Igeo**	0.003	Fair	0.22	**D20**	**Zn_PI**	0.040	Slight	0.20
D10	**PLI**	0.014	Fair	0.20	**D60**	**RI**	0.048	Slight	0.18
D20	**PLI**	0.014	Fair	0.20	**D70**	**RI**	0.048	Slight	0.18
D50	**PLI**	0.014	Fair	0.20	**D60**	**Cd_CRc**	0.048	Slight	0.18
D60	**PLI**	0.014	Fair	0.20	**D80**	**Pb_EF**	0.008	Slight	0.19
D70	**PLI**	0.014	Fair	0.20	**D90**	**Ni_EF**	0.024	Slight	0.16
D70	**Cd_CRc**	0.023	Fair	0.22	**ADP**	**Cd_Igeo**	0.030	Slight	0.15
D10	**Zn_Igeo**	0.024	Slight	0.16	**dw**	**RI**	0.047	Slight	0.17
D40	**Cd_CRa**	0.029	Fair	0.30	**rw**	**Cd_PI**	0.040	Fair	0.27
D70	**Cd_CRa**	0.029	Fair	0.30	**dw**	**Cr_CRa**	0.025	Slight	0.20
D80	**Cd_CRa**	0.029	Fair	0.30	**dw**	**Cr_EF**	0.025	Slight	0.20
D30	**PLI**	0.034	Slight	0.17	**dw**	**Cd_CRc**	0.020	Fair	0.21
D40	**PLI**	0.034	Slight	0.17	**Imax**	**Ni_EF**	0.024	Slight	0.16
D80	**PLI**	0.034	Slight	0.17					

6.1.1 Correlation and PCA

Based on the correlation (section 5.1.2), in the constructed-wetland/storage-tank (CW/ST) only found a correlation of 0.85 between Cu and D100. For MR, between Pb and D10 of 0.54, D20 of

0.43, D60 of 0.40, and D70 of 0.41. Finally, the Arzobispo River (AR) is the place with most correlated variables.: Cd with D10 to D50 and a correlation between -0.92 and -0.74, Cr with D10 to D80 from -0.95 to -0.73, Ni with D10 to D60 from -0.91 to -0.74, and Pb with D10 to D40 and D80 with a variation between -0.92 to -0.87 and -0.71, respectively. As for PCA, similarly to the AR and CW/ST correlation, they have a relationship between all metals with all PSD diameters, except Zn in CW/ST, which only has a relation with D60 and D100. For MR, all HM are related to D100, and Pb is associated with D10 to D90.

Secondly, correlation analysis between HM and hydrology variables only shows a coefficient of 0.74 for Cu in AR, an inverse relationship with rainy days (rw), and a direct relationship with dry days (dw). While by PCA, relationships were found between HM and all hydrological variables for AR and CW/ST. For MR, Zn is related to the antecedent dry weather period (ADP), and Cd, Cr, and Ni are related to the other hydrological variables. The similarities between the relationships found for AR and CW/ST may be from land use and hydrology since as mentioned in section 1.3 they have the same land use, and precipitation data is downloaded from the same station.

From the above, although there are relationships between HM concentrations and PSD, it is evident that there are no similar patterns between the associations of metal concentrations and grain size for all the places. Not only because of the different relationships but also because, in the case of AR, they are inverse, while MR and CW/ST are direct (See Appendix C for all correlation diagrams and PCA data). Thus, it is not recommended to extrapolate data from one basin to another.

6.2 Molinos River

Risk indices and sediment accumulation are considered for data analysis in MR as *Y* variables. As *X* variables: precipitation height (H), average rain intensity (I_{ave}), maximum rain intensity (I_{max}), antecedent dry weather period (ADP), number of dray days (dw), number of rainy days (rw), flow runoff (Q), and D1 to D100. The results obtained following the methodology described in Figure 24 are presented below.

6.2.1 Variables relationship

According to the results of Cohen's Kappa shown in Table 25, the dependent variables (*Y*) are accumulatio, the geo-accumulation index (I_{geo}) risk index by Zn, the enrichment factor (EF) by Pb and Ni. Accumulation has a p-value of 0.013 with ADP, with a moderate agreement, and a coefficient of 0.45. Furthermore, ADP has a fair agreement and a coefficient of 0.35 with D10, D20, and D30 (p-value = 0.039). On the other hand, Zn_I_{geo} has a fair agreement and a coefficient of 0.32 with some PSDs (p-value =0.048), specifically with the finest ones: D10 to D40. In turn, D10 to D40 have a moderate agreement and a coefficient of 0.44 with hydrological variables such as precipitation height (H) and I_{ave} (p-value = 0.014). No agreement was found for the other *Y* variables analyzed with hydrology or PSD.

Table 25 Molinos rives Cohen's Kappa Coefficient. Accum: sediments accumulation (%), Zn_I_{geo}: Zn geo-accumulation index, Pb_EF: enrichmdent factor by Pb, Ni_EF: enrichmdent factor by Ni, ADP: antecedent dry weather period (days), H: precipitation height (mm), I_{ave}: average intensity (mm/h). Q: flow runoff (m3/s)

var1	var2	p-value	Agreement	Estimate	var1	var2	p-value	Agreement	Estimate
D60	**Pb_EF**	0.004	Fair	0.31	**D40**	**Pb_EF**	0.015	Fair	0.25
ADP	**Accum**	0.013	Moderate	0.45	**D50**	**Pb_EF**	0.015	Fair	0.25
H	**D10**	0.014	Moderate	0.44	**D20**	**Ni_EF**	0.023	Slight	0.20
I_{ave}	**D10**	0.014	Moderate	0.44	**D30**	**Ni_EF**	0.023	Slight	0.20
Q	**D10**	0.014	Moderate	0.44	**D40**	**Ni_EF**	0.023	Slight	0.20
H	**D20**	0.014	Moderate	0.44	**ADP**	**D10**	0.039	Fair	0.35
I_{ave}	**D20**	0.014	Moderate	0.44	**ADP**	**D20**	0.039	Fair	0.35
Q	**D20**	0.014	Moderate	0.44	**ADP**	**D30**	0.039	Fair	0.35
H	**D30**	0.014	Moderate	0.44	**D20**	**Pb_EF**	0.043	Slight	0.20
I_{ave}	**D30**	0.014	Moderate	0.44	**D30**	**Pb_EF**	0.043	Slight	0.20
Q	**D30**	0.014	Moderate	0.44	**D70**	**Pb_EF**	0.043	Slight	0.20
H	**D40**	0.014	Moderate	0.44	**D80**	**Pb_EF**	0.043	Slight	0.20
I_{ave}	**D40**	0.014	Moderate	0.44	**D10**	**Zn_I_{geo}**	0.048	Fair	0.32
Q	**D40**	0.014	Moderate	0.44	**D20**	**Zn_I_{geo}**	0.048	Fair	0.32
H	**D90**	0.014	Moderate	0.44	**D30**	**Zn_I_{geo}**	0.048	Fair	0.32
I_{ave}	**D90**	0.014	Moderate	0.44	**D40**	**Zn_I_{geo}**	0.048	Fair	0.32
Q	**D90**	0.014	Moderate	0.44					

Therefore, the *X* variables for the accumulation are ADP, D10, D20, and D30. For Zn_I_{geo} are: D10, D20, D30, D40, H, I_{ave}, ADP, and Q. For Pb_EF are: D20 to D80, H, I_{ave}, ADP, and Q. For Ni_EF are: D20, D30, D40, H, I_{ave}, ADP, and Q. As mentioned above, Q depends directly on I_{ave}, so it will not be considered for the following analyses.

6.2.2 Variables correlations and limits

The correlation values and limits for the *X* variables from the previous section with direct relation were analyzed. The graphic correlation matrix found a significance level of 10% between accumulation and ADP (Figure 25). Despite inverse correlation between Zn_I_{geo} and PSD variables, the p-value in all cases is higher than 0.05. Similarly, Ni_EF correlates with the hydrological variables, but the p-value is greater than 0.05 in any case.

Considering that Pb_EF is a non-parametric variable, to analyze the correlation, Spearman's coefficient should be used (Figure 26). The graphic correlation for Pb_EF found a p-value lower than 0.05 with D70, lower than 0.01 with D20, D30, and D60, and lower than 0.001 with D40 and D50.

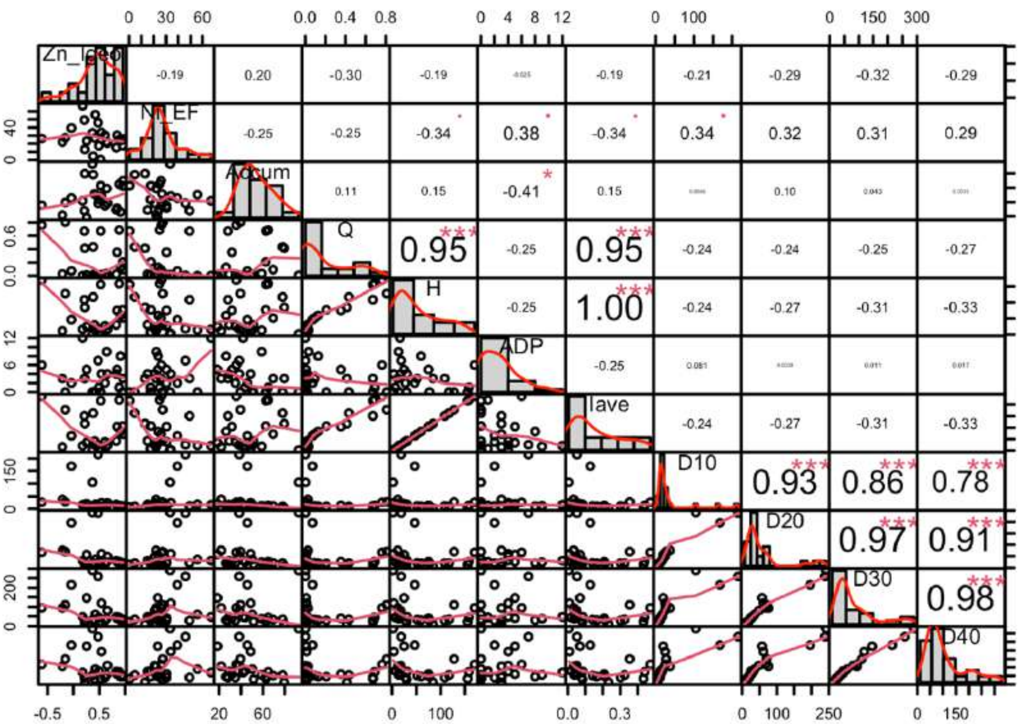

*Figure 25 Molinos river Pearson correlation matrix. • p-value ≤0.1, * p-value ≤0.05, ** p-value ≤0.01, *** p-value ≤0.001. Accum: sediments accumulation (%), Zn_I_{geo}: Zn geo-accumulation index, Ni_Pb: enrichment factor by Ni, ADP: antecedent dry weather period (days), H: precipitation height (mm), I_{ave}: average intensity (mm/h), Q: flow runoff (m^3/s)*

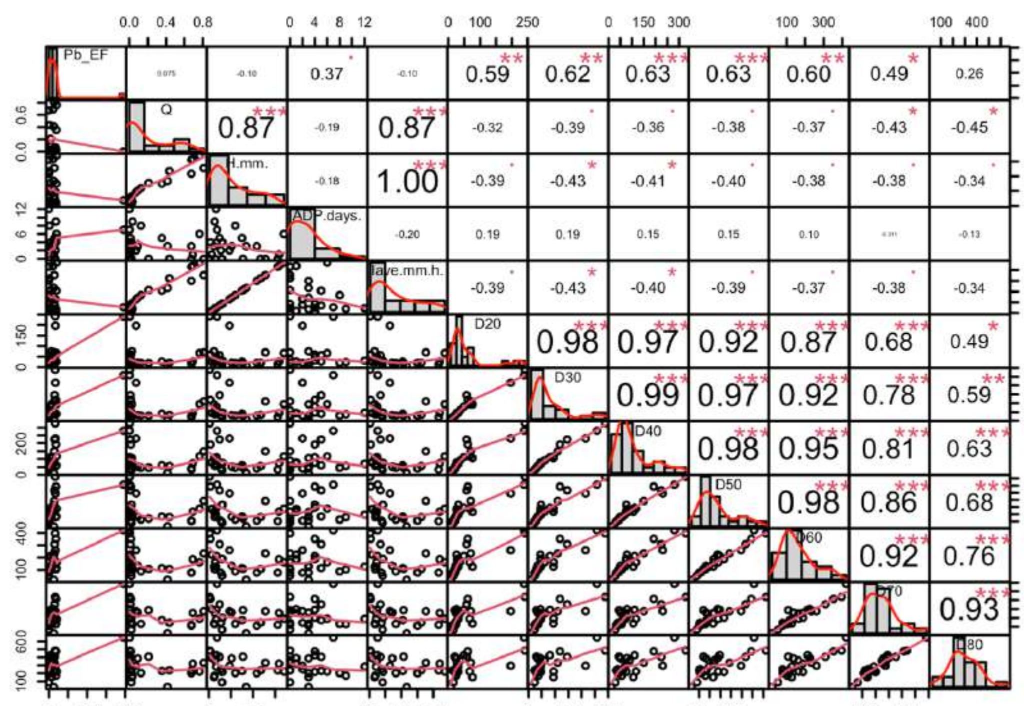

*Figure 26 Molinos river Spearman correlation matrix. • p-value ≤0.1, * p-value ≤0.05, ** p-value ≤0.01, *** p-value ≤0.001. Pb_EF: enrichment factor by Pb, ADP: antecedent dry weather period (days), H: precipitation height (mm), I_{ave}: average intensity (mm/h), Q: flow runoff (m^3/s)*

Table 26 shows the limits values for the Y variables defined. Since the correlation between accumulation and ADP is negative, the amount of sediment in the channel is not expected to increase with more dry weather days. Results can be explained because there are no sediment contributions to the channel in dry weather since the sediments come from the stormwater runoff. For $Zn\_I_{geo,}$ the limits are calculated for the relations with PSD. As the relationship is also inverse, the probability of risk increases as the particle size decreases. Finally, the limits for Ni_EF and Pb_EF have a direct relationship as the particle size increases the enrichment factor also increases.

Table 26 Molinos River accumulation (Accum), Zn geo-accumulation, Ni and Pb enrichment factor limits

Variable Y	Variable X_i	Limit	Variable Y	Variable X_i	Limit
Accum	ADP (days)	0	Pb_EF	D20 (μm)	48
Zn_I_{geo}	D10 (μm)	25	Pb_EF	D30 (μm)	80
Zn_I_{geo}	D20 (μm)	61	Pb_EF	D40 (μm)	105
Zn_I_{geo}	D30 (μm)	80	Pb_EF	D50 (μm)	137
Zn_I_{geo}	D40 (μm)	90	Pb_EF	D60 (μm)	162
Ni_EF	D20 (μm)	15	Pb_EF	D70 (μm)	254
Ni_EF	D30 (μm)	22	Pb_EF	D80 (μm)	387
Ni_EF	D40 (μm)	40			

In addition, the Monte Carlo method was used to evaluate the variation of the limits using the calibration data. For accumulation, the limit varies between 0 and 3 days of ADP. For Zn_I_{geo}, the PSD variations are between 16 μm to 216 μm for D10, 30 μm to 242 μm for D20, 45 μm to 290 μm for D30, and 69 μm to 328 μm for D40. For Ni_EF the PSD variations are between 15 to 21 μm for D20, from 22 to 34 μm for D30, and from 40 to 55 μm for D40. Finally, the PSD variation for Pb_EF are from 20 to 76 μm for D20, from 29 to 146 μm for D30, from 45 to 224 μm for D40, from 62 to 246 μm for D50, from 88 to 233 μm for D60, from 130 to 287 μm for D70, and from 300 to 475 μm for D80.

6.2.3 Accumulation linear regression model

The simple linear regression model is made to predict accumulation using the ADP, obtaining Equation 22, where the coefficient ranges of variation for the thousand iterations are expressed in parentheses. Figure 27 shows the differences between the obtained models' results and the measured data for each sample. This model's median validation data error is 40%, varying between 15% and 88%. Only some of the predicted data agree with the measured ones, so despite the existing correlation, it is not recommended to use this model since it would generate errors in decision-making, mainly because it overestimates the accumulation.

$$Accum = [43.81; 68.53] - [0.46; 7.26]ADP$$

Equation 22 Accumulation simple linear regression model

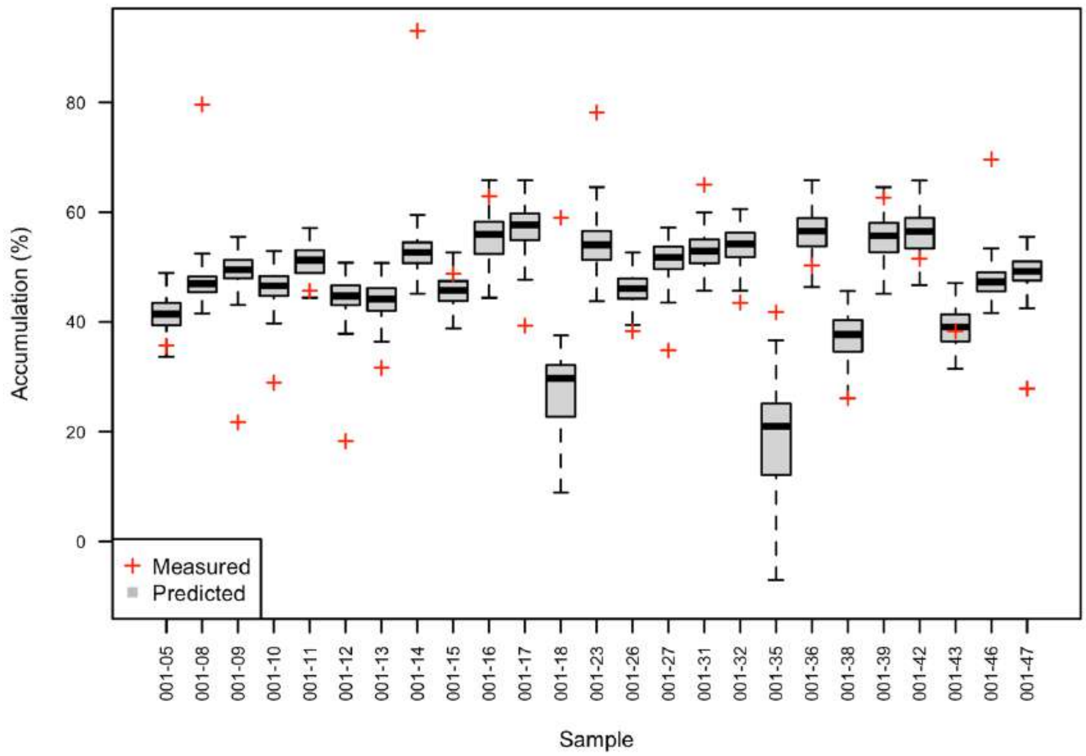

Figure 27 Accumulation simple linear regression model results (validation data) and measured for each sample.

Regarding the multiple linear regression model, in addition to ADP, it includes the PSD variables that agree with the ADP based on Cohen's Kappa coefficient. The model for the accumulation is described in Equation 23 with a median validation error of 50%, varying between 19% and 1494%. Figure 28 shows the results of the thousand iterations and the measured data for each sample. For this modeling proposal, significant variations are generated in the amount of accumulation in samples 001-11, 001-14, and 001-43; these samples have the highest D10, D20, and D30 (>100 μm). However, it is possible to identify outliers and avoid erroneous modeling values. Therefore, the outliers are the samples 001-08, 001-09, 001-11, 001-14, 001-18, and 001-43 (See Appendix C for additional data).

$$Accum = [39.31; 84.72] + [-5.77; 0.16]ADP + [-13.89; 1.92]D10 + [-2.03; 5.85]D20 + [-1.51; 0.89]D30$$

Equation 23 Accumulation multiple linear regression model

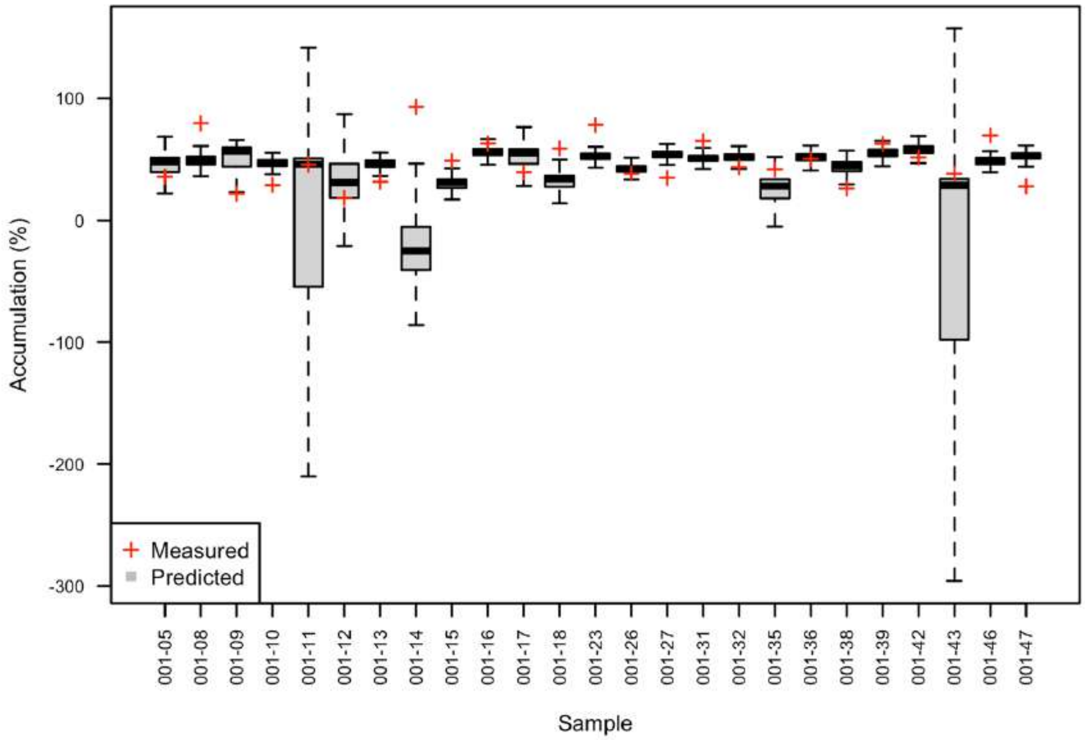

Figure 28 Accumulation multiple linear regression model results (validation data) and measured for each sample.

Since there is only one correlation between accumulation and ADP, the linear model can only be used to predict accumulation with errors greater than 40% in data validation. However, it is a methodology that allows the identification of outliers. On the other hand, it is not a suitable methodology to model Zn_I_{geo} since there is no linear relationship with any *X* variable. Therefore, implementing models that can solve nonlinear problems, such as SVM, could help reduce data prediction errors (See Appendix C for additional data).

6.2.4 PCA accumulation and Zn_I_{geo}

With the *Y* variables identified, a multivariate analysis of up to six components is proposed to establish the influence of the related *X* variables, the variables related to accumulation (Figure 29), Zn_I_{geo} (Figure 30) and Pb_EF (**¡Error! No se encuentra el origen de la referencia.**). *X* variables are in ascending order using the coordinate of the columns concerning the components with the most significant influence. For accumulation and Zn_I_{geo}, ADP is the variable with the most binding effect, and for Pb_Ef is D60. The *X* variables are ordered as follows (i) for accumulation: D20, D30, I_{max}, D10, H, rw, and ADP; (ii) for Zn_I_{geo}: Accum, D40, rw, D30, H, D20, D10 I_{max}, and ADP (See Appendix C for PCA results).

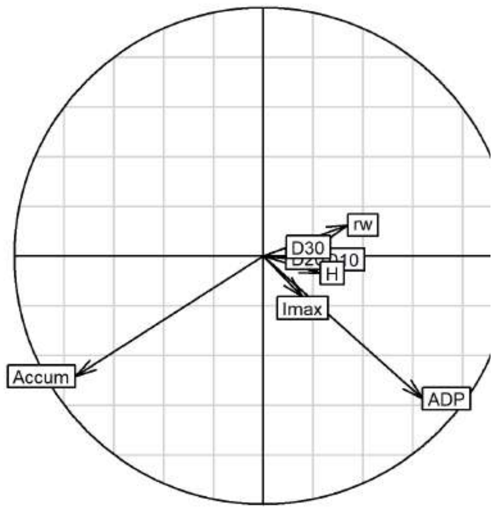

Figure 29 Molinos River accumulation PCA. x = component 3, y = component 4

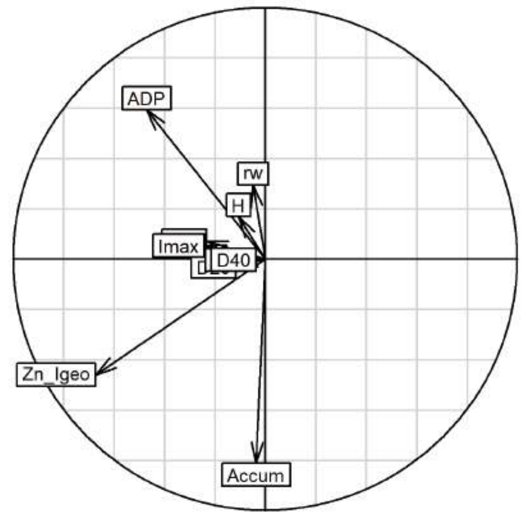

Figure 30 Molinos River Zn geo-accumulation index PCA. x = component 4, y = component 5.

6.2.5 SVM Accumulation and Zn_I_{geo}.

SVM regression models were implemented, considering that there are no accumulation classifications and most MR Zn_I_{geo} classifications are G1 (uncontaminated to moderately contaminated). In this sense, implementing a classification model is not considered appropriate. Nevertheless, it is possible to implement a classification SVM model if observations of *Y* variables have enough classes for the validation process.

The best model for the accumulation prediction is obtained using all the related variables and the ANOVA kernel. The minimum error between the predicted and measured data is 19%, and the maximum is 59%, with a median of 39%. Figure 31 shows that the predicted data is highly underestimated in samples 001-08 and 001-14 and overestimated, especially in samples 001-38 and 001-47. However, this accumulation model fits better than the linear regression options and proves that the proposed methodology works. Thereby, it is possible to apply regression SVM to predict the accumulation in MR and use it as a decision-making tool.

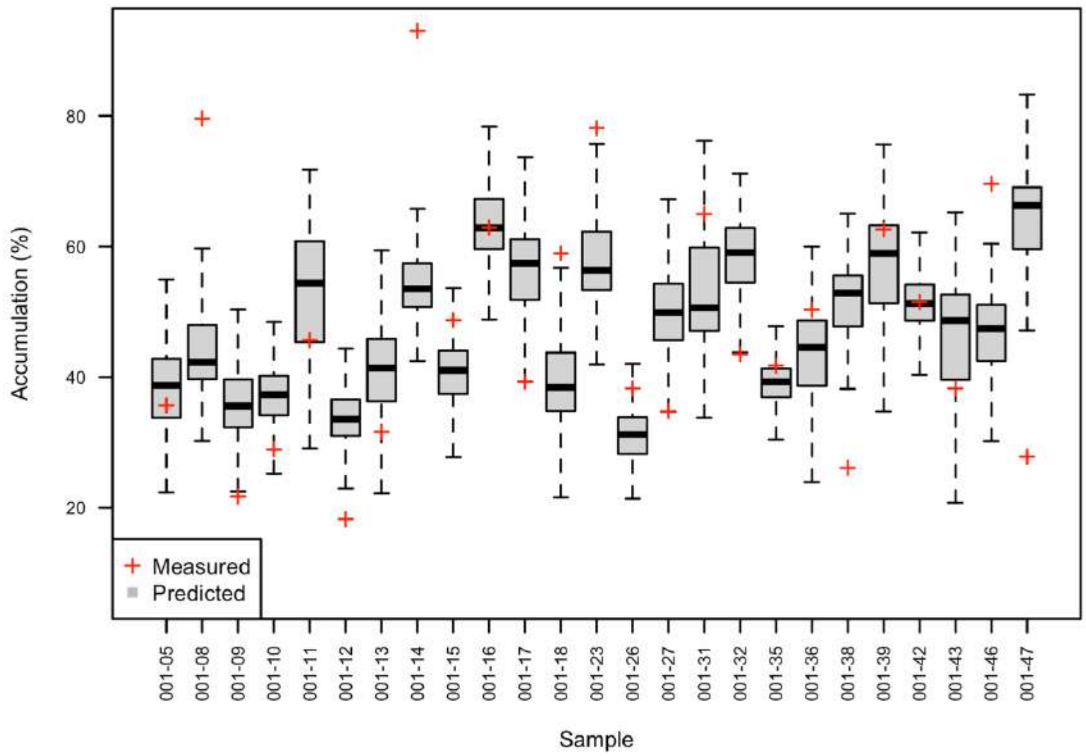

Figure 31 Accumulation support vector machine results (validation data) and measured for each sample

The best Zn_I_{geo} prediction model is obtained using all the related variables and the rbfd kernel. The minimum error between the predicted and measured data is 32%, and the maximum is 109%, with a median of 63%. Figure 32 shows the variation between the measured and predicted data, and the model does not work for values less than zero. For uncontaminated environments (G0), the model predicts a slightly contaminated environment (G1) (see section 3.2.1 for I_{geo} classification values). Although none of the previous classifications is risky, different categories can be expected in scenarios with risk for I_{geo} > 1. Due to MR conditions in which there is no sediment risk by Zn_I_{geo}, the model can be used as a decision-making tool. However, to accurately assess the model's behavior, it would be convenient to apply the proposed methodology to a group of observations with more significant data variability to define its effectiveness.

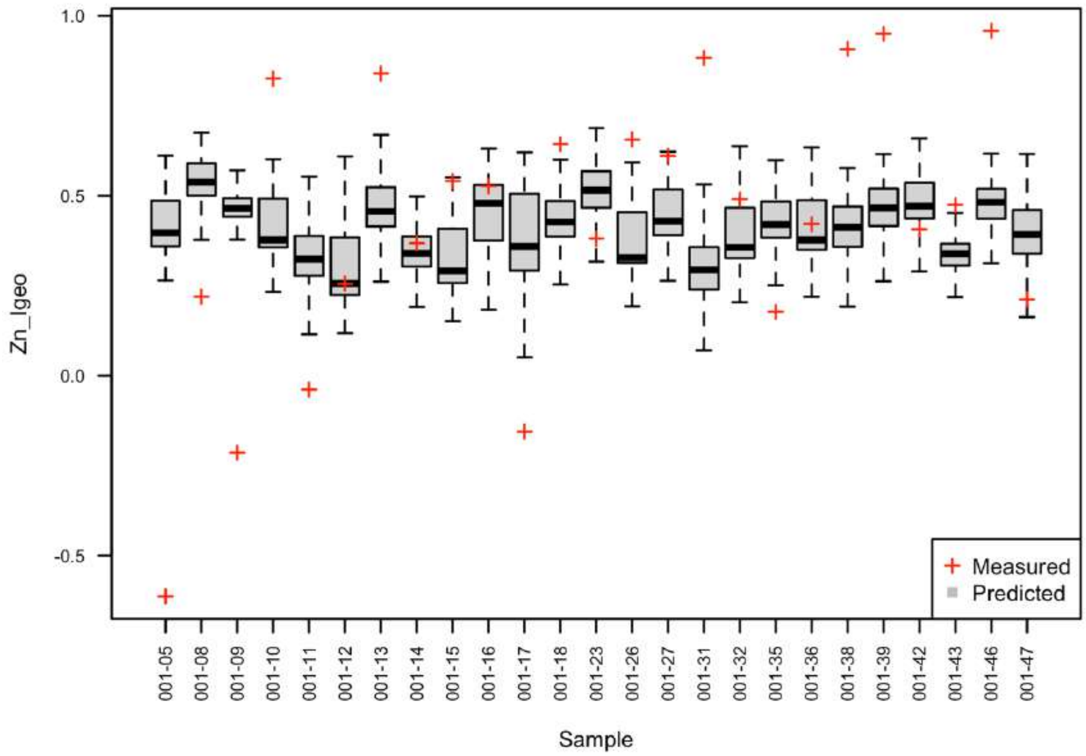

Figure 32 Zn geo-accumulation index (I_{geo}) support vector machine results (validation data) and measured for each sample

Based on the MR results, the proposed methodology to determine variables relationships and data prediction shows that it can be replicated for other urban stormwater drainage structures and avoid expensive laboratory tests to evaluate sediment characteristics.

6.2.6 Accumulation modeling without outliers

According to outliers defined in section 0, these observations are removed from the data, and a new modeling scenario was considered. Cohen's Kappa coefficient analysis is initially rerun to identify new accumulation relationships. As shown in Table 27, a moderate agreement (coefficient 0.59) between accumulation and ADP with a p-value of 0.005 was found, and ADP has a substantial agreement (coefficient 0.69) with D10 and a p-value of 0.002, and a moderate agreement (coefficient 0.47) with D20 and D30 and a p-value of 0.021. Following the proposed methodology, through PCA, it is identified that ADP is the most influential variable in accumulation. The ADP and D10, D20, and D30 were used for the SVM model as independent variables. The best prediction model is obtained using ADP and kernel ANOVA, with a median validation error of 33%, varying between 16% and 51% (Figure 33).

Table 27 Cohen's Kappa Coefficient without outliers for Molinos River accumulation (Accum). ADP: antecedent dry weather period, H: precipitation height, I_{ave}: average intensity, I_{max}: maximum intensity (mm/h), dw: dray weather days, Pb_EF: enrichment factor by Pb, Cd_EF: enrichment factor by Cd.

var1	var2	p-value	Agreement	Estimate	var1	var2	p-value	Agreement	Estimate
H	**D90**	0.001	Substantial	0.69	**Iave**	**D30**	0.019	Moderate	0.48
Iave	**D90**	0.001	Substantial	0.69	**Imax**	**D30**	0.019	Moderate	0.48
ADP	**D10**	0.002	Substantial	0.68	**Imax**	**D90**	0.019	Moderate	0.48
ADP	**Accum**	0.005	Moderate	0.59	**ADP**	**D20**	0.021	Moderate	0.47
dw	**D90**	0.007	Moderate	0.57	**ADP**	**D30**	0.021	Moderate	0.47
rw	**D90**	0.017	Moderate	0.49	**Imax**	**Pb_EF**	0.041	Fair	0.39
H	**D30**	0.019	Moderate	0.48	**rw**	**Cd_EF**	0.045	Fair	0.24

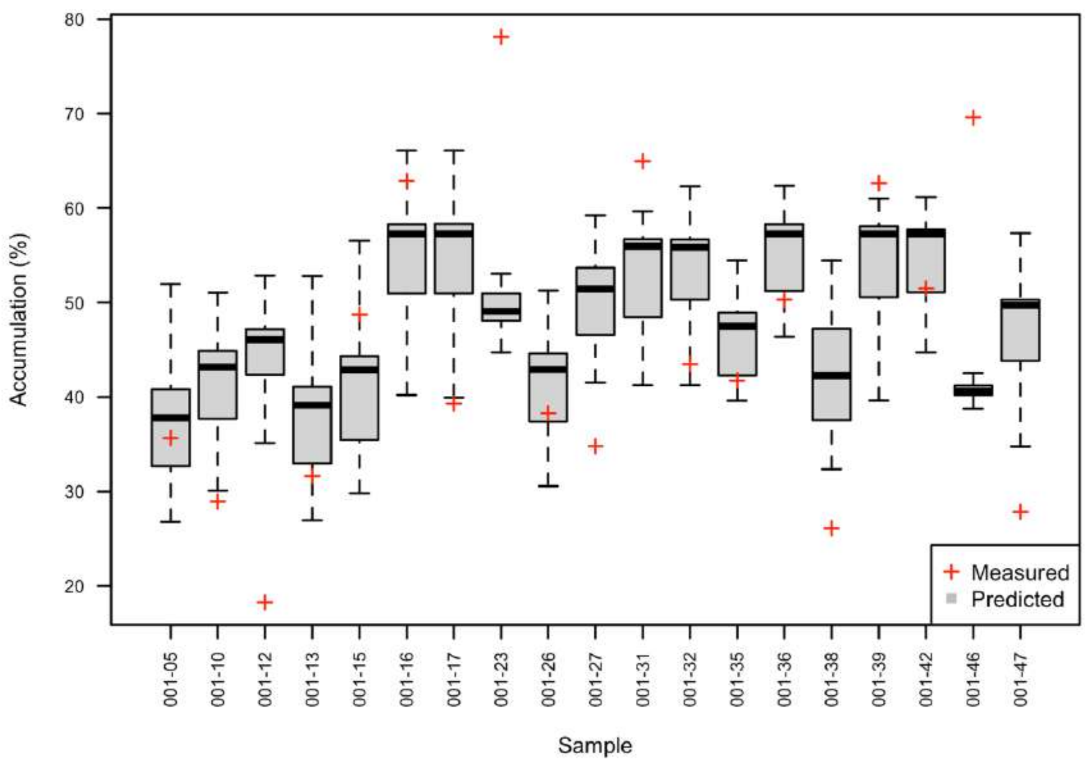

Figure 33 Support vector machine model (validation data) without outliers for Molinos River accumulation

A model with sufficient reliability for data prediction could be obtained despite not finding a model in which there are no differences between the predicted and measured data if having more observations. However, the results of the proposed methodology to analyze the variables show that it can effectively be replicated in another database.

CONCLUSIONS PART C

According to the results of correlation and principal components analysis, there are relationships between heavy metals (HM) concentrations and particle size distribution (PSD) and between HM concentrations and hydrological variables such as antecedent dry weather period (ADP), precipitation height (H) and average rain intensity (I_{ave}). However, these relationships are not consistent between the sampling points, only for the hydrological variables in the Arzobispo River (AR) and the constructed-wetland/storage-tank (CW/ST), since the same pluviometric station was used for both. Therefore, it is not recommended to extrapolate data from one sampling point to another, even if they are in the same basin. Then, it is necessary to carry out sampling campaigns at the points of interest since different results can be obtained from those presented in this thesis.

As a case study, to evaluate the proposed methodology for analyzing relationships and predicting variables, data from the Molinos River (MR) were used. Accumulation geo-accumulation index by Zn (Zn_I_{geo}), and enrichment factor by Pb and Ni were defined as dependent variables based on Cohen's Kappa coefficient. Only an inverse correlation was found between accumulation and ADP. In addition, according to PCA, the ADP is the variable with the most significant influence on the objective variables. Thus, with the relationships found, it was possible to implement the linear regression model and support vector machine (SVM). Founding that SVM for accumulation is a better prediction model than linear regression. Secondly, the linear regression model proved to be a tool to detect outliers, which must be removed, to repeat the analysis process and thus obtain a prediction model with a lower error percentage based on more confident samples and experimental results. Therefore, it is possible to replicate the methodology proposed in this thesis to predict variables for other points of interest or the same place under different hydrological conditions. However, more data is needed to validate the models to replicate them in AR and CW/ST. For accuracy and future research, it is recommended to replicate this methodology by having more observations.

The statistical and modeling analysis presented in this Part demonstrates the importance of understanding some variables' influence on others. In some way, it seeks to inform urban storm drainage stakeholders to focus efforts on decision-making for sediment management. Thus, based on the results, it is necessary to know at least the rainfall characteristics and the sediments' PSD.

REFERENCES PART C

Asuero, A. G., Sayago, A., & González, A. G. (2006). The Correlation Coefficient: An Overview. Critical Reviews in Analytical Chemistry, 36(1), 41–59. https://doi.org/10.1080/10408340500526766

Bąk, Ł., Szeląg, B., Sałata, A., & Studziński, J. (2019). Modeling of Heavy Metal (Ni, Mn, Co, Zn, Cu, Pb, and Fe) and PAH Content in Stormwater Sediments Based on Weather and Physico-Geographical Characteristics of the Catchment-Data-Mining Approach. Water, 11(3), 626. https://doi.org/10.3390/w11030626

Blecken, G.-T., Rentz, R., Malmgren, C., Öhlander, B., & Viklander, M. (2012). Stormwater impact on urban waterways in a cold climate: variations in sediment metal concentrations due to untreated snowmelt discharge. Journal of Soils and Sediments, 12(5), 758–773. https://doi.org/10.1007/s11368-012-0484-2

Bro, R., & Smilde, A. K. (2014). Principal component analysis. Anal. Methods, 6(9), 2812–2831. https://doi.org/10.1039/C3AY41907J

Charters, F. J., Cochrane, T. A., & O'Sullivan, A. D. (2015). Particle size distribution variance in untreated urban runoff and its implication on treatment selection. Water Research, 85(Supplement C), 337–345. https://doi.org/10.1016/j.watres.2015.08.029

Cohen, J. (1960). A Coefficient of Agreement for Nominal Scales. Educational and Psychological Measurement, 20(1), 37–46. https://doi.org/10.1177/001316446002000104

Dray, S., Dufour, A.-B., & Thioulouse, J. (2017). Package ‘ade4.’

Galarza-Molina, S. (2017). Decision-making tool for the operation of a stormwater harvesting system. Pontificia Universidad Javeriana.

Gorgoglione, A., Bombardelli, F., Pitton, B., Oki, L., Haver, D., & Young, T. (2018). Role of Sediments in Insecticide Runoff from Urban Surfaces: Analysis and Modeling. International Journal of Environmental Research and Public Health, 15(7), 1464. https://doi.org/10.3390/ijerph15071464

Hernández, N., Caradot, N., Sonnenberg, H., Rouault, P., & Torres, A. (2021). Support Vector Machines Used for the Prediction of the Structural Conditions of Pipes in Bogota’s Sewer System. Ingenieria y Universidad, 25. https://doi.org/10.11144/Javeriana.iued25.svmu

Karatzoglou, A., Smola, A., Hornik, K., & Zeileis, A. (2004). kernlab - An S4 Package for Kernel Methods in R. Journal of Statistical Software, 11(9), 1–20.

Karlavičienė, V., Švedienė, S., Marčiulionienė, D. E., Randerson, P., Rimeika, M., & Hogland, W. (2009). The impact of storm water runoff on a small urban stream. Journal of Soils and Sediments, 9(1), 6–12. https://doi.org/10.1007/s11368-008-0038-9

Kim, J.-Y., & Sansalone, J. J. (2008). Event-based size distributions of particulate matter transported during urban rainfall-runoff events. Water Research, 42(10–11), 2756–2768. https://doi.org/10.1016/j.watres.2008.02.005

Landis, J. R., & Koch, G. G. (1977). The Measurement of Observer Agreement for Categorical Data. Biometrics, 33(1), 159. https://doi.org/10.2307/2529310

Li, Z., Zhang, W., & Shan, B. (2019). The effects of urbanization and rainfall on the distribution of, and risks from, phenolic environmental estrogens in river sediment. Environmental Pollution, 250, 1010–1018. https://doi.org/10.1016/j.envpol.2019.04.108

Liu, A., Duodu, G. O., Mummullage, S., Ayoko, G. A., & Goonetilleke, A. (2017). Hierarchy of factors which influence polycyclic aromatic hydrocarbons (PAHs) distribution in river sediments. Environmental Pollution, 223, 81–89. https://doi.org/10.1016/j.envpol.2016.12.034

Ma, H., Ding, F., & Wang, Y. (2022). A novel multi-innovation gradient support vector machine regression method. ISA Transactions. https://doi.org/10.1016/j.isatra.2022.03.006

Ma, Y., Hao, S., Zhao, H., Fang, J., Zhao, J., & Li, X. (2018). Pollutant transport analysis and source apportionment of the entire non-point source pollution process in separate sewer systems. Chemosphere, 211, 557–565. https://doi.org/10.1016/j.chemosphere.2018.07.184

Ma, Y., He, W., Zhao, H., Zhao, J., Wu, X., Wu, W., Li, X., & Yin, C. (2019). Influence of Low Impact Development practices on urban diffuse pollutant transport process at catchment scale. Journal of Cleaner Production, 213, 357–364. https://doi.org/10.1016/j.jclepro.2018.12.198

Nakazawa, M. (2021). fmsb: Functions for Medical Statistics Book with some Demographic Data (R package version 0.7.2.).

Peterson, B. G., & Carl, P. (2020). PerformanceAnalytics: Econometric Tools for Performance and Risk Analysis. (R package version 2.0.4.).

R Core Team. (2021). R: A language and environment for statistical computing. R Foundation for Statistical Computing, Vienna, Austria. https://www.r-project.org/

Sansalone, J. J., Buchberger, S. G., Koran, J. M., & Smithson, J. A. (1997). Relationship between particle size distribution and specific surface area of urban roadway stormwater solids. Transportation Research Record, 1601(1), 95–108.

Sivalingam, P., al Salah, D. M. M., & Poté, J. (2021). Sediment Heavy Metal Contents, Ostracod Toxicity and Risk Assessment in Tropical Freshwater Lakes, Tamil Nadu, India. Soil and Sediment Contamination: An International Journal, 30(2), 231–252. https://doi.org/10.1080/15320383.2020.1835822

Tranmer, M., Murphy, J., Elliot, M., & Pampaka, M. (2020). Multiple linear regression. Hummedia.Manchester.Ac.Uk. http://hummedia.manchester.ac.uk/institutes/cmist/archive-publications/working-papers/2020/multiple-linear-regression.pdf

Wang, Q., Zhang, Q., Dzakpasu, M., Chang, N., & Wang, X. (2019). Transferral of HMs pollution from road-deposited sediments to stormwater runoff during transport processes. FRONTIERS OF ENVIRONMENTAL SCIENCE & ENGINEERING, 13(1). https://doi.org/10.1007/s11783-019-1091-x

Wang, Q., Zhang, Q., Wang, X. C., Huang, J., & Ge, Y. (2020). Impacts of key factors on heavy metal accumulation in urban road-deposited sediments (RDS): Implications for RDS management. Chemosphere, 261. https://doi.org/10.1016/j.chemosphere.2020.127786

Wijesiri, B., Egodawatta, P., McGree, J., & Goonetilleke, A. (2016). Understanding the uncertainty associated with particle-bound pollutant build-up and wash-off: A critical review. Water Research, 101, 582–596. https://doi.org/10.1016/j.watres.2016.06.013

Wold, S., Esbensen, K., & Geladi, P. (1987). Principal component analysis. Chemometrics and Intelligent Laboratory Systems, 2(1–3), 37–52.

Zhao, H., & Li, X. (2013). Understanding the relationship between heavy metals in road-deposited sediments and washoff particles in urban stormwater using simulated rainfall. Journal of Hazardous Materials, 246–247, 267–276. https://doi.org/10.1016/j.jhazmat.2012.12.035

PART D: SEDIMENT MANAGEMENT

INTRODUCTION PART D

The progressive increase of contaminated sediments in aquatic environments has highlighted the need to establish guidelines for monitoring and management, mainly due to the water quality deterioration caused by diffuse sources associated with urban stormwater runoff (Sharley et al., 2017). There are few studies on the ecological quality of urban drains, so there is a critical need to develop standardized integrative methodologies aligned with a statistical approach to monitoring, evaluating the environmental quality, and managing urban storm drains (Arakel, 1995; Tixier et al., 2011; Wang et al., 2018).

Bearing in mind that for the proper drainage of stormwater runoff, sediments must be periodically removed and disposed of appropriately because they reduce the capacity of drainage systems and produce overflow pollution during heavy rainfall events (Nawrot & Wojciechowska, 2017; Wang et al., 2018). In addition, dredging produces large volumes of material per year, representing a key management element for local authorities. Urban drainage managers need relevant information to estimate dredging frequency to prevent the accumulation of urban runoff sediment and its associated pollutants (Lintern et al., 2016; Selbig, 2015; Wiest et al., 2018). It is known that the discharge of sediments for long periods generates affectations in the disposal areas and their surroundings due to the migration of pollutants, which creates concern about the accumulation of contaminants in the soil and underground water (Bhairappanavar et al., 2018). In this regard, the main zones in which sediments are deposited most frequently must be considered to improve sustainable management and different potential uses according to their quality characterization and risk assessment (Merchan et al., 2014; Sébastian et al., 2014; Wu et al., 2018).

As stated by Köthe, (2003), "*Sediment management means all the steps in sediment handling (uptake/dredging, transport and disposal) including characterisation and assessment of the sediment quality.*" Using the urban basin as a small-scale management element is critical for the proper territorial planning of cities. Urban drainages are generally impermeable, increasing the chances of a flood event occurring. In addition to the hydraulic impact, they also represent environmental, social, and economic influence (Lipeme Kouyi et al., 2018).

Therefore, in PARTD, management options are proposed based on sediment characterization and data analysis presented in previous parts. In CHAPTER 7, the possible management elements to be implemented are presented. In CHAPTER 8, the applicability of the elements is evaluated with the results obtained for the three sampling sites analyzed.

CHAPTER 7 MANAGEMENT OPTIONS

Among the management alternatives proposed by different researchers, the possibility of carrying out treatment or reuse according to the quantity and quality of the sediments in civil engineering applications has been raised. Considering that 90 percent of the dredged material is acceptable for alternative reuses as the dredged material consists mainly of natural sediments such as gravel, sand, silt, clay, and organic particles. However, economic suitability and environmental acceptability still need to be considered (Bhairappanavar et al., 2018; El-Mufleh Al Husseini et al., 2013; Sébastian et al., 2014). The elements presented in this chapter are tools for the manager to decide the dredging time of the sediments and appropriate disposal or reuse.

The results obtained in the previous parts are elements for sediment management. Management options such as reusing sediments, formulating protocols for disposal and extraction, or decision-making systems can be considered. Figure 34 presents a scheme of the proposal for implementing the previous results on sediment management.

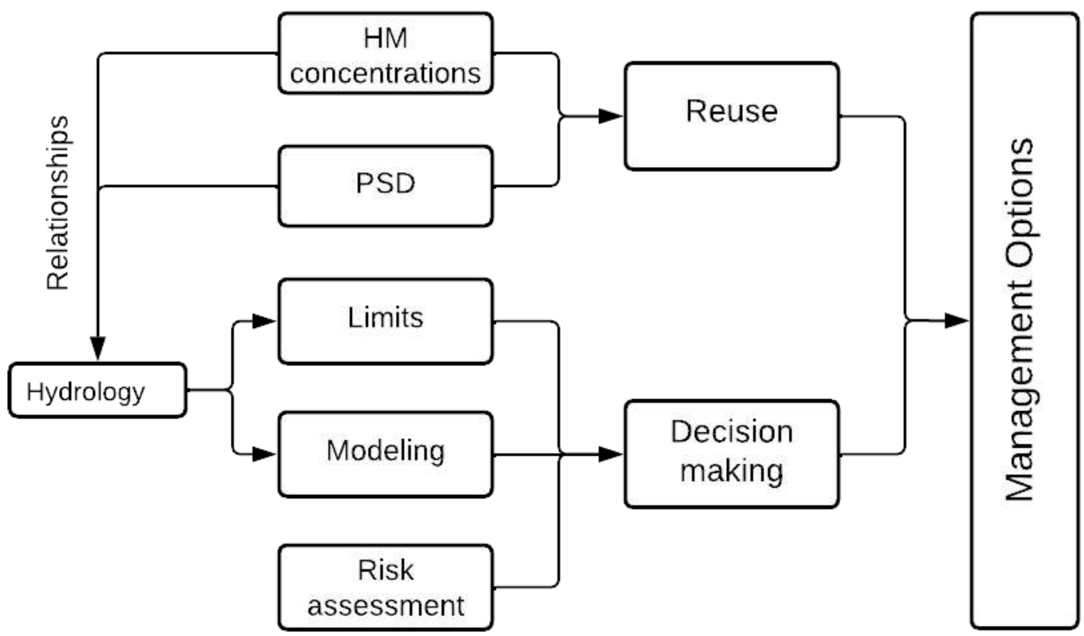

Figure 34 Management options proposal. HM: heavy metals. PSD: particle size distribution.

7.1 Sediment reuse

Regarding the characterization of sediments (PART A), reuse options can be established based on the permissible limit heavy metals (HM) concentrations or particle size distribution (PSD) for different activities such as agriculture and construction. According to the chemical characteristic, to reuse some waste, the pollutants concentrations in materials must be lower than the threshold established in some guidelines (Table 28). These guidelines usually define the permissible values for reuse materials in agriculture, gardening, and soil restoration. In addition to the characteristics of the particles analyzed in this research, these guidelines include other parameters that should be considered to determine their applicability.

In Colombia, through the manual of good engineering practices in title F, the limit concentrations are established to reuse material in three categories: category A, for agricultural use; category A - other uses, for restoration of contaminated soils; and category B, for the stabilization of slopes or soil cover eroded by mining (Ministerio de Vivienda, 2012). For the distribution of waste on land for agricultural reuse, different guides establish maximum concentration limits of HM: the Food and Agriculture Organization of the United Nations (FAO), countries such as Denmark, South Africa, and the Australian state of Tasmania (Danish Environmental Protection Agency, 2001; Pescod & Rome, 1992; Snyman & Herselman, 2006; Tasmanian Biosolids Reuse Guidelines, 1999). Additionally, the United States of America (USA) has a regulation for reuse in soil restoration and Tasmania for application in residential gardens, which is more restricted due to direct contact with children (Tasmanian Biosolids Reuse Guidelines, 1999; Biosolids Technology Fact Sheet Land Application of Biosolids, 2000).

*Table 28. Threshold heavy metal concentrations for material reuse expressed in mg/kg. * South Africa, USA, and Colombia -Other uses have the same limits.*

COUNTRY	Reuse option	Cd	Cr	Cu	Pb	Ni	Zn
Colombia[a]	Cat A / Agriculture	0.7	70	70	45	25	200
	Cat A / Other Uses	39.0	1200	1500	300	420	2800
	Cat B	85.0	3000	4300	840	420	7500
Denmark[b]	Agriculture	0.5	30	40	40	15	100
FAO[c]	Agriculture	3.0	400	80	300	50	200
Tasmania[d]	Home gardens	3.0	100	100	150	60	200
	Agriculture	20.0	500	1000	420	270	2500
USA[e]	Land Applications	39.0	-	1500	300	420	2800
South Africa[f]	Agriculture	40.0	1200	1500	300	420	2800

Source: a (Ministerio de Vivienda, 2012)*, b* (Danish Environmental Protection Agency, 2001)*, c (Pescod & Rome, 1992), d* (Tasmanian Biosolids Reuse Guidelines, 1999)*, e* (Biosolids Technology Fact Sheet Land Application of Biosolids, 2000)*, f (Snyman & Herselman, 2006)*

According to Colombian legislation, materials used in embankments are classified into five categories based on the material's intrinsic characteristics: selected soils, adequate soils, tolerable soils, marginal soils, and unsuitable soils. In addition to the particle size, the amount of organic matter, the content of soluble salts, and the liquid limit, among others, are considered (Capítulo 2: Especificaciones Generales de Construcción de Carreteras 2022, 2022). Only the conditions related to grain size will be considered to reuse sediments in embankments. Tests must be carried out to evaluate the other parameters required by the standard. The characteristics of each type of soil are described below.

- Selected soils: the maximum size of the aggregate (D_{max}) ≤ 100 mm and the percentage that passes the No. 40 sieve (0.425 mm) ≤ 15%. If the last condition is not met, it is mandatory that the percentage passing the No. 10 (2 mm) sieve < 80%, the percentage passing the No. 40 sieve < 75%, and the percentage passing the No. 200 (0.075 mm) sieve < 25%. Its use is recommended for the area of the crest, foundation, core, or erosion control soil.

- Suitable soils: D_{max} ≤ 100mm, the percentage passing the No. 10 sieve < 80%, and the percentage passing the No. 200 sieve < 35%. Its use is recommended for the area of the crest, foundation, core, or erosion control soil.
- Tolerable soils: D_{max} ≤ 100mm. Its use is recommended for the foundation, core, or erosion control soil.
- Marginal soils: percentage passing 3/4-inch (19 mm) sieve > 70% or percentage passing No. 200 sieve > 35%. Additional studies are required to justify its use.
- Unsuitable soils: those that do not meet the requirements for other types of soils.

7.2 Decision-making

Decision-making is a sediment management element based on the available information, that is, the characterization of sediments, risk analysis, among others. Accordingly, protocols can be generated to protect the environment and people's health (section 7.2.1), activate alert systems based on indicators (section 7.2.2), or implement prediction tools (section 7.2.3).

7.2.1 Protocols

Estimating the risk indexes (CHAPTER 4) for the fauna, the environment, and human health, are elements to define protocols and avoid affectations on the receiving bodies due to the discharge of sediments in the disposal sites by the magnification of contaminants and people's health affectations. For the protocol proposal, it is advisable to develop interdisciplinary working groups in which public health, environmental, and biologists participate, as well as experts in urban drainage management, who are generally in charge of decision-making for the dredging of sediments.

For the development of this section, a working group was formed through the Instituto Javeriano del Agua of the Pontificia Universidad Javeriana, with the maintenance staff of the University campus, public health officers, medical students, biologists, and civil engineers. The constructed-wetland/storage-tank (CW/ST) was selected as a working point to develop a protocol for the safe approach by workers exposed to the sediments accumulated in the sand traps, focused on the impact of carcinogenic heavy metals (HM) on health (section 3.3). Therefore, the health risks associated with HM exposure were identified, and a proposal for risk mitigation was developed.

7.2.2 Warning indicators

Warning indicators are tools to detect real impacts, provide information to implement management decisions to avoid harm, and use standard measurements with known reliability and low measurement error (van Dam et al., 1998). The development of warning indicators helps predict changes in ecosystems associated with anthropogenic activities and develop management strategies based on the identification of tipping points (Burthe et al., 2016).

The lack of knowledge about the characteristics of the sediments and the adverse effects of excessive accumulation in urban drainage structures highlights the need to develop alert systems for sediment management. The determination of the breaking points is based on decision-making about the risk, accumulation, or concentration of a contaminant, which are the dependent or Y variables. For them, it is necessary to know with which variable or variables the Y variable is related, which ideally should be easier to measure or obtain data (X variables). Therefore, identifying inflection points can define alert indicators in managing urban sediments. Since they are based on the continuous measurement of the X variables, they are a corrective and not a preventive tool. To decide if it is necessary to dredge the channel due to a high accumulation of sediments, it is required to know the variables with which the accumulation is related and to have the data of these variables. Suppose the sediments of the structure have been extracted. In that case, the X variables must be analyzed, which allows identifying concentrations or risks to define adequate disposal or reuse.

Based on the data analysis presented in the previous chapter, the limits based on the relationships between pairs of variables (section 5.1.3) will be used as elements to establish the warning indicators. As demonstrated in section 6.1, since it is impossible to extrapolate the information from one sampling point to another, the implementation of this management strategy has the limitation that turning points must be established for each study site.

7.2.3 Prediction tools

Data modeling is a valuable tool for predicting and preventing. It is a preventive tool to reduce the flooding risk due to the clogging of structures or human health and environmental risk due to the accumulation of pollutants. Through modeling, scenarios based on historical data can be created to predict future behavior or create scenarios in which unfortunate events may occur to establish early warning systems. The methodology for modeling sediment characteristics proposed in section 5.2 is an additional tool to transport modeling widely used by other researchers to understand the behavior of particles in drainage systems and their composition.

7.3 Molinos River management elements

The last combination of validation and calibration observations according to the Monte Carlo method (section 5.2) was used to evaluate management strategies as the base scenario for decision-making, as shown in Figure 35.

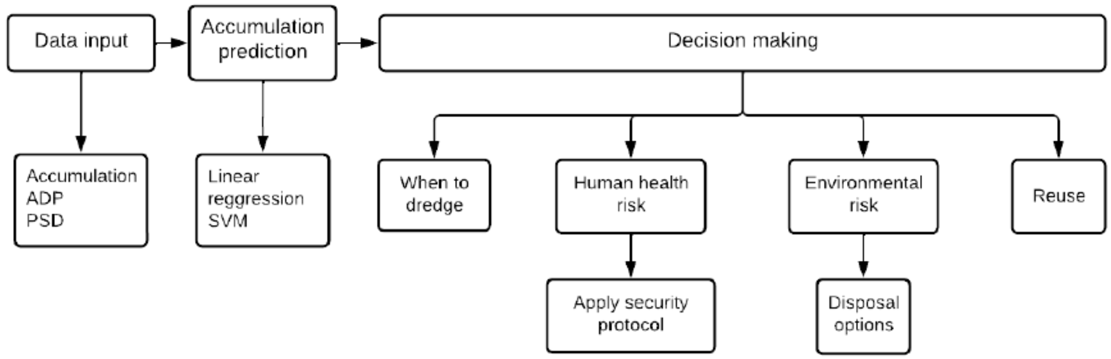

Figure 35 Molinos River Decision making

Calibration observations (Table 29) will be taken as input data for the model following the results of the methodology proposed in section 5.2 to predict the accumulation in the validation observations using the antecedent dry weather period (ADP), which are 4,5,5,0,1 and 3 days. Once the percent accumulation is predicted, it is decided whether to do a sediment dredge. On the other hand, the heavy metal (HM) concentrations and associated risks from the validation observations will be used to make decisions regarding safety protocols, disposal, and reuse options.

Table 29 Input data used to predict accumulation in Molinos River. ADP: antecedent dry weather period

Sample	ADP	Accumulation	Sample	ADP	Accumulation
001-05	6	35.7%	**001-35**	12	41.8%
001-15	4	48.7%	**001-36**	0	50.3%
001-16	0	62.9%	**001-38**	8	26.1%
001-17	0	39.3%	**001-39**	0	62.6%
001-26	4	38.3%	**001-42**	0	51.5%
001-27	2	34.8%	**001-47**	3	27.8%
001-32	1	43.5%			

CHAPTER 8 SEDIMENT MANAGEMENT ASSESSMENT

This chapter presents the results of the management options based on the results obtained in previous parts. That is, the reuse options in section 8.1, and management elements based on available information in section 8.2

8.1 Reuse options

Reuse options are analyzed for each sampling site, starting with comparing the HM concentrations against the limits established in each guide. As shown in Figure 36, all the sediment samples from the three points meet the concentrations to be reused in Colombia to restore contaminated soils and stabilize slopes or soil covers eroded by mining. They also comply with the limits to covering agricultural soils in South Africa and Tasmania and restoring soils in the United States of America.

MR does not comply with the other legislations for reuse in agriculture in Colombia, Denmark, and FAO, and for reuse in residential gardens in Tasmania due to the high concentrations of Cu, since 96% of the maximum concentrations measured in the sediment samples exceed the limit values. Additionally, 68% and 44% of the samples exceed the Denmark limits of Ni and Zn, respectively. Similarly, Arzobispo River (AR) does not comply with Cu limits concentrations for gardening (Tasmania) and agricultural reuse (Colombia, Denmark, and FAO) because 87.5% of the sediment samples are above the threshold. Besides, according to Colombia, for use in agricultural soil, some samples do not comply with Cd and Zn concentrations; in Denmark, with the limits for Cd, Ni, and Pb, and finally, FAO and gardening in Tasmania with the Cd concentrations. Finally, the sediments collected from the CWST have significant restrictions since only the Cr concentration met the established values for agricultural reuse in Colombia and Denmark. On the other hand, following FAO and Tasmania gardening recommendations, 71.4% of the samples do not comply with the Cu and Zn limits (see section 2.2.2 for sediments HM concentrations).

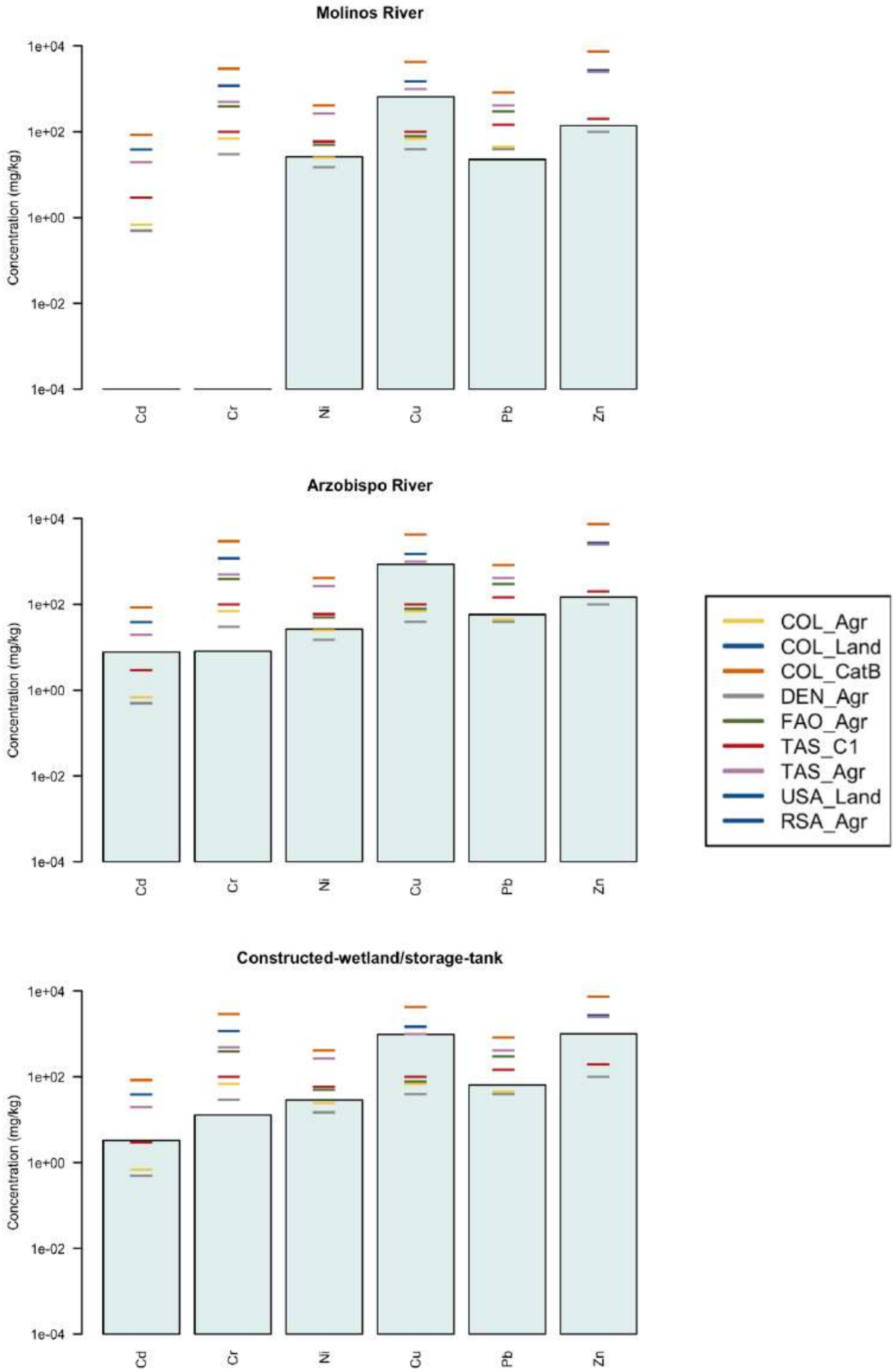

*Figure 36 Comparison between maximum measured heavy metals concentrations in sediments and limit concentrations for reuse. COL: Colombia, DEN: Denmark, TAS: Tasmanian, USA: United States of America, RSA: South Africa. Agr: agricultural reuse, Land: soil restoration, CatB: stabilization of slopes or soil cover eroded by mining, C1: residential gardens. *COL_Land, USA_Land, and RSA_Agr have the same limits.*

For the reuse of sediments collected, from the three sampling points, as material for embankments, following Colombian regulations, the D_{max} is met since the maximum particle size measured is 1000 mm. Alike complies with the requirements of tolerable soils to be used in the foundation zone, core, or as cover soil. As shown in Table 30 sediments are composed mainly of fine particles; therefore, they are inadequate to be used as suitable or selected soils. Besides, 64%, 62.5%, and 71.4% of the sediment samples collected in MR, AR, and CW/ST are classified as marginal soils, implying that additional analyses must consider their reuse (see section 2.2.1 for sediments PSD).

Table 30 Percentage of samples that meet the requirements to be used in embankments.MR: Molinos River, AR: Arzobispo River, CW/ST: constructed-wetland/storage-tank

Sive	Passing	MR	AR	CW/ST
3/4 in	**>70%**	100%	100%	100%
No. 10	**< 80%**	0%	0%	0%
No. 40	**≤ 15%**	0%	0%	0%
	< 75%	12%	12.5%	0%
No. 200	**< 25%**	32%	37.5%	0%
	< 35%	36%	37.5%	28.6%
	> 35%	64%	62.5%	71.4%

8.2 Management decision-making.

8.2.1 A safe protocol for sediment management

Although there are methodologies to assess the health risk due to accidental exposure to sediments loaded with carcinogenic HM (section 3.3), no studies were found in which the secondary effects on health are evaluated, specifically for those workers who dredge the material of the different urban storm drainage structures. The impacts on workers' health by heavy metals, Cd is recognized as a probable carcinogen, and Cr and Ni as confirmed carcinogens, all three with evidence in the development of lung cancer (US EPA, 2022).

The proposed risk mitigation plan for workers in contact with the CW/ST sediments included a series of interventions. (I) Inform workers about the risk with the support of expert staff from the Faculty of Engineering and Medicine. (ii) The minimum recommended personal protection elements are a cap, helmet, high-efficiency mask (N-95), face shield or glasses made of non-glass material, waterproof gloves, ideally non-slip, and PVC boots. (iii) Develop visual supports that facilitate understanding and guarantee safe maintenance in which the proposed protection elements are clarified, information on risks and healthy behaviors in the work environment, separated into three moments: before, during, and after exposure present in the CW/ST (Serna-Henao et al., 2022) (See Appendix D for the graphic supports).

8.2.2 Molinos River management

The evaluation of decision-making in sediment management is made for MR based on the results obtained in section 6.2. This will be done for the accumulation and the geo-accumulation index by Zn (Zn_I_{geo}), the dependent variables found by Cohen's Kappa coefficient.

The accumulation negatively correlates with ADP. That is, there will be more sediment accumulation in the channel as the days in dry weather decrease. As an inflection point, it was found that from zero days in ADP, the accumulation increases. It is estimated that the primary source of the sediments is runoff due to the conformation of the basin at the sampling point, which is mainly surrounded by impervious surfaces for residential land use (section 1.1). Thus, the contribution of sediments increases as there is daily rainfall. Otherwise, when there are days without rain, there will be no contribution of particles to the channel by runoff. Therefore, for decision-making regarding sediment dredging, the number of consecutive days with rainfall must be counted for estimating the amount of accumulated material. However, to predict the accumulation in the channel, it is possible to implement the modeling methodology since it uses ADP as an input variable, for which different scenarios based on dry days can be established and thus estimate the percentage of accumulation in the channel.

On the other hand, Zn_I_{geo} has a negative correlation with D10, D20, D30, and D40. This means that as the size of the particle increases, the risk index decreases. The alert value is for a condition where there is a risk, $Zn\_I_{geo}>1$, equivalent to moderately contaminated (G2) (section 4.2). This implies that there will be a safe scenario if the particle size is greater than 25, 61, 80, and 90 μm for D10, D20, D30, and D40, respectively. A safe scenario implies that it is possible to dispose of the sediments without affecting the environment since the influence of anthropogenic factors on Zn concentrations will not be significant.

Following the proposed methodology in section 7.3, the accumulation predicted by the model for the validation samples are shown in Table 31. As expected from the data limits, the most significant accumulation occurs on fewer ADP days: samples 001-23 and 001-31. Thus, sediments will accumulate in rainy seasons in the channel, implying that sediment dredging can be scheduled during a dry period after the accumulation occurs.

Table 31 Accumulation predicted and measured for Molinos Revier in validation samples

Sample	Accumulation		Sample	Accumulation	
	Predicted	Measured		Predicted	Measured
001-10	37.0%	28.9%	**001-23**	50.9%	78.13%
001-12	36.1%	18.3%	**001-31**	47.7%	65.0%
001-13	36.1%	31.6%	**001-46**	39.5%	69.6%

For the same samples in which the accumulation was predicted, the risk index by Zn_I_{geo} is evaluated based on the limits determined in section 6.2.2, which uses D10 to D40 (Table 32). Thus, the only sample of those analyzed that would have a risk would be 001-12 since the values of D30 and D40 exceed the established limit (Table 26). Therefore, based on this index, except for sample 001-12, the samples are considered environmentally safe to be disposed of.

Table 32 Molinos River granulometry values used for predicting Zn_Igeo

Sample	D10	D20	D30	D40	Sample	D10	D20	D30	D40
001-10	17.34	30.63	47.64	75.10	**001-23**	10.10	20.43	34.21	54.66
001-12	20.40	57.03	145.94	224.12	**001-31**	13.99	26.33	44.46	72.82
001-13	14.03	26.10	40.31	59.55	**001-46**	11.55	21.19	33.03	51.47

Additionally, according to the HM concentrations (Table 33), for the samples analyzed following Colombian regulations, the sediments can be reused in soil remediation or as construction raw material. Regarding the worker's health risk, there is a tolerable risk for Ni, so it is recommended to follow all the safety health instructions. These concentrations carry low-risk indices for Cd, Cr, Ni, and Pb; hence the sediments can be disposed of anywhere without causing damage. However, according to the concentrations of Zn and Cu according to the pollution index (PI), the samples are moderately and highly contaminated, and according to I_{geo}, they are weakly (G1) and heavily polluted (G4), respectively (section 3.2). Therefore, due to the degree of contamination associated with Cu, the secondary effects that may be generated in the disposal sites must be considered.

Table 33 Molinos River decision-making heavy metals concentrations

	Cd	Cr	Ni	Cu	Pb	Zn
001-10	0.21	0.00	21.85	607.05	19.36	127.55
001-12	0.00	0.00	19.96	545.36	13.49	85.94
001-13	0.00	0.00	21.06	650.81	13.99	128.86
001-23	0.00	0.00	16.43	532.43	8.52	93.74
001-31	0.00	0.00	17.32	557.79	7.75	132.73
001-46	0.00	0.00	14.33	570.47	3.06	139.86

CONCLUSIONS PART D

As a management tool, sediments could be reused in different activities according to their characteristics. In this regard, in Colombia, the collected sediments from the Molinos River (MR), Arzobispo river (AR), and the constructed-wetland/storage-tank (CW/ST), meet heavy metal specifications to be reused for soil restoration and as raw construction material. However, construction reuse must also comply with a specified particle size. The three sampling points have fine particles and meet the requirements of tolerable soils for use in embankments. According to the results, reuse as an alternative for sediment disposal breaks the paradigm that sediments are waste. A cost analysis is recommended to determine the economic benefits of implementing sediment reuse.

A protocol is proposed for the safe management of sediments accumulated in the CW/ST based on the risk to workers' health due to concentrations of carcinogenic heavy metals. Decision-making is based on data analysis, is necessary to have characterized the sediments. However, only a few sampling campaigns are needed to establish the protocols per basin.

The results of decision-making in MR show that an accumulation greater than 45% is generated in the channel for days in antecedent dry weather period (ADP) <1; thus, for rainy seasons, a high accumulation of particles is expected, which must be dredged complying with safety protocols for the health of workers due to the tolerable risk of developing cancer associated with Ni concentrations. On the other hand, once these sediments are dredged, they can be reused for soil restoration and construction due to their chemical characteristics; however, due to the particle size, they only meet the conditions to be reused as tolerable material for slopes. Moreover, as usual in dumps, disposing of the material does not threaten the environment. Therefore, decision-making is based on complete sediment management, dredging, and disposal. To make decisions regarding management in other basins, it is necessary to have sufficient information, especially on the characteristics of the particles, that allows following the methodology proposed throughout this document.

According to the analysis, it is possible to establish alternatives that improve the management of urban drainage systems, including sediments. However, for the application, the managers must have the characterization of the sediments as basic information to continue with the application of the proposed methodology, in addition to all the parameters required for the reuse to comply with the specifications determined in each place.

REFERENCES PART D

Arakel, A. V. (1995). Towards developing sediment quality assessment guidelines for aquatic systems: An Australian perspective. Australian Journal of Earth Sciences, 42(4), 335–369. https://doi.org/10.1080/08120099508728207

Bhairappanavar, S., Liu, R., & Coffman, R. (2018). Beneficial uses of dredged material in green infrastructure and living architecture to improve resilience of Lake Erie. Infrastructures, 3(4). https://doi.org/10.3390/infrastructures3040042

Burthe, S. J., Henrys, P. A., Mackay, E. B., Spears, B. M., Campbell, R., Carvalho, L., Dudley, B., Gunn, I. D. M., Johns, D. G., Maberly, S. C., May, L., Newell, M. A., Wanless, S., Winfield, I. J., Thackeray, S. J., & Daunt, F. (2016). Do early warning indicators consistently predict nonlinear change in long-term ecological data? Journal of Applied Ecology, 53(3), 666–676. https://doi.org/10.1111/1365-2664.12519

Danish Environmental Protection Agency. (2001). Soil. In Environmental Factors and Healt. https://www2.mst.dk/udgiv/publications/2001/87-7944-519-5/html/kap06_eng.htm#kap6.1.2

El-Mufleh Al Husseini, A., Béchet, B., Gaudin, A., & Ruban, V. (2013). Trace metal fractionation as a mean to improve on the management of contaminated sediments from runoff water in infiltration basins. Environmental Technology, 34(10), 1255–1266. https://doi.org/10.1080/09593330.2012.745619

Capítulo 2: Especificaciones generales de construcción de carreteras 2022, (2022).

Köthe, H. (2003). Existing sediment management guidelines: an overview. Journal of Soils and Sediments 2003 3:3, 3(3), 139–143. https://doi.org/10.1065/JSS2003.08.082

Lintern, A., Leahy, P. J., Heijnis, H., Zawadzki, A., Gadd, P., Jacobsen, G., Deletic, A., & Mccarthy, D. T. (2016). Identifying heavy metal levels in historical flood water deposits using sediment cores. Water Research, 105, 34–46. https://doi.org/10.1016/j.watres.2016.08.041

Lipeme Kouyi, G., Barraud, S., Becouze-Lareure, C., Blaha, D., Perrodin, Y., Wiest, L., Aubin, J.-B., Toussaint, J.-Y., Vareilles, S., Mandon, C., Marjolet, L., & Cournoyer, B. (2018). Characterization of and new management insights for sediments in a stormwater detention basin | Caractérisation des sédiments d'un bassin de retenue-décantation des eaux pluviales et éléments pour la gestion. Techniques - Sciences - Methodes, 113(9), 65–75. https://doi.org/10.1051/tsm/201809065

Merchan, C. G., Perrodin, Y., Barraud, S., Sébastian, C., Becouze-Lareure, C., Bazin, C., & Kouyi, G. L. (2014). Spatial variability of sediment ecotoxicity in a large storm water detention basin. Environmental Science and Pollution Research, 21(8), 5357–5366. https://doi.org/10.1007/s11356-013-2325-2

Ministerio de Vivienda, C. y T. (2012). TÍTULO F Sistemas de Aseo Urbano.

Nawrot, N., & Wojciechowska, E. (2017). Review on the quality of sediments from the stormwater drainage system in the urban area. E3S Web of Conferences, 17, 00064. https://doi.org/10.1051/e3sconf/20171700064

Pescod, M. B., & Rome, N. (1992). Food and Agriculture Organization of the United. http://files/345/Pescod y Rome - Food and Agriculture Organization of the United.pdf

Sébastian, C., Barraud, S., Ribun, S., Zoropogui, A., Blaha, D., Becouze-Lareure, C., Kouyi, G. L., & Cournoyer, B. (2014). Accumulated sediments in a detention basin: Chemical and microbial hazard assessment linked to hydrological processes. Environmental Science and Pollution Research, 21(8), 5367–5378. https://doi.org/10.1007/s11356-013-2397-z

Selbig, W. R. (2015). Characterizing the distribution of particles in urban stormwater: advancements through improved sampling technology. Urban Water Journal, 12(2), 111–119. https://doi.org/10.1080/1573062X.2013.820334

Serna-Henao, D., Zúñiga-Castro, S. P., Suárez-Carreño, M. J., Zambrano-González, M. L., Vargas-Fierro, M. J., Ruiz-Cossío, V., Pimiento, M. A., & Palencia-Sánchez, F. (2022). Protocolo para manejo seguro de sedimentos de escorrentía pluvial en el campus de la Pontificia Universidad Javeriana Bogotá.

Sharley, D. J., Sharp, S. M., Marshall, S., Jeppe, K., & Pettigrove, V. J. (2017). Linking urban land use to pollutants in constructed wetlands: Implications for stormwater and urban planning. Landscape and Urban Planning, 162, 80–91. https://doi.org/10.1016/j.landurbplan.2016.12.016

Snyman, H. G., & Herselman, J. E. (2006). Selection of Management Options. In Guidelines for the Utilisation and Disposal of Wastewater Sludge (2nd ed., Vol. 1, Issue 5).

Tasmanian Biosolids Reuse Guidelines, 73 (1999).

Tixier, G., Lafont, M., Grapentine, L., Rochfort, Q., & Marsalek, J. (2011). Ecological risk assessment of urban stormwater ponds: Literature review and proposal of a new conceptual approach providing ecological quality goals and the associated bioassessment tools. Ecological Indicators, 11(6), 1497–1506. https://doi.org/10.1016/j.ecolind.2011.03.027

Biosolids Technology Fact Sheet Land Application of Biosolids, EPA 832-F-00-064 (2000).

US EPA. (2022, November 14). Integrated Risk Information System | US EPA. https://www.epa.gov/iris

van Dam, R. A., Camilleri, C., & Finlayson, C. M. (1998). The potential of rapid assessment techniques as early warning indicators of wetland degradation: A review. Environmental Toxicology and Water Quality, 13(4), 297–312. https://doi.org/10.1002/(SICI)1098-2256(1998)13:4<297::AID-TOX3>3.0.CO;2-2

Wang, J., Zhao, Y., Zhang, P., Yang, L., Xu, H., & Xi, G. (2018). Adsorption characteristics of a novel ceramsite for heavy metal removal from stormwater runoff. Chinese Journal of Chemical Engineering, 26(1), 96–103. https://doi.org/10.1016/j.cjche.2017.04.011

Wiest, L., Baudot, R., Lafay, F., Bonjour, E., Becouze-Lareure, C., Aubin, J.-B., Jame, P., Barraud, S., Kouyi, G. L., Sébastian, C., Sébastian, C., & Vulliet, E. (2018). Priority substances in accumulated sediments in a stormwater detention basin from an industrial area. Environmental Pollution, 243, 1669–1678. https://doi.org/10.1016/j.envpol.2018.09.138

Wu, X., Yu, J., Qiu, H., & Fang, H. (2018). Pollution and ecological risk assessment of nutrients associated with deposited sediments collected from roof and road surfaces. Environmental Science and Pollution Research, 25(9), 8943–8950. https://doi.org/10.1007/s11356-017-1132-6

GENERAL CONCLUSIONS

Understanding the characterization of the sediments retained in urban runoff drainage systems is essential for their management since contamination indices can be established, safety protocols developed, and decision-making facilitated. Thus, sediment particle size distribution (PSD), heavy metals (HM) concentrations, and accumulation were analyzed for three stormwater systems in Bogotá, Colombia: Molinos River (MR), Arzobispo River (AR), and the Constructed-wetland/storage-tank (CW/ST) from the Pontificia Universidad Javeriana. On the other hand, the daily precipitation information in the city's early warning system was downloaded from stations near the sampling points to analyze the hydrology and flow runoff. This research proposes experimental and statistical modeling methodologies that allow management alternatives for the sediments retained in urban stormwater systems.

PSD shows that the sediments collected in the three sampling points can be classified as fine particles due to the D50 being around 110 μm and the D90 being less than 500 μm. Additionally, approximately 37% of the samples are lower than 63 μm. On the other hand, MR is the one with the lowest HM concentrations, and AR is the one with the highest, except for Cu and Zn, which are higher in constructed-wetland/storage-tank CW/ST. Being fine particles with the capacity to adsorb high loads of HM that affects the stormwater quality since these do not dissolve, and their concentrations tend to magnify. Further investigation is needed to know the relation between land use and HM concentrations to establish their source.

Concerning the results of the environmental indices, the concentrations of Cu and Zn represent a threat to this basin, in addition to the fact that they come from anthropic activities, which is why they widely exceed background concentrations. Regarding human health, sediments represent a high risk for children and above tolerable risk for adults associated with carcinogenic metals (Cr, Cd, and Ni), primarily due to accidental ingestion followed by dermal contact due to Ni content. In terms of environmental conservation, it is necessary to remove sediments from urban areas in the source before they are discharged into natural water bodies since most pollutants come from human activities and remain attached to the particles, causing environmental contamination and pollutant magnification. In cases where manual extraction is carried out, the health risk increases for the workers in charge of these tasks, and inadequate disposal may increase exposure to different population groups.

According to the results of correlation and principal components analysis, relationships are not consistent between the three sampling points. Therefore, it is not recommendable to extrapolate data characterization from one sampling point to another, even if they are in the same basin. Then, it is necessary to carry out sampling campaigns at the points of interest since different results can be obtained from those presented in this thesis. The MR (used as a study case) accumulation, geo-accumulation index by Zn (Zn_I_{geo}), and enrichment factor by Pb and Ni were the variables which have relationships based on Cohen's Kappa coefficient, with an inverse correlation between accumulation and antecedent dry weather period (ADP). Founding that support vector machine (SVM) for accumulation is a better prediction model than linear regression. Secondly, the linear regression model proved to be a tool to detect outliers, which must be removed, to repeat the analysis process and thus obtain a prediction model with a lower error percentage based on more confident samples and experimental results. Therefore, it is possible to replicate the methodology proposed in this thesis to predict variables for other points of interest or the same place under different hydrological conditions. However, more data is needed to validate the models to replicate them in AR and CW/ST.

As a management tool, sediment could be reused in different activities according to their characteristics. In this regard, in Colombia, the collected sediments from the MR, AR, and CW/ST, meet HM specifications to be reused for soil restoration and as raw construction material. The three sampling points have fine particles and meet the requirements of tolerable soils for use in embankments. The results of decision-making in MR show that an accumulation greater than 45% is generated in the channel for days in ADP <1; thus, for rainy seasons, a high accumulation of particles is expected, which must be dredged complying with safety protocols for the health of workers due to the tolerable risk of developing cancer associated with Ni concentrations. On the other hand, once these sediments are dredged, they can be reused for soil restoration and construction due to their chemical characteristics; however, due to the particle size, they only meet the conditions to be reused as tolerable material for slopes. Moreover, as usual in dumps, disposing of the material does not threaten the environment. Therefore, decision-making is based on complete sediment management, dredging, and disposal. To make decisions regarding management in other basins, it is necessary to have sufficient information, especially on the characteristics of the particles and the volume extraction that allows following the methodology proposed throughout this document.

The sediment characterization in the three sampling points showed that they are fine particles with high concentrations of Cu and Zn, which are of anthropogenic origin and represent a risk to the environment. On the other hand, the Ni concentrations represent a risk of developing cancer due to accidental ingestion. The results found were used as elements for management as reuse alternatives and sediment accumulation predictions. The above implies that it is possible to use sediments as a resource and not necessarily be discarded as waste, safeguarding the integrity of humans, and conserving the environment. For future work, it is recommended to analyze other basins, evaluate other types of pollutants, and estimate the costs associated with the different disposal alternatives.

HIGHLIGHTS

The concentrations of HM allow the determination of human health risk indexes, with which it is possible to establish protocols to protect the workers' health in charge of the sediment dredging and the inhabitants who live near the disposal sites. It is also helpful information to estimate various environmental indices, which help to know if the origin of the metals is from natural or anthropogenic sources, as well as the effects on fauna. With them, the degree of contamination is established for the receiving water bodies and the disposal sites. In terms of management, it is possible to develop quality guidelines to safeguard the streams' quality, or it is possible to determine if they comply with the limits established in national legislation to be reused in activities such as agriculture, soil restoration, or construction material.

Implementing a series of statistical tests that allow finding relationships between variables was proposed to reduce laboratory analysis, which are expensive, and the results can take time. Based on this, it is impossible to extrapolate information from one basin to another to implement management strategies. Therefore, it will be necessary to conduct laboratory analysis in each basin that is to be intervened. On the other hand, the statistical analysis makes it possible to find the most influential variables for each basin and, in turn, what they are related to. Thus, models can be made, determining inflection points as alert systems, and making decisions regarding the accumulation of particles in drainage structures and disposal.

PART A: Data Characterization

Sediment trap dimensions

Table A-1 Molinos River (MR) sediment trap dimensions and installation dates

Trap code	1	2	3	4	5	6	7	8	9
Installation date	4/2/2020	31/03/2020		9/11/2020			5/11/2020	10/2/2021	9/3/2021
diameter (cm)	5	4	6	6	6	7.62	6	4.5	6x4
high (cm)	10	5	10	4.5	9.4	9	5.5	6	8
Volume (cm3)	196.35	62.83	282.74	127.23	265.78	410.43	155.51	95.43	192

Table A-2. Constructed-wetland/storage-tank (CW/ST) trap dimensions and installation dates.

Trap code	1	2
Installation date	9/2/2020	9/2/2020
diameter (cm)	9	8
high (cm)	4.5	6
Volume (cm3)	286.28	301.59

Hydrology data

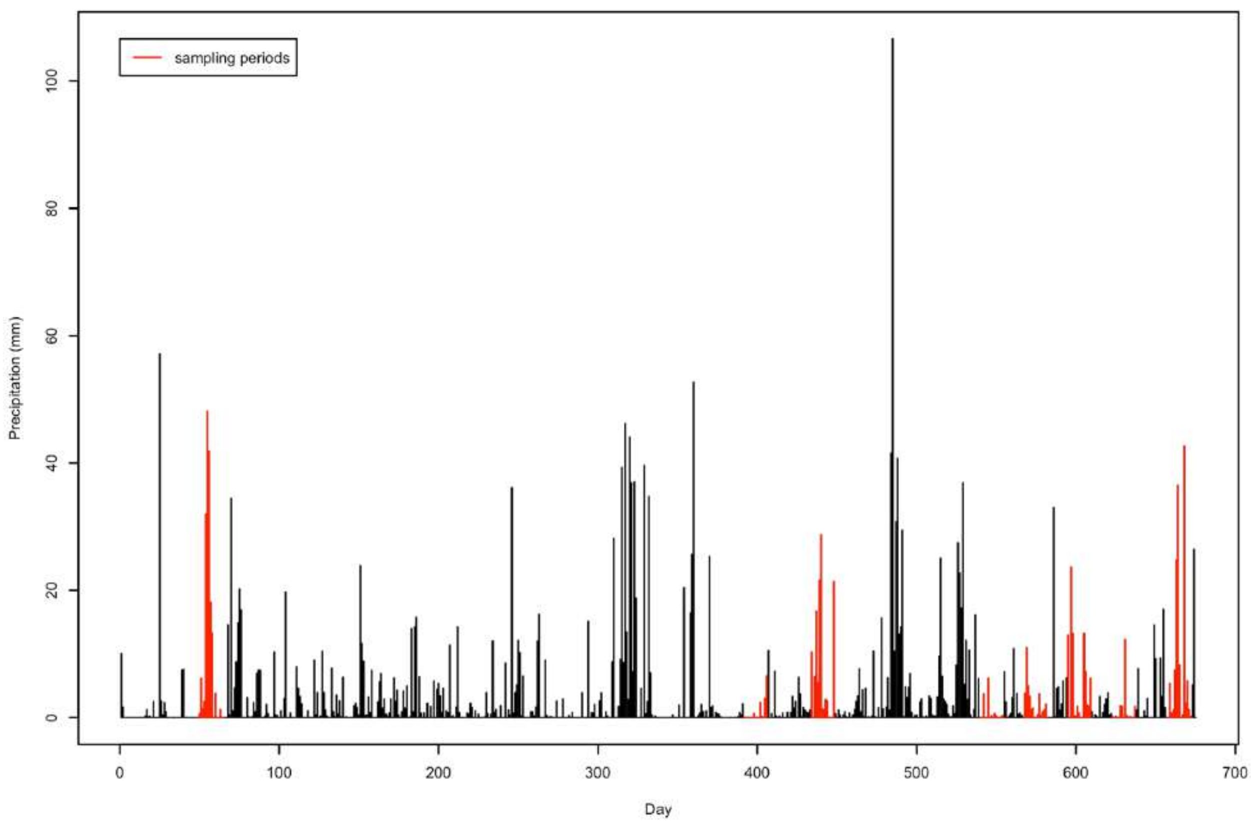

Figure A-1 Pluviometric station "El paraiso" precipitation data from 1 January 2020 until 28 October 2021, and Arzobispo River sampling periods

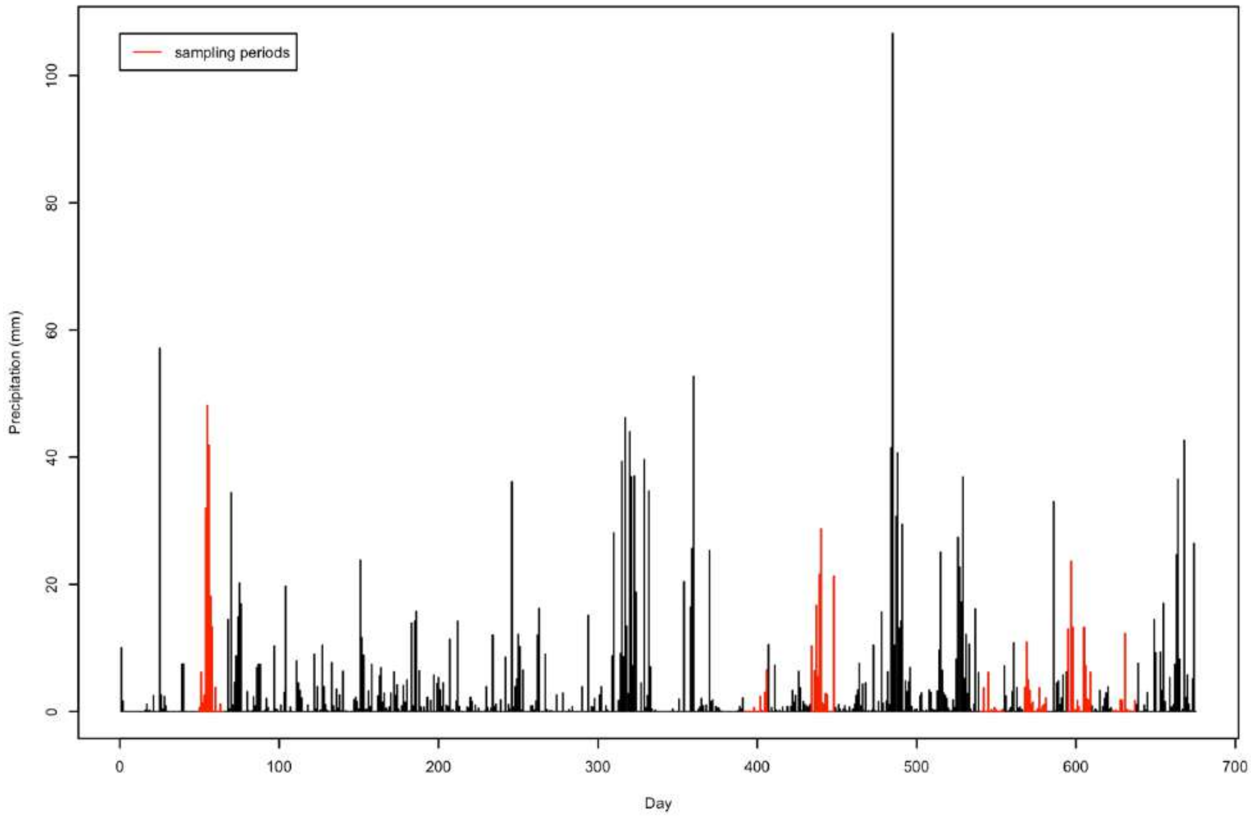

Figure A-2 Pluviometric station "El paraiso" precipitation data from 1 January 2020 until 28 October 2021, and Constucted-wetland/storage-tank sampling periods

Table A-3 Hydrology Data. H: total precipitation height, Iave: average intensity, Imax: maximum intensity, dw: number of days with dry weather, rw: number of days with rainfall weather, ADP: antecedent dry weather period. MR: Molinos River, AR: Arzobispo River, CW/ST: Constructed wetland storage tank.

Sample	Site	H(mm)	t(days)	dw(days)	rw(days)	ADP(days)	Iave(mm/h)	Imax(mm/h)
001-5	MR	169.8	15	4	11	6	0.471	1.263
001-7	AR	168.7	15	4	11	9	0.469	2.004
001-8	MR	84.3	15	6	9	3	0.234	0.883
001-9	MR	11.8	15	9	6	3	0.033	0.233
001-10	MR	30.7	15	8	7	4	0.085	0.554
001-11	MR	46.5	15	8	7	2	0.129	0.871
001-12	MR	24.9	15	10	5	5	0.069	0.504
001-13	MR	75.1	15	8	7	5	0.209	0.879
001-14	MR	2.2	15	13	2	0	0.006	0.050
001-15	MR	3.5	15	12	3	4	0.010	0.067
001-16	MR	155.93	15	4	11	0	0.433	1.652
001-17	MR	127.65	15	6	9	0	0.355	1.652
001-18	MR	13.4	15	13	2	9	0.037	0.508
001-20	AR	12.4	15	11	4	6	0.034	0.271
001-21	CW/ST	44.4	22	10	12	0	0.084	0.438
001-23	MR	117.2	15	5	10	0	0.326	1.400
001-24	AR	118.1	15	4	11	0	0.328	1.196
001-25	CW/ST	127.1	22	5	17	0	0.241	1.196
001-26	MR	17.7	15	9	6	4	0.049	0.396
001-27	MR	27.5	15	8	7	2	0.076	0.308
001-28	CW/ST	86.7	36	17	19	3	0.100	0.888
001-29	CW/ST	319.7	30	12	18	0	0.444	4.442
001-31	MR	158.4	15	3	12	1	0.440	1.554

Sample	Site	H(mm)	t(days)	dw(days)	rw(days)	ADP(days)	Iave(mm/h)	Imax(mm/h)
001-32	MR	6.8	16	14	2	1	0.018	0.229
001-33	CW/ST	231	43	19	24	3	0.224	1.538
001-34	AR	10.4	15	12	3	2	0.029	0.254
001-35	MR	16.4	16	10	6	12	0.043	0.292
001-36	MR	14.4	13	6	7	0	0.046	0.221
001-37	AR	33.1	15	5	10	2	0.092	0.454
001-38	MR	59.8	15	8	7	8	0.166	1.013
001-39	MR	77	15	6	9	0	0.214	0.867
001-40	CW/ST	82.2	15	5	10	0	0.228	0.983
001-41	AR	82.2	15	5	10	0	0.228	0.983
001-42	MR	29.9	15	10	5	0	0.083	0.517
001-43	MR	18.9	15	9	6	7	0.053	0.321
001-44	CW/ST	17.4	15	11	4	5	0.048	0.508
001-45	AR	17.4	15	11	4	5	0.048	0.508
001-46	MR	51.5	15	10	5	3	0.143	1.350
001-47	MR	108.4	15	4	11	3	0.301	0.842
001-48	AR	135.6	15	4	11	2	0.377	1.775

Runoff coefficients and flow rates

Table A-4 Constructed-wetland/storage-tank runoff coefficients and flow rates

Sample	S	C	Q_max	Q_ave
001-21	71.641	0.200	0.919	0.177
001-25	71.641	0.543	6.806	1.370
001-28	71.641	0.419	3.905	0.442
001-29	28.222	0.901	41.992	4.198
001-33	71.641	0.705	11.368	1.655
001-40	71.641	0.402	4.143	0.962
001-44	71.641	0.007	0.039	0.004

Table A-5 Arzobispo River runoff coefficients and flow rates

Sample	S	C	Q_max	Q_ave
001-7	71.641	0.625	64.693	15.126
001-20	71.641	0.004	0.060	0.008
001-24	71.641	0.520	32.103	8.807
001-34	71.641	0.022	0.288	0.033
001-37	71.641	0.118	2.762	0.559
001-41	71.641	0.402	20.400	4.737
001-45	71.641	0.007	0.191	0.018
001-48	13.368	0.891	81.652	17.327

Particle size distribution

Table A-6 Particle Size Distribution µm. MR: Molinos River, AR: Arzobispo River, CW/ST: Constructed wetland storage tank

Sample	Site	D10	D20	D30	D40	D50	D60	D70	D80	D90	D100
001-05	MR	26.56	66.90	94.30	116.93	139.57	162.29	189.37	222.26	267.05	792.84
001-07	AR	44.69	89.40	122.07	150.85	180.16	209.88	239.92	271.90	312.59	740.38
001-08	MR	3.25	6.59	9.15	11.90	15.26	19.40	24.23	30.21	39.44	426.86
001-09	MR	37.63	75.52	93.67	105.48	115.90	126.22	137.33	151.62	415.11	873.40
001-10	MR	17.34	30.63	47.64	75.10	166.02	188.26	202.61	218.11	235.08	635.00
001-11	MR	168.55	196.16	215.24	230.63	245.77	260.18	275.26	294.56	318.67	551.28
001-12	MR	20.40	57.03	145.94	224.12	267.51	309.26	353.63	406.67	495.63	1043.00
001-13	MR	14.03	26.10	40.31	59.55	84.49	115.40	174.59	228.54	316.63	873.40
001-14	MR	105.31	241.70	289.49	327.78	362.34	396.79	436.29	485.73	560.38	1043.00
001-15	MR	25.21	60.69	118.70	192.68	294.36	352.36	414.28	475.09	573.29	1043.00
001-16	MR	7.24	13.63	22.01	33.52	51.38	77.29	121.14	236.03	517.82	1043.00
001-17	MR	27.82	70.25	110.26	149.61	192.50	233.11	274.33	332.35	426.00	899.33
001-18	MR	12.55	23.84	37.56	55.65	79.36	103.58	129.84	171.20	252.53	650.87
001-20	AR	24.26	62.23	189.22	221.62	246.09	271.28	306.43	415.43	574.39	981.67
001-21	CW/ST	14.83	25.93	39.02	57.18	100.51	143.38	164.52	186.27	227.02	740.38
001-23	MR	10.10	20.43	34.21	54.66	80.33	107.73	146.11	238.55	423.33	1043.00
001-24	AR	25.84	66.19	128.01	197.91	274.19	354.94	444.22	547.21	689.77	1043.00
001-25	CW/ST	17.62	30.61	45.79	64.26	86.81	114.37	155.46	231.86	374.98	1043.00
001-26	MR	24.70	48.32	80.44	111.14	146.20	213.09	291.39	426.36	581.20	1043.00
001-27	MR	11.13	19.96	28.98	39.85	54.32	76.93	144.70	251.40	499.80	1043.00
001-28	CW/ST	20.19	39.64	66.49	99.32	138.08	183.80	242.33	315.08	450.62	1043.00
001-29	CW/ST	19.64	33.18	48.66	66.96	89.74	120.31	170.12	255.77	432.56	1043.00
001-31	MR	13.99	26.33	44.46	72.82	118.17	186.03	254.48	321.13	418.49	947.52
001-32	MR	12.52	24.81	44.84	78.03	137.04	223.85	298.17	390.98	534.07	1043.00
001-33	CW/ST	29.30	52.03	76.96	104.72	138.23	183.43	244.65	331.55	488.42	1043.00
001-34	AR	6.84	14.06	22.62	32.92	45.46	65.69	100.29	139.78	308.89	925.25
001-35	MR	16.27	30.45	47.35	69.43	96.20	127.51	186.43	284.44	483.12	1043.00
001-36	MR	18.05	35.72	60.00	89.53	118.58	162.10	248.19	361.02	525.01	1043.00
001-37	AR	6.43	11.81	18.01	25.79	37.32	57.42	94.48	160.95	314.25	1043.00
001-38	MR	10.69	20.12	30.55	44.69	62.45	88.06	133.05	203.80	344.06	915.28
001-39	MR	10.41	18.91	29.37	44.81	70.09	108.28	287.13	409.72	461.28	870.69
001-40	CW/ST	14.03	23.27	32.25	42.55	55.37	72.10	94.29	124.80	183.26	1024.87
001-41	AR	5.55	10.11	17.76	28.49	142.61	153.87	164.18	176.09	190.41	590.72
001-42	MR	8.56	15.29	22.31	29.99	39.72	51.75	66.32	88.18	123.52	602.29
001-43	MR	215.78	239.14	258.43	280.32	306.70	421.76	584.80	650.83	726.33	1043.00
001-44	CW/ST	21.86	36.93	50.82	67.12	90.37	130.09	219.46	356.71	573.58	1043.00
001-45	AR	1.45	1.60	1.73	1.85	1.98	2.13	2.48	6.93	7.66	241.72

Sample	Site	D10	D20	D30	D40	D50	D60	D70	D80	D90	D100
001-46	MR	11.55	21.19	33.03	51.47	82.16	135.22	260.06	387.43	530.83	1043.00
001-47	MR	11.54	20.19	28.94	40.10	55.16	77.62	111.55	201.25	440.27	1043.00
001-48	AR	5.95	19.55	52.50	90.93	120.98	140.13	156.08	173.67	197.03	715.13

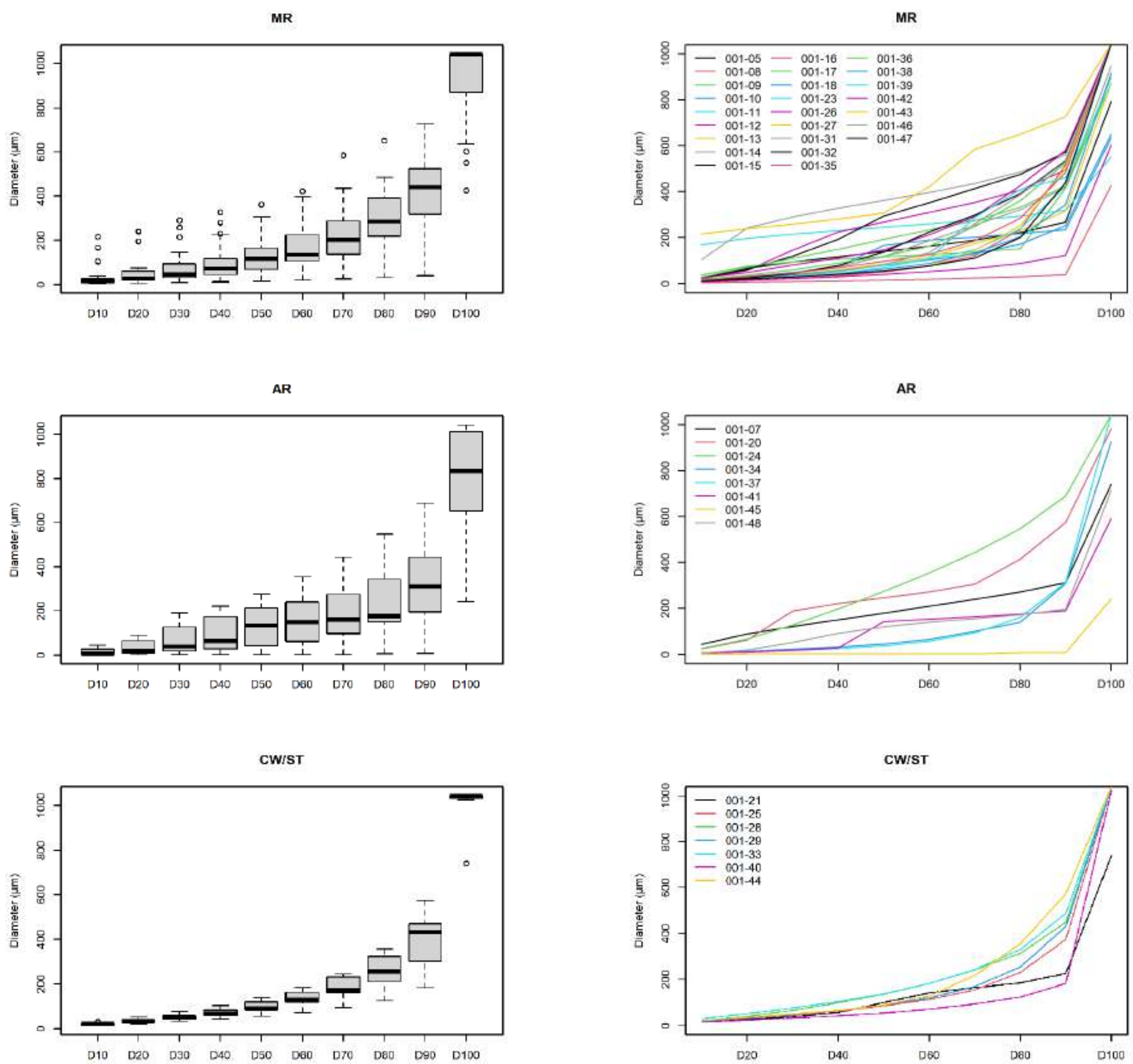

Figure A-3 Particle Size Distribution (μm). Diameter variation by D – left. Granulometric curve by sample- right. MR: Molinos River, AR: Arzobispo River, CW/ST: Constructed wetland storage tank

Heavy metals

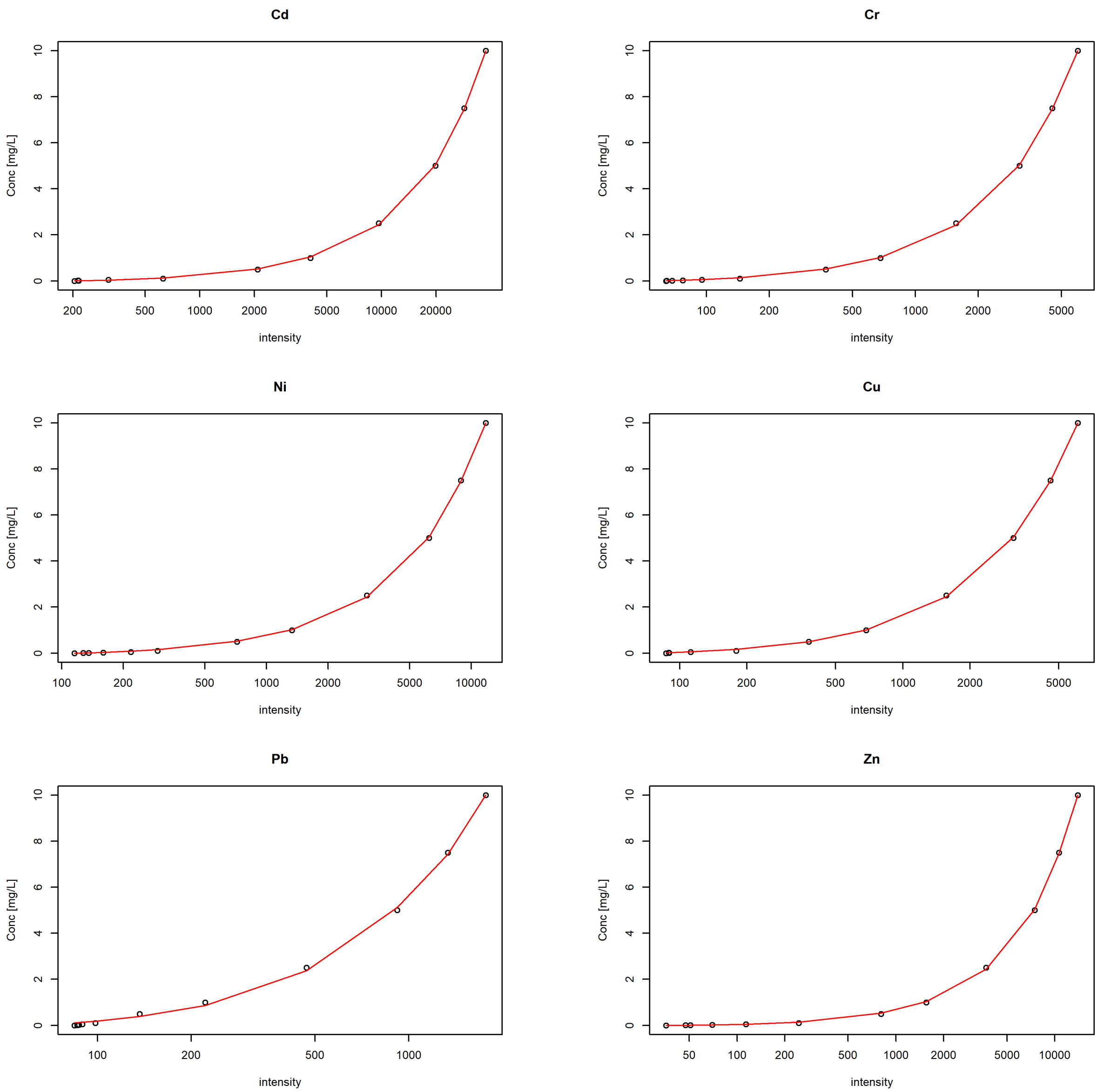

Figure A-4 Heavy metals calibration curves

Table 8 Calibration curve equations by heavy metals.

HM	Calibration curve equations
Cd	$C = -2.39 * 10^{-18}x^4 + 1.87 * 10^{-13}x^3 - 4.03 * 10^{-9}x^2 + 2.81 * 10^{-4}x - 4.85 * 10^{-2}$
Cr	$C = -3.79 * 10^{-15}x^4 + 4.23 * 10^{-11}x^3 - 1.22 * 10^{-7}x^2 + 1.72 * 10^{-3}x - 1.00 * 10^{-1}$
Ni	$C = -2.69 * 10^{-16}x^4 + 6.05 * 10^{-12}x^3 - 3.60 * 10^{-8}x^2 + 8.84 * 10^{-4}x - 1.05 * 10^{-1}$
Cu	$C = -2.62 * 10^{-16}x^4 + 2.90 * 10^{-12}x^3 - 4.29 * 10^{-9}x^2 + 1.64 * 10^{-3}x - 1.22 * 10^{-1}$
Pb	$C = 1.05 * 10^{-12}x^4 - 3.77 * 10^{-9}x^3 + 4.17 * 10^{-6}x^2 + 4.44 * 10^{-3}x - 2.93 * 10^{-1}$
ZN	$C = -1.46 * 10^{-16}x^4 + 3.89 * 10^{-12}x^3 - 2.59 * 10^{-8}x^2 + 7.17 * 10^{-4}x - 3.45 * 10^{-2}$

Table A-7 Total and soluble Heavy Metal concentration in mg/kg. MR: Molinos River, AR: Arzobispo River, CWST: Constructed wetland storage tank.

Sample	Site	Cd (mg/kg)		Cr (mg/kg)		Ni (mg/kg)		Cu (mg/kg)		Pb (mg/kg)		Zn (mg/kg)	
		TOT	SPLP	TOT	SPLP	TOT	SPLP	TOT	SPLP	TOT	SPLP	TOT	SPLP
001-5	MR	0.000	0.000	0.000	0.000	19.980	0.970	586.870	34.020	15.780	0.650	47.070	3.110
001-7	AR	0.000	0.000	0.000	0.000	16.580	0.960	585.770	23.280	9.190	0.010	76.980	0.620
001-8	MR	0.350	0.100	0.000	0.000	22.440	1.140	600.680	41.080	22.560	1.370	83.820	8.330
001-9	MR	0.000	0.000	0.000	0.000	15.500	1.110	501.780	35.280	5.070	1.310	62.070	4.940
001-10	MR	0.210	0.020	0.000	0.000	21.850	1.020	607.050	52.190	19.360	0.740	127.550	23.120
001-11	MR	0.000	0.000	0.000	0.000	19.520	0.910	492.400	37.350	8.980	0.290	70.090	11.360
001-12	MR	0.000	0.000	0.000	0.000	19.960	0.960	545.360	48.360	13.490	0.580	85.940	15.800
001-13	MR	0.000	0.000	0.000	0.000	21.060	1.150	650.810	35.150	13.990	0.450	128.860	13.790
001-14	MR	0.000	0.000	0.000	0.000	19.410	1.150	571.810	30.770	10.170	0.200	92.910	4.060
001-15	MR	0.000	0.000	0.000	0.000	21.250	1.290	554.750	42.470	12.150	0.640	104.730	21.050
001-16	MR	2.300	0.120	2.730	0.000	25.850	1.330	608.550	27.960	37.520	0.880	103.690	2.290
001-17	MR	0.000	0.000	0.000	0.000	21.520	1.230	524.580	34.340	11.530	0.800	64.620	6.980
001-18	MR	0.230	0.090	0.000	0.000	21.860	1.200	610.570	40.180	18.980	0.820	112.440	13.130
001-20	AR	0.000	0.000	0.000	0.000	15.370	0.950	795.980	26.700	4.260	0.000	294.130	1.170
001-21	CW/ST	0.000	0.000	0.000	0.000	14.260	0.970	408.620	25.260	0.000	0.000	43.560	21.160
001-23	MR	0.000	0.000	0.000	0.000	16.430	1.600	532.430	28.040	8.520	1.070	93.740	2.780
001-24	AR	1.960	0.000	0.000	0.000	18.550	1.040	526.500	34.010	20.890	1.340	104.760	3.680
001-25	CW/ST	0.000	0.000	0.000	0.000	17.340	0.890	792.940	26.650	14.090	0.120	344.860	0.810
001-26	MR	0.000	0.000	0.000	0.000	16.320	1.230	603.820	38.210	3.720	0.750	113.440	9.030
001-27	MR	0.000	0.000	0.000	0.000	15.670	0.810	498.150	27.970	0.320	0.000	109.920	2.700
001-28	CW/ST	2.800	0.000	6.600	0.000	27.310	0.970	1192.940	32.360	39.450	0.130	476.090	0.960
001-29	CW/ST	3.290	0.000	13.040	0.000	29.160	1.100	818.240	29.580	64.830	0.240	929.790	1.530
001-31	MR	0.000	0.000	0.000	0.000	17.320	0.930	557.790	25.440	7.750	0.060	132.730	2.520
001-32	MR	0.000	0.000	0.000	0.000	17.140	0.840	521.060	22.710	12.120	0.000	101.120	1.390
001-33	CW/ST	0.000	0.000	0.000	0.000	18.890	0.860	881.250	24.700	23.790	0.000	364.980	1.020
001-34	AR	7.780	0.170	6.750	0.000	26.260	1.150	859.120	31.130	50.120	0.340	149.430	0.710
001-35	MR	0.000	0.000	0.000	0.000	15.210	0.740	529.960	25.330	0.000	0.000	81.400	18.620
001-36	MR	0.000	0.000	0.000	0.000	13.550	0.710	548.470	25.470	0.000	0.000	96.380	1.340
001-37	AR	6.820	0.030	6.210	0.330	23.850	0.840	669.790	28.470	40.330	0.010	139.160	0.620
001-38	MR	0.000	0.000	0.000	0.000	14.190	0.780	588.520	23.790	1.110	0.000	135.030	1.290
001-39	MR	0.000	0.000	0.000	0.000	13.990	0.800	610.080	23.380	3.580	0.050	139.060	0.810
001-40	CW/ST	2.970	0.000	5.020	0.570	20.830	0.980	813.320	30.050	53.820	0.210	1016.310	1.970
001-41	AR	6.890	0.030	8.160	0.000	23.610	0.890	625.790	31.890	57.850	0.090	123.820	0.630
001-42	MR	0.000	0.000	0.000	0.000	13.760	0.480	594.380	25.460	0.000	0.000	95.460	1.270
001-43	MR	0.000	0.000	0.310	0.000	12.960	0.430	589.530	24.750	59.740	0.000	100.000	1.180

Sample	Site	Cd (mg/kg)		Cr (mg/kg)		Ni (mg/kg)		Cu (mg/kg)		Pb (mg/kg)		Zn (mg/kg)	
		TOT	SPLP	TOT	SPLP	TOT	SPLP	TOT	SPLP	TOT	SPLP	TOT	SPLP
001-44	CW/ST	1.660	0.000	5.100	0.000	27.910	0.750	975.860	25.520	33.600	0.000	704.900	2.350
001-45	AR	5.050	0.060	5.920	0.000	22.370	0.970	583.840	31.400	45.820	0.240	92.850	0.750
001-46	MR	0.000	0.000	0.000	0.000	14.330	1.120	570.470	33.070	3.060	0.590	139.860	0.880
001-47	MR	0.000	0.000	0.000	0.000	13.620	0.830	554.940	29.060	0.000	0.000	83.370	0.840
001-48	AR	4.520	0.030	4.730	0.000	22.310	0.960	601.520	27.240	48.250	0.140	100.860	0.460

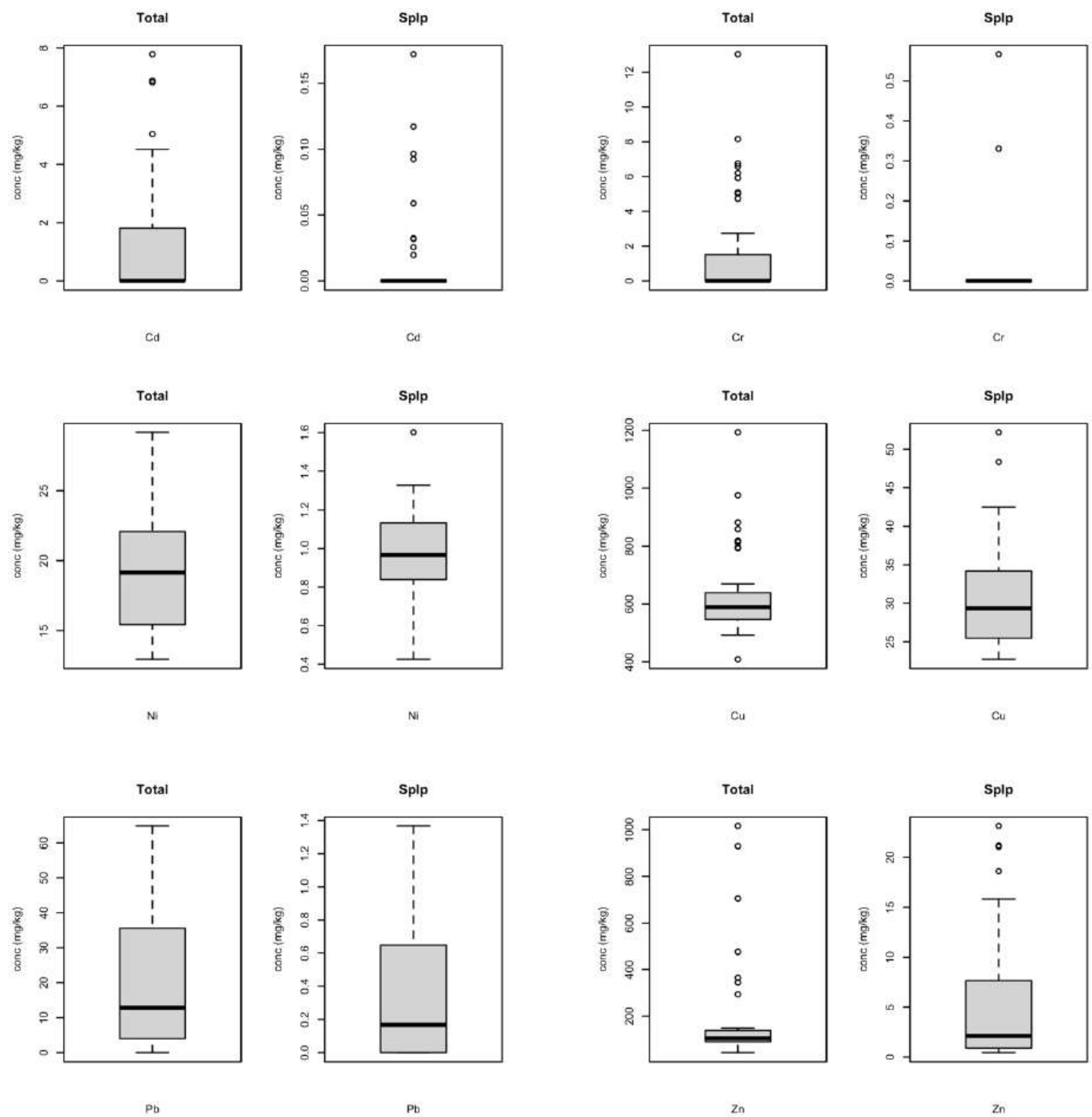

Figure A-5 Total and soluble Heavy metals concentrations (mg/kg)

PART B: Sediments Pollution

Human health risk

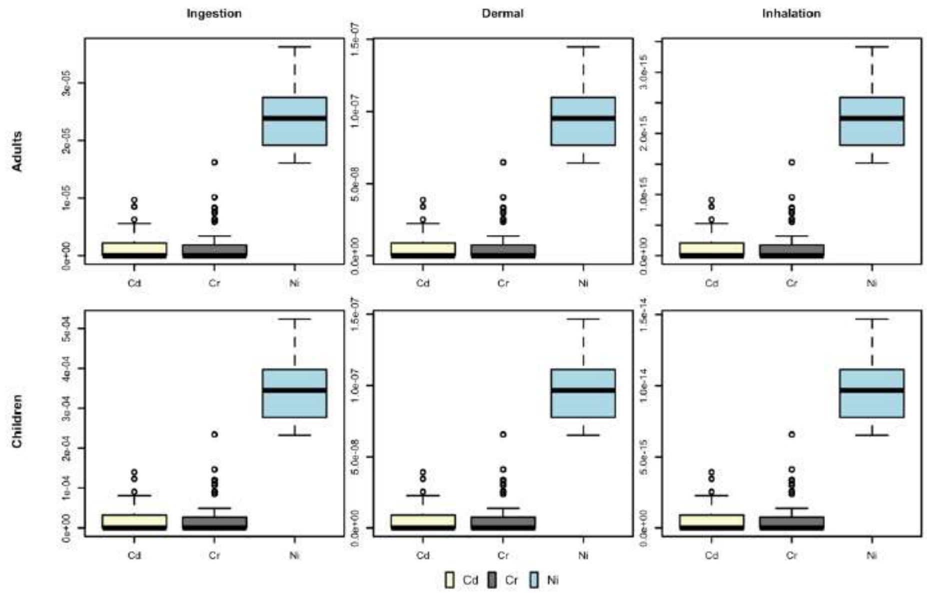

*Figure B-1 Average daily dose (ADD) for carcinogenic HM for each pathway in children and adults [mg/(kg*day)]. MR: Molinos River, AR: Arzobispo River, CW/ST: Constructed wetland storage tank.*

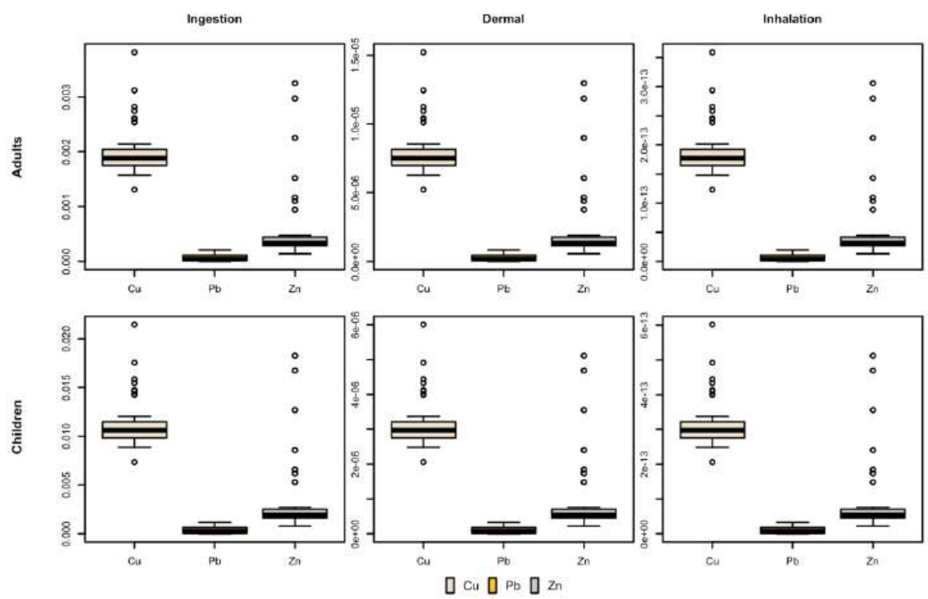

*Figure B-2 Average daily dose (ADD) for no carcinogenic HM for each pathway in children and adults [mg/(kg*day)]. MR: Molinos River, AR: Arzobispo River, CW/ST: Constructed wetland storage tank.)*

PART C: Statistics and modeling

Heavy metals and particle size distribution correlations

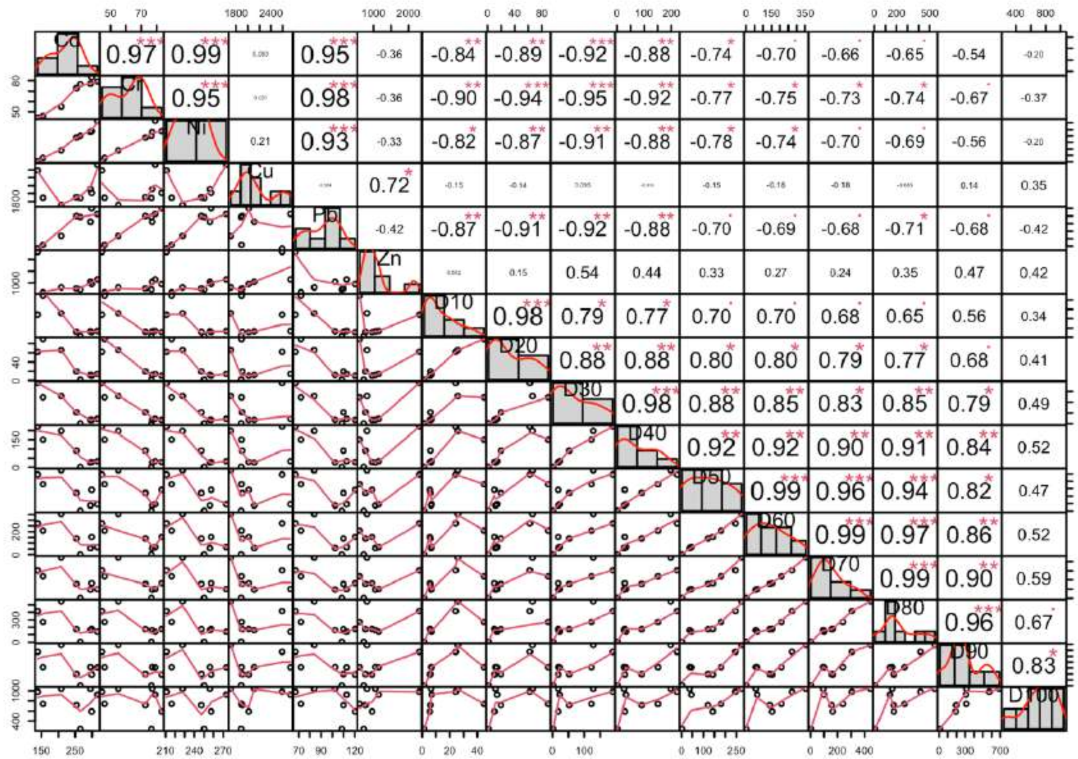

Figure C-1 Arzobispo river heavy metals and particle size distribution correlation

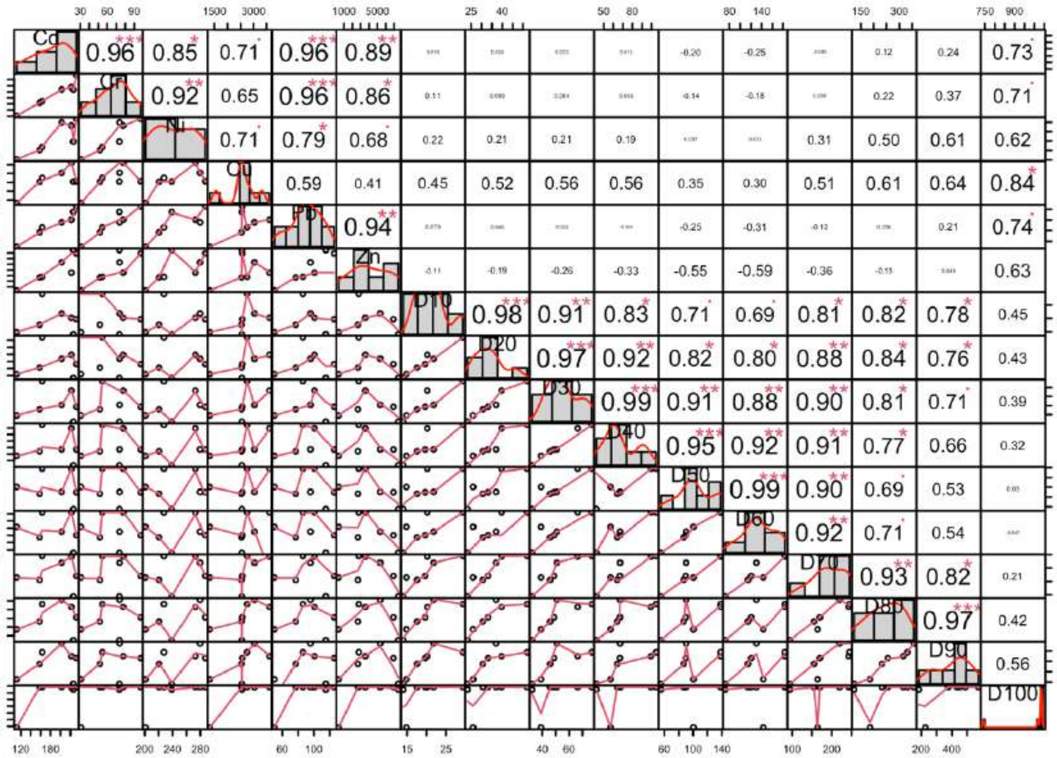

Figure C-2 Constructed-wetland/storage-tank heavy metals and particle size distribution correlation

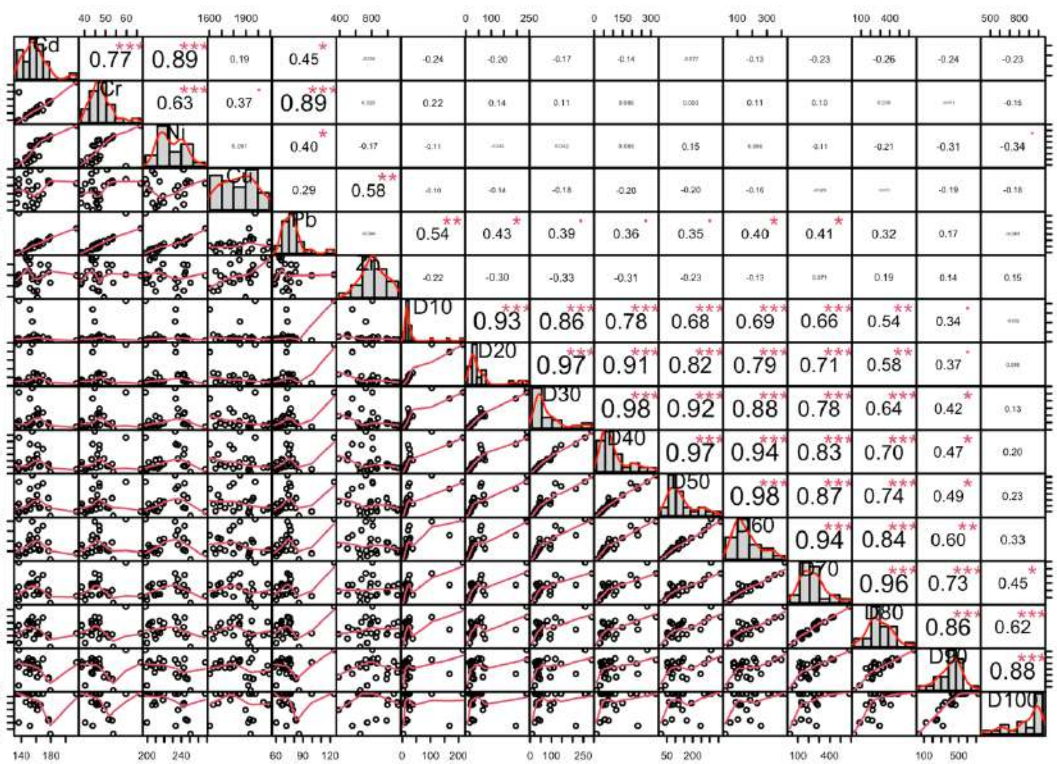

Figure C-3 Molinos river heavy metals and particle size distribution correlation

Heavy metals and hydrology correlations

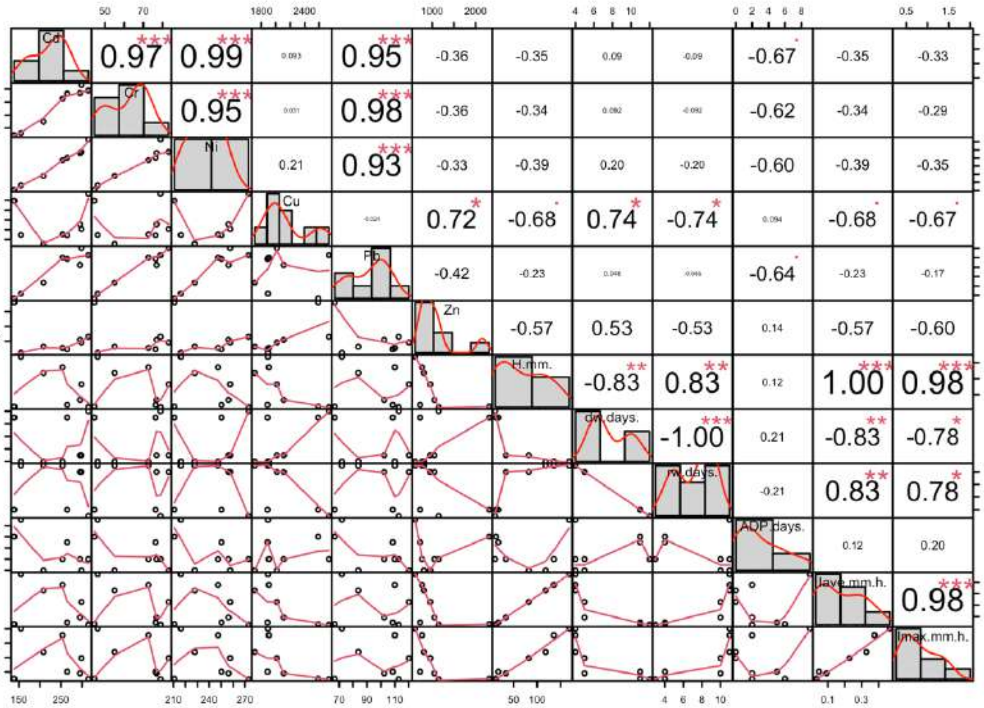

Figure C-4 Arzobispo river heavy metals and hydrology correlation

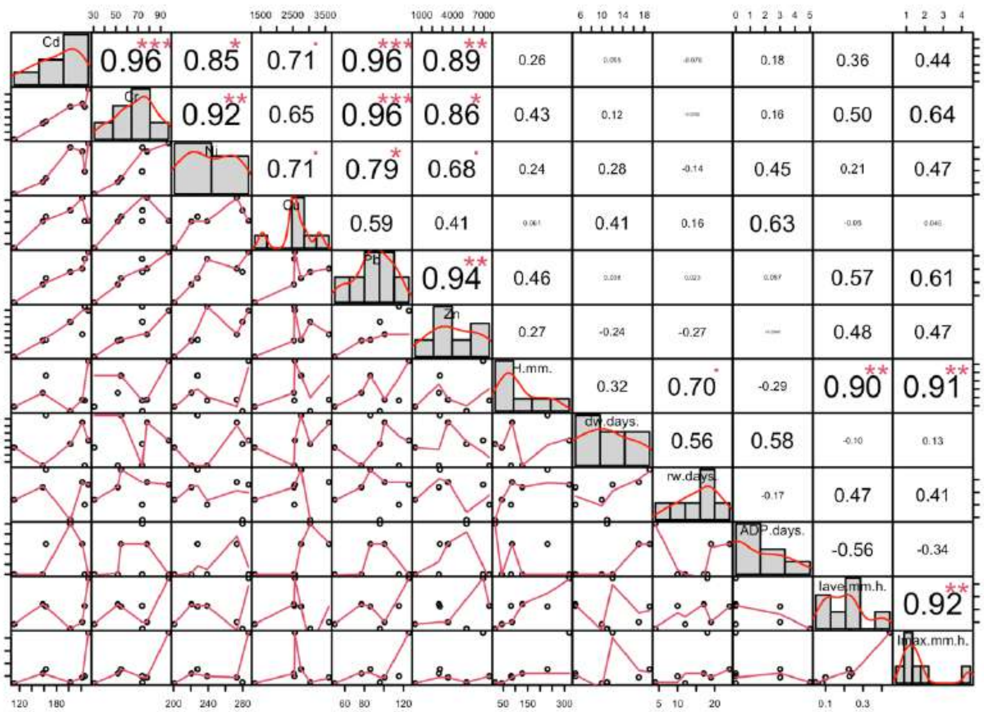

Figure C-5 Constructed-wetland/storage-tank heavy metals and hydrology correlation

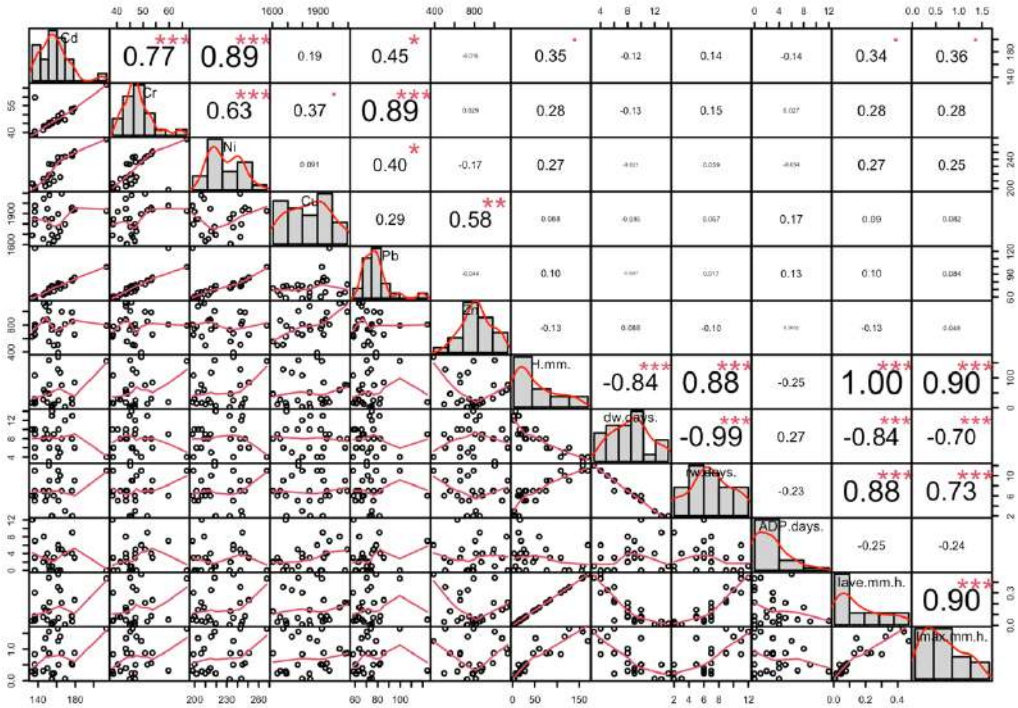

Figure C-6 Molinos river heavy metals and hydrology correlation

Principal Component Analysis heavy metals and hydrology

Table C-1 Molinos River heavy metals and hydrology principal component analysis

	Comp1	Comp2	Comp3	Comp4	Comp5	Comp6
Cd	-0.554	-0.687	-0.210	0.289	-0.216	0.054
Cr	-0.516	-0.804	0.020	-0.102	0.236	-0.060
Ni	-0.444	-0.671	-0.359	0.206	-0.349	0.128
Cu	-0.172	-0.383	0.805	-0.011	-0.041	0.335
Pb	-0.300	-0.744	0.021	-0.324	0.467	-0.140
Zn	0.088	-0.117	0.851	0.374	-0.079	-0.232
H.mm.	-0.949	0.235	0.005	-0.056	-0.081	-0.055
dw.days.	0.832	-0.418	-0.108	0.120	-0.116	-0.201
rw.days.	-0.854	0.409	0.088	-0.159	0.075	0.138
ADP.days.	0.282	-0.239	0.188	-0.764	-0.478	-0.079
Iave.mm.h.	-0.950	0.236	0.006	-0.054	-0.078	-0.052
Imax.mm.h.	-0.875	0.183	0.084	0.066	-0.151	-0.341

Table C-2 Constructed-wetland/storage-tank heavy metals and hydrology principal component analysis

	Comp1	Comp2	Comp3	Comp4	Comp5	Comp6
Cd	0.916	-0.304	0.157	-0.167	0.006	-0.129
Cr	0.975	-0.171	0.083	0.043	-0.093	-0.055
Ni	0.844	-0.416	-0.057	0.247	-0.225	-0.017
Cu	0.609	-0.569	-0.369	-0.365	-0.119	0.150
Pb	0.967	-0.089	0.165	-0.103	0.127	-0.058
Zn	0.840	-0.149	0.460	-0.032	0.246	0.007
H.mm.	0.605	0.703	-0.331	0.103	0.083	0.115
dw.days.	0.175	-0.132	-0.926	0.177	0.124	-0.218
rw.days.	0.165	0.577	-0.720	-0.346	-0.025	-0.027
ADP.days.	0.087	-0.799	-0.492	0.209	0.139	0.222
Iave.mm.h.	0.644	0.747	0.100	-0.012	0.030	0.126
Imax.mm.h.	0.741	0.600	-0.051	0.275	-0.109	0.024

Table C-3 Arzobispo river heavy metals and hydrology principal component analysis

	Comp1	Comp2	Comp3	Comp4	Comp5	Comp6
Cd	0.553	-0.824	0.026	-0.052	-0.076	0.076
Cr	0.534	-0.826	0.082	-0.007	-0.092	-0.134
Ni	0.607	-0.763	0.119	-0.153	-0.035	0.098
Cu	0.725	0.418	-0.060	-0.531	-0.045	0.103
Pb	0.450	-0.860	0.107	-0.072	0.045	-0.200
Zn	0.449	0.723	-0.450	-0.164	-0.049	-0.209
H.mm.	-0.951	-0.206	0.055	-0.197	0.105	0.001
dw.days.	0.822	0.429	0.306	0.019	0.213	-0.020
rw.days.	-0.822	-0.429	-0.306	-0.019	-0.213	0.020
ADP.days.	-0.256	0.686	0.615	-0.044	-0.282	-0.061
Iave.mm.h.	-0.951	-0.206	0.055	-0.197	0.105	0.001
Imax.mm.h.	-0.923	-0.213	0.188	-0.216	0.083	-0.106

Principal Component Analysis heavy metals and particle size distribution

Table C-4 Molinos River heavy metals and particle size distribution principal component analysis

	Comp1	Comp2	Comp3	Comp4	Comp5	Comp6
Cd	0.197	-0.850	-0.184	0.393	0.116	0.066
Cr	-0.138	-0.881	-0.331	0.050	-0.288	0.011
Ni	0.043	-0.846	0.052	0.365	0.336	0.024
Cu	0.166	-0.329	-0.572	-0.601	0.168	-0.374
Pb	-0.454	-0.720	-0.262	-0.108	-0.390	0.005
Zn	0.170	0.127	-0.773	-0.379	0.277	0.341
D10	-0.817	-0.137	0.228	-0.358	-0.287	0.160
D20	-0.888	-0.117	0.288	-0.227	-0.083	0.014
D30	-0.936	-0.101	0.271	-0.099	0.051	-0.051
D40	-0.949	-0.080	0.218	0.006	0.163	-0.074
D50	-0.934	-0.088	0.128	0.077	0.283	-0.024
D60	-0.959	-0.033	-0.014	0.065	0.209	0.000
D70	-0.937	0.087	-0.249	-0.029	0.115	0.027
D80	-0.855	0.222	-0.416	0.047	0.059	0.027
D90	-0.668	0.379	-0.482	0.336	-0.197	0.021
D100	-0.368	0.506	-0.525	0.490	-0.155	-0.164

Table C-5 Constructed-wetland/storage-tank heavy metals and particle size distribution principal component analysis

	Comp1	Comp2	Comp3	Comp4	Comp5	Comp6
Cd	0.227	0.946	-0.048	-0.213	0.016	-0.072
Cr	0.296	0.920	0.086	-0.159	-0.141	0.115
Ni	0.470	0.777	0.389	-0.140	-0.071	0.019
Cu	0.711	0.541	-0.081	-0.104	0.417	-0.106
Pb	0.186	0.949	-0.155	-0.100	-0.175	0.029
Zn	-0.079	0.969	-0.084	0.079	-0.167	-0.121
D10	0.889	-0.130	-0.184	0.317	-0.236	-0.049
D20	0.940	-0.176	-0.201	0.154	-0.139	-0.045
D30	0.951	-0.212	-0.215	-0.046	-0.046	0.015
D40	0.929	-0.256	-0.190	-0.179	0.014	0.054
D50	0.819	-0.475	-0.066	-0.311	-0.020	0.041
D60	0.800	-0.519	0.040	-0.294	-0.042	-0.004
D70	0.932	-0.281	0.208	-0.063	0.009	-0.072
D80	0.924	-0.040	0.322	0.193	0.046	-0.034
D90	0.871	0.141	0.343	0.313	0.036	0.069
D100	0.522	0.700	-0.292	0.271	0.255	0.118

Table C-6 Arzobispo River heavy metals and particle size distribution principal component analysis

	Comp1	Comp2	Comp3	Comp4	Comp5	Comp6
Cd	0.889	-0.230	0.382	-0.078	-0.047	-0.016
Cr	0.942	-0.138	0.285	0.078	-0.041	0.055
Ni	0.896	-0.277	0.288	-0.131	-0.128	-0.055
Cu	0.038	-0.855	-0.418	-0.138	-0.266	-0.050
Pb	0.913	-0.067	0.328	0.145	-0.157	0.065
Zn	-0.402	-0.748	-0.402	0.315	0.072	0.059
D10	-0.845	0.312	-0.147	-0.357	-0.170	0.046
D20	-0.928	0.237	-0.087	-0.245	-0.123	0.011
D30	-0.975	-0.080	-0.173	0.088	-0.007	0.010
D40	-0.984	-0.032	-0.004	0.097	0.005	-0.017
D50	-0.923	0.015	0.243	0.232	-0.159	0.098
D60	-0.920	0.018	0.332	0.167	-0.119	0.027
D70	-0.910	-0.021	0.396	0.092	-0.070	-0.038
D80	-0.918	-0.132	0.358	0.069	0.025	-0.070
D90	-0.850	-0.369	0.329	-0.070	0.091	-0.133
D100	-0.546	-0.599	0.349	-0.404	0.190	0.139

Molinos river linear regression model

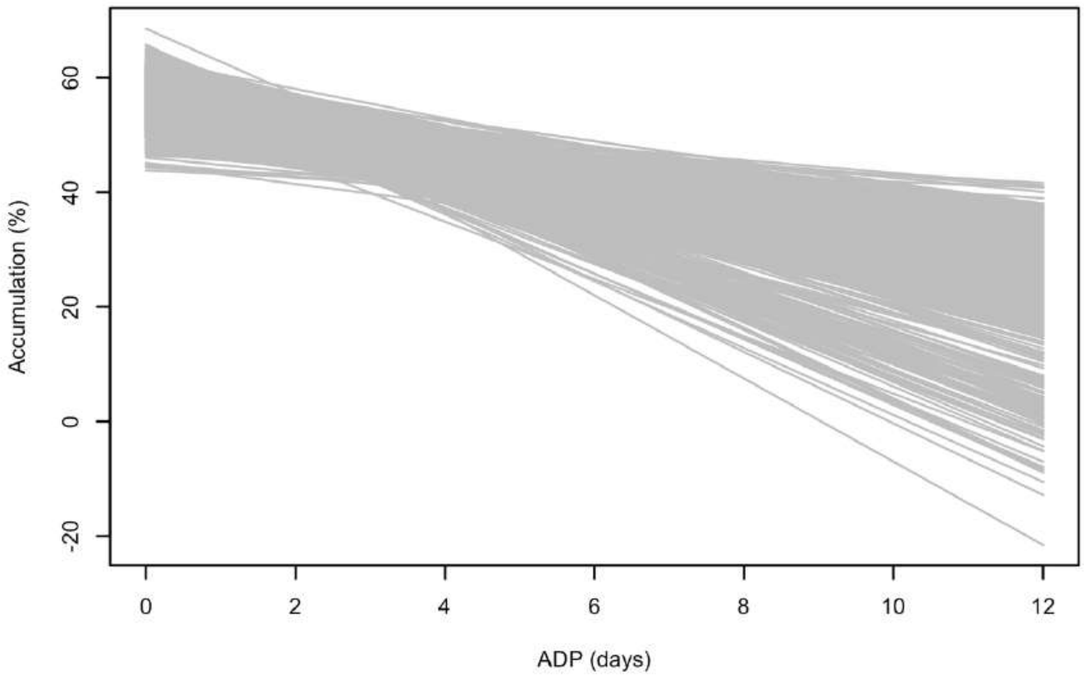

Figure C-7 Simple linear regression model for accumulation in Molinos River

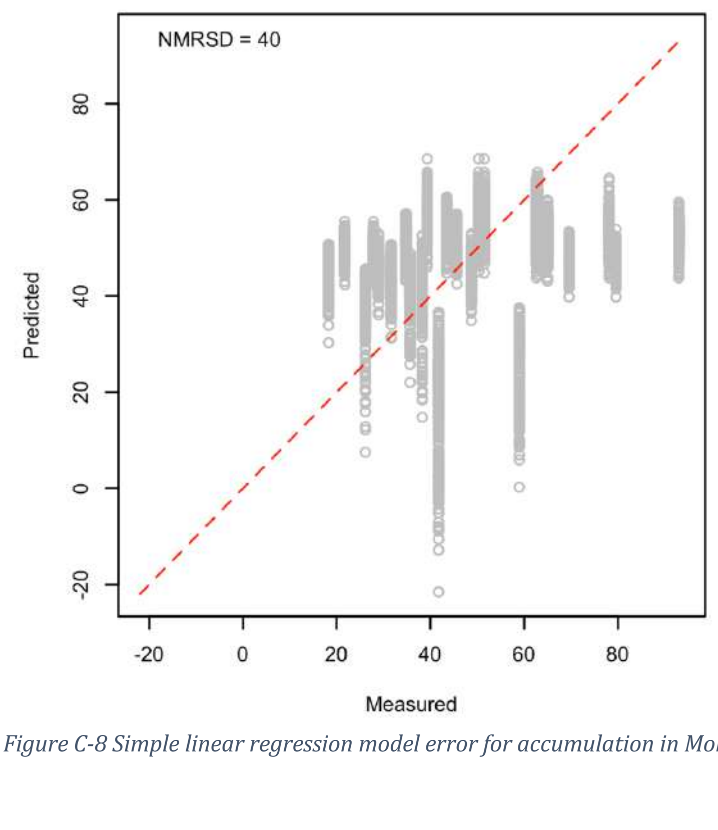

Figure C-8 Simple linear regression model error for accumulation in Molinos River

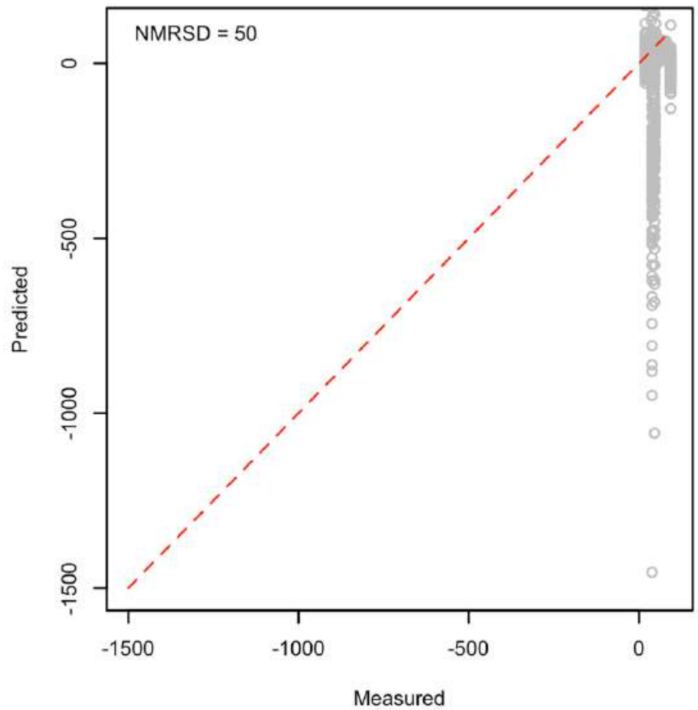

Figure C-9 Multiple linear regression model error for accumulation in Molinos River

Modeling PCA

Table C-7 Accumulation principal component analysis

Variables	Comp1	Comp2	Comp3	Comp4	Comp5	Comp6
D20	-0.804	-0.58	0.091	-0.009	0.003	-0.053
D30	-0.817	-0.517	0.091	0.037	0.097	-0.2
Imax	0.754	-0.517	0.157	-0.163	0.305	0.125
D10	-0.745	-0.564	0.229	-0.013	-0.08	0.251
H	0.774	-0.551	0.229	-0.068	0.033	-0.143
rw	0.731	-0.473	0.339	0.126	-0.322	-0.013
ADP	-0.246	0.445	0.64	-0.573	-0.049	-0.034
Accum	0.09	-0.413	-0.756	-0.483	-0.124	-0.006

Table C-8 Accumulation principal component analysis % of variance

Comp 1	Comp 2	Comp 3	Comp 4	Comp 5	Comp 6
45.48	26.07	15.53	7.64	2.89	1.79

Table C-9 Zn_Igeo principal component analysis

Variables	Comp1	Comp2	Comp3	Comp4	Comp5	Comp6
Accum	0.054	0.322	-0.811	-0.037	-0.472	0.085
D40	-0.908	0.282	-0.002	-0.038	0.064	-0.247
rw	0.604	0.649	0.294	-0.049	0.116	0.251
D30	-0.925	0.344	-0.003	-0.061	0.037	-0.114

Variables	Comp1	Comp2	Comp3	Comp4	Comp5	Comp6
H	0.621	0.729	0.17	-0.108	-0.051	-0.097
D20	-0.903	0.389	-0.029	-0.118	0.011	0.067
D10	-0.825	0.375	0.074	-0.235	0.066	0.274
Imax	0.626	0.66	0.054	-0.243	-0.047	-0.218
ADP	-0.161	-0.446	0.595	-0.471	-0.442	-0.001
Zn_Igeo	0.321	-0.352	-0.459	-0.674	0.319	-0.011

Table C-10 Zn_Igeo principal component analysis % of variance

Comp 1	Comp 2	Comp 3	Comp 4	Comp 5	Comp 6
44.10	23.43	14.23	7.65	5.49	2.78

Modeling SVM

Table C-11 Accumulation super vector machine

	rbfdot			polydot			vanilladot			tanhdot		
	NRMSD	min	max	NRMSD	min	max	NRMSD	min	max	NRMSD	min	max
D20	41	19	62	49	23	77	49	23	77	50	25	81
D30	41	19	62	49	22	78	49	22	78	49	15	84
Imax	41	21	63	48	22	77	48	22	77	50	18	84
D10	42	20	63	46	21	72	46	21	72	52	21	85
H	42	21	63	43	19	67	43	19	67	48	20	78
rw	42	22	64	43	22	65	43	22	65	45	20	74
ADP	41	18	65	40	19	62	40	19	62	43	22	65

	laplacedot			besseldot			anovadot			splinedot		
	NRMSD	min	max	NRMSD	min	max	NRMSD	min	max	NRMSD	min	max
D20	42	20	63	39	18	61	39	19	59	70	25	234
D30	42	19	66	41	19	62	39	19	61	68	20	178
Imax	42	20	63	43	21	64	40	18	61	72	19	186
D10	42	18	66	43	19	66	40	20	61	60	19	144
H	42	21	63	44	19	69	41	17	65	51.5	16	95
rw	42	21	63	43	20	68	40	19	62	47	16	84
ADP	42	19	66	40	17	62	40	19	62	41	18	63

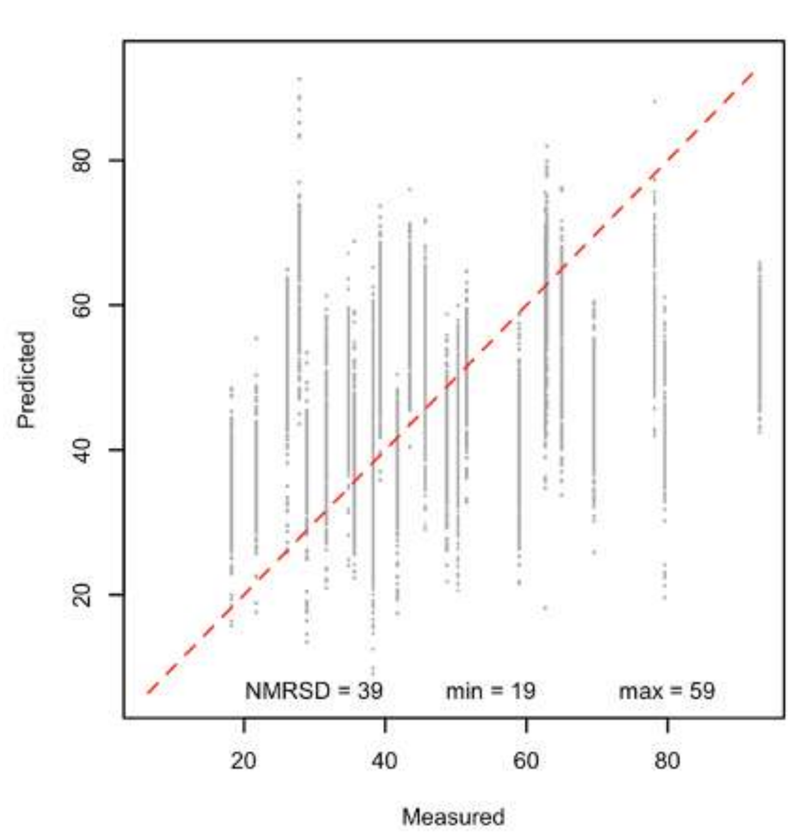

Figure C-10 Support vector machine error for accumulation in Molinos River

Table C-12 Zn_Igeo super vector machine

	rbfdot			polydot			vanilladot			tanhdot		
	NRMSD	min	max	NRMSD	min	max	NRMSD	min	max	NRMSD	min	max
Accum	63	32	109	75	30	151	75	30	151	81	24	142
D40	65	32	111	74	32	140	74	32	140	78	30	133
rw	65	32	113	74	29	138	74	29	138	78	33	140
D30	65	32	112	72	30	136	72	30	136	77	27	133
H	67	33	114	74	29	136	74	29	136	78	36	136
D20	67	31	116	72	30	137	72	30	137	68.5	28	120
D10	69	32	118	80	31	154	80	31	154	68	29	124
Imax	69	33	120	68	32	133	68	32	133	68.5	23	122
ADP	69	32	121	66.5	32	114	66.5	32	114	67	27	117

	laplacedot			besseldot			anovadot			splinedot		
	NRMSD	min	max	NRMSD	min	max	NRMSD	min	max	NRMSD	min	max
Accum	64	32	107	64	31	110	67	27	122	190.5	36	1783
D40	64	32	110	65	32	113	67	26	121	140	34	729
rw	64	32	110	66	32	116	66.5	32	119	133	32	766
D30	64	32	110	64	32	114	64	30	114	120	34	425
H	65	33	113	65	33	114	66	32	119	100	32	275

D20	65	32	111	65	31	115	65	31	115	84	30	195
D10	67	34	113	67	33	117	71	32	124	82	33	169
Imax	68	34	116	67	34	115	74	36	130	75	34	146
ADP	70	32	121	66	32	110	67	32	119	66	32	114

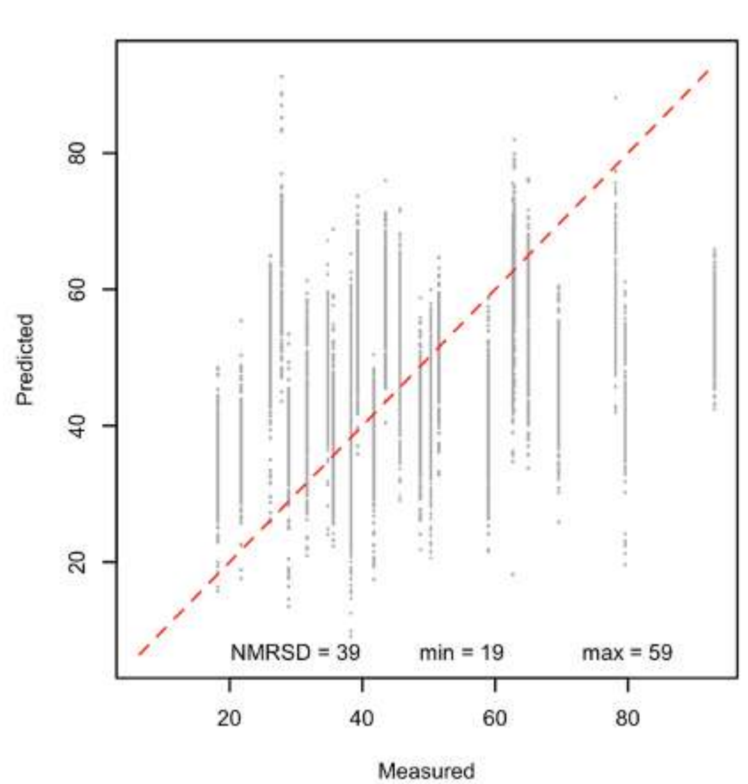

Figure C-11 Support vector machine error for Zn_I_{geo} in Molinos Reiver

PART D: Sediment management

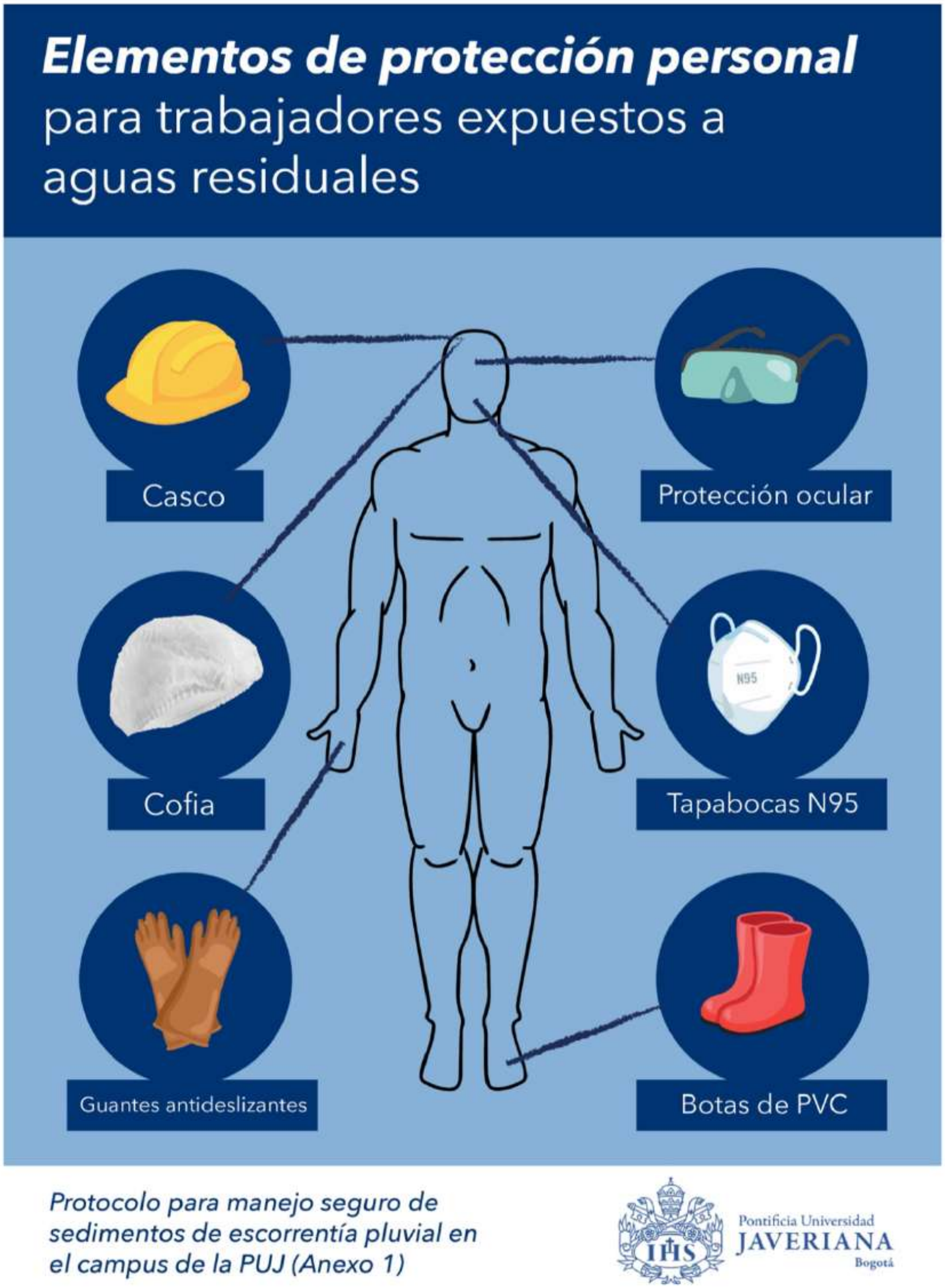

Figure D-1 Personal protection items. Source:(Serna-Henao et al., 2022)

Figure D-2 Sediment Handling Precautions Source:(Serna-Henao et al., 2022)